U L T I M A T E L O A D B E H A V I O U R O F

P L Y W O O D S T R E S S E D – S K I N P A N E L S

Thesis submitted for the degree of

Doctor of Philosophy

of London University

by

Mu Kattil Surendranath B.E., M.Sc.,

Department of Civil Engineering,

Imperial College of Science and

Technology,

London, S.W.7.

1982

DEDICATION

To the memory of my beloved parents.

ABSTRACT

Ultimate load behaviour of Plywood stressed-skin panels

The ultimate load behaviour of single skin and double skin panels with rigid connections between flanges and ribs has been investigated treating them as a series of T beams and I beams respectively. The sections with non-layered flanges and layered flanges (appropriate to the plywood flanges) have been considered. Plastic behaviour in compression and brittle failure in tension, the properties which are attributable to the timber, have been taken into account. As the ultimate tensile stress of the rib is considered to be dependent upon the volume of the rib and the type of loading, Weibull's statistical strength theory has been applied to the tensile zone of the rib of the T sections to predict the ultimate tensile stress at a desired probability of failure.

Computer programs have been written to calculate the resisting moments of the sections and to find the modes of failure.

Results of the pilot tests are also reported.

ACKNOWLEDGEMENTS

The author wishes to express his profound gratitude to the supervisor, Dr. L.G.Booth, for the constant guidance and advice given during the course of the work. He is also deeply indebted to Professor B.G.Neal, head of the Civil Engineering Department, for the understanding and kindness he has shown during the adverse situations. The guidance given by Mr. F.H.Potter on the experimental work is gratefully acknowledged.

The author is very grateful to Dr. R.O.Foschi of the Western Forest Product Laboratory, Vancouver, for his valuable advice on Weibull's statistical strength theory and the size effect problem in timber.

Thanks are due to Mr. J.Neal, Mr. R.Philpott, Mr. A.J.Leete and other members of the Engineering Structures Laboratory and Carpentry shop of the Imperial College, who gave assistance in the making of the model beams and experimental work. Thanks are also due to the members of the Civil Engineering Laboratory of the University College, London, who helped the author to conduct experiments on timber veneers using ultrasonic pulse technique.

During the course of the work, the author had many opportunities to visit the Princess Risborough Laboratory of the Building Research Establishment. The valuable help given by the staff of the Laboratory, especially Mr. W.T.Curry, Mr. J.R.Tory, Mr. A.R.Fewell, Mr. M.F. Houldsworth and Mr. C.B.Pierce, by way of numerous discussions and by providing data from the experiments conducted at PRL and other relevant informations, is thankfully acknowledged.

The author is grateful to his previous employers, Medway Buildings Ltd., for permission to engage in part-time research work at Imperial College. Help given by his present employers, Montague L. Meyer Ltd., is also gratefully acknowledged. Thanks are due to Thames Plywood Manufacturers Ltd., for supplying, free of charge, the timber veneers used in the experiments. Thanks are also due to the Council of the Forest Industries of British Columbia for donating the timber joists.

The author is grateful to Science Research Council for granting a scholarship for one year, thus enabling him to engage in the full-time research work during that period.

The author also express his thanks to all colleagues at Medway Buildings Ltd., Montague L Meyer Ltd., and Imperial College who gave valuable help by providing constructive criticism during the discussions and by reading the manuscript.

Special thanks are due to the author's wife, Padmini, for typing the thesis. The author wishes to record his deep appreciation of her patience and constant support throughout the period of this research work.

CONTENTS

			Page No.
NOTATION			9
CHAPTER	1	INTRODUCTION	
	1.1	General	11
	1.2	Review of previous work	12
	1.3	Object and scope of present investigation	17
CHAPTER	2	ANALYSIS OF T SECTION WITH NON-LAYERED FLANGE	
	2.1	Stress-strain relationship of the materials of flange and rib	20
	2.2	Assumptions for T section in bending	20
	2.3	Modes of failure	21
	2.4	Derivation of governing equations	23
	2.5	Analysis of T sections using computer	36
CHAPTER	3	ANALYSIS OF I SECTION WITH NON-LAYERED FLANGES	
	3.1	Assumptions	42
	3.2	Analysis	42
CHAPTER	4	ANALYSIS OF T SECTION WITH LAYERED FLANGE	
	4.1	Assumptions	47
	4.2	Additional assumptions	47
	4.3	Additional notation	48
	4.4	Derivations of governing equations	49
	4.5	Analysis of T sections with layered flange using computer	61

	4.6	Analysis of I sections with layered flanges	71
CHAPTER	5	STATISTICAL ANALYSIS OF SIZE EFFECT	
	5.1	Introduction	73
	5.2	Weakest link theory	73
	5.3	Weibull's statistical strength theory	74
	5.4	Brittle fracture	74
	5.5	Material types	74
	5.6	Development of statistical strength theory	75
	5.7	Non-uniform stress	77
	5.8	Comparison of two volumes at same probability of failure	78
	5.9	Tensile stress at a particular probability of failure	79
	5.10	Application of Weibull's theory to predict the ultimate resisting moment of a T beam in bending	82
	5.11	Method of development of an expression for $\int_V \sigma^k dv$ in the tension zone	84
	5.12	Derivation of the values of k and K_0 from the test results	107
	5.13	Solutions for typical examples using Weibull's theory	113
CHAPTER	6	EXPERIMENTAL INVESTIGATION	
	6.1	Preliminary test series	128
	6.2	Pilot test series on T beams with non-layered flange to investigate size effect problem	146
CHAPTER	7	COMPUTER PROGRAMS	
	7.1	Introduction	172
	7.2	Computer programs	172

CHAPTER 8 SUMMARY, CONCLUSIONS & FUTURE WORK

8.1 Summary 179

8.2 Conclusions 181

8.3 Future work 182

BIBLIOGRAPHY 183

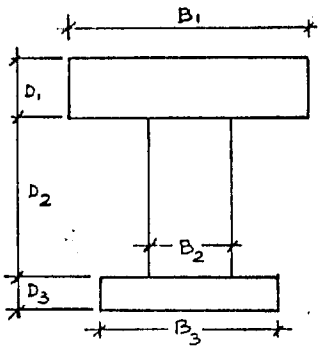
APPENDIX 1 Iteration procedure 186

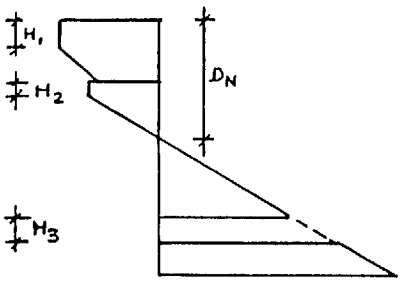
APPENDIX 2 Fortran program for iteration algorithm 188

APPENDIX 3 Application of Gauss quadrature 189

APPENDIX 4 Bending test results obtained from Princes Risborough Laboratory (PRL) 192

a) I and T sections with non-layered flanges





TYPICAL STRESS DIAGRAM

B_1 Breadth of top flange

B_2 Breadth of rib

B_3 Breadth of bottom flange. For T section $B_3 = 0$

C_1 Coefficient for Neutral Axis such that $D_N = C_1 D_1$

C_2 Coefficient for Ultimate resisting moment such that

$$ULTM = C_2 F_4 \frac{B_2 D_2^2}{6}$$

D_1 Depth (thickness) of top flange

D_2 Depth of rib

D_3 Depth (thickness) of bottom flange

D_N Depth of Neutral Axis from top of the top flange

E_1 Modulus of elasticity of top flange

E_2 Modulus of elasticity of rib

E_3 Modulus of elasticity of bottom flange

F_1 Ultimate compressive stress of top flange

F_3 Ultimate compressive stress of rib

F_4 Ultimate tensile stress of rib

F_5 Ultimate tensile stress of bottom flange

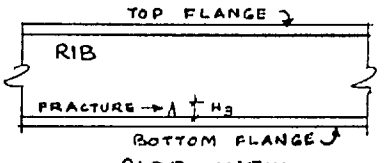
Note: E_1 to F_5 are properties parallel to the span

H_1 Depth of yield penetration in top flange

H_2 Depth of yield penetration in rib

H_3 Ineffective depth of rib

ULTM Ultimate resisting moment of the section



SIDE VIEW

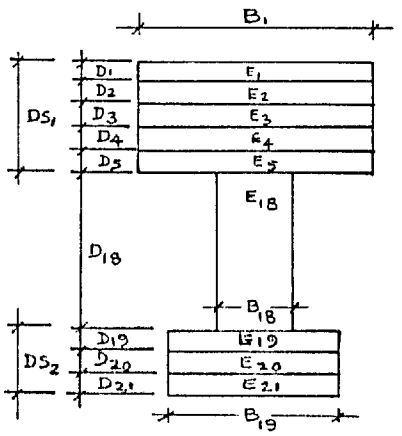
$$\alpha = \frac{D_2}{D_1} \qquad \beta = \frac{B_1}{B_2} \qquad \gamma = \frac{E_2}{E_1} \qquad \rho_1 = \frac{F_1}{F_4}$$

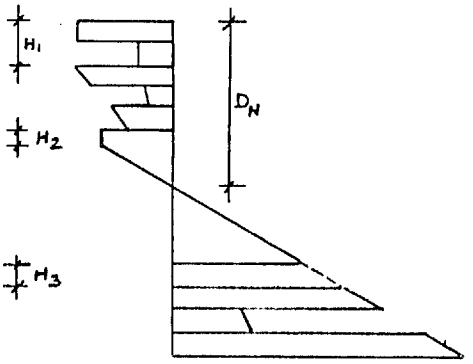
$$\rho_2 = \frac{F_3}{F_4} \qquad \phi_1 = \frac{H_1}{D_1} \qquad \phi_2 = \frac{H_2}{D_2}$$

σ_{i1} Stress at the extreme top fibre of the i^{th} element

σ_{i2} Stress at the extreme bottom fibre of the i^{th} element

b) I and T sections with layered flanges





TYPICAL STRESS DIAGRAM

Note: Up to 17 layers in each flange are considered in this thesis. Therefore rib and first layer of bottom skin are named as 18th and 19th element respectively.

B_1 Breadth of top flange

B_{18} Breadth of rib

B_{19} Breadth of bottom flange. For T section $B_{19} = 0$

D_i Depth of i^{th} element counting from top

DS_1 Depth of top flange

DS_2 Depth of bottom flange

E_i Modulus of elasticity of i^{th} element

F_1 Ultimate compressive stress of first layer of top flange

F_2 Ultimate compressive stress of second layer of top flange

F_3 Ultimate compressive stress of rib

F_4 Ultimate tensile stress of rib

F_5 Ultimate tensile stress of 19^{th} element (first layer of bottom flange)

F_6 Ultimate tensile stress of 20^{th} element (second layer of bottom flange)

Note: E_i to F_6 are properties parallel to the span
D_N, H_1, H_2, H_3 & ULTM have the same meanings as in case (a)

N_1 Number of layers in top flange

N_2 Number of layers in bottom flange

σ_{i1} Stress at the extreme top fibre of the i^{th} element

σ_{i2} Stress at the extreme bottom fibre of the i^{th} element

CHAPTER 1

INTRODUCTION

1.1 GENERAL

Traditionally, timber structural components were made at building sites by skilled carpenters. However, the increase in cost of site labour has lead to an increase in the use of factory made structural components. The scarcity and the resulting high price of timber has necessitated a more efficient use of timber in these components. One such structural component is the "stressed-skin panel". The development of the stressed-skin plywood panel started in the early 1930s at the U.S Forest Product Laboratory. These panels are now widely used in prefabricated timber buildings.

Plywood stressed-skin panels consist of plywood sheets effectively attached to one or both sides of solid longitudinal timber framing members. They are used as floors, roofs and walls in prefabricated timber buildings. In conventional system, plywood acts as a surface covering only, whereas in stressed-skin panels the plywood acts integrally with the longitudinal timber joists to resist bending stresses. With the plywood thus sharing the load with the joists, it becomes possible to use smaller joists to support the load. The benefits of the reduction of joist size achieved by this efficient use of materials are numerous. Not only is the cost of materials reduced but also a lightweight panel is obtained. Reduction in volume and weight results in economy of storage and transportation of the prefabricated units. These panels are easy to handle and they reduce site work and speed up erection.

Structurally, a double skin panel can be considered as a series of parallel I beams in which the longitudinal framing joists form the webs and the plywood the flanges. Similarly, a single skin panel can be considered as a series of T beams.

The plywood is connected to the joists by pressure-gluing, nail-gluing or simply by nailing. Staples are sometimes used as an alternative to nails. Nail (or staple) joints are least efficient because of nail slip and the consequent incomplete shear transfer between rib and flange. The use of nails to impart pressure on the glue line during curing can achieve a better result. However, there are areas of uncertainty in nail-gluing resulting from uneven pressure and one cannot be sure of its stress-carrying capabilities. The best joint is achieved by pressure-gluing. The visual proof of the adequate uniform pressure applied along the joint is given by pressure gauges attached to the press. To obtain the full stress skin effect it is essential that the plywood is firmly bonded throughout the length of all longitudinal joists. In this thesis panels only with perfect bond between the flanges and ribs are considered.

1.2 Review of previous work

1.2.1 Stressed-skin panels

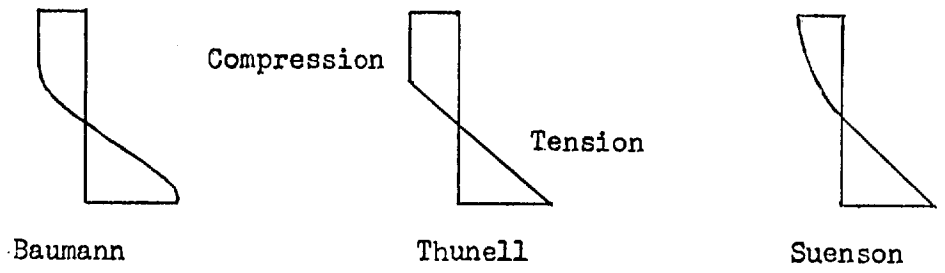
All known previous work is limited to elastic analysis. Amana (1967) has given an exhaustive survey of the work done by the other investigators on the behaviour of stressed-skin panels within the limit of elasticity. Amana considered stressed-skin panels as stiffened plywood plates and obtained a membrane solution. Foschi (1969) studied the influence of geometric and elastic parameters

on the stress distribution in multi-web-type plywood stressed-skin panels. Booth and Pierce (1971) presented a 'combined beam and plate analysis' for plywood panels stiffened with timber beams.

1.2.2 Solid timber beams in bending

Kollmann and Cotē (1968) make reference to the work of Baumann, Ros, Thunell and Suenson on the ultimate load behaviour of solid timber beams.

The following sketches show a comparison of the stress distribution adopted by them.



Stress distribution for the cross-section of a bent timber beam

Baumann's stress diagram shows plastic behaviour both in the compression and tension zones, even though the plasticity in tension zone is very small and not as predominant as in the compression zone. Thunell and Suenson assumed linear distribution of stress throughout the tension zone. In the compression zone, Ros and Thunell assumed trapezoid-like stress distribution whereas Suenson used a parabolic curve to represent the compressive stress distribution.

Dietz (1942), Comben (1957) and Ramos (1961) were interested in the strain distribution across the depth of the timber beams. Dietz observed non-linear strain distribution when he tested Douglas-fir beams. However, Comben's experiments indicated that the strain distribution is approximately linear across the depth, except at high

compression region where it is slightly non-linear. Ramos also observed basically linear strain distribution.

On the basis of the conclusions of the previous investigators the following assumptions can be made in deriving the governing equations of the ultimate load behaviour of a timber beam.

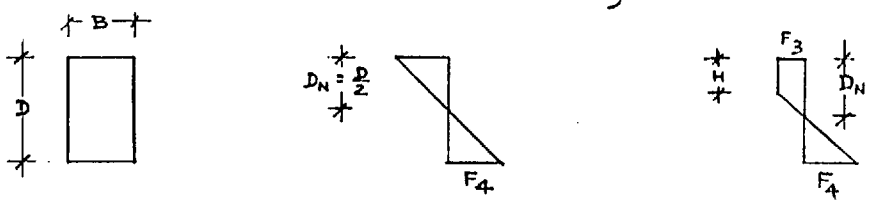
Assumptions:

1. Plane sections remain plane until the collapse moment is reached.
2. Moduli of elasticity in tension and compression are same.
3. Ultimate load is reached when extreme bottom fibre attains ultimate tensile stress.
4. Compression strain is unlimited.
5. Plastic deformation can take place in the compression zone only, not in the tension zone.

In the case of structural size timber there are two possible modes of failure according to the relative magnitude of ultimate tensile and compressive stresses.

Mode 1. When ultimate compressive stress (F_3) $\nless$ ultimate tensile stress (F_4)

Mode 2. When ultimate compressive stress (F_3) $<$ ultimate tensile stress (F_4)



Beam section Mode 1 Mode 2

Stress distributions of failure modes

In the case of Mode 2 trapezoid-like stress distribution is assumed in the compression zone.

Mode 1. In this mode the section remains elastic until the collapse moment is reached.

$$D_N = \tfrac{1}{2} D \qquad \text{-- 1.1}$$

$$\text{ULTM} = F_4 \frac{BD^2}{6} \qquad \text{-- 1.2}$$

Mode 2. In this mode the section is in the elasto -plastic state.

Total tension $T = \tfrac{1}{2}F_4B(D - D_N)$

Total compression $C = -\left[F_3BH + \tfrac{1}{2}F_3B(D_N - H)\right]$

For equilibrium $T + C = 0$

From this we obtain $H = \frac{D}{\rho_2} - D_N \left(\frac{1}{\rho_2} + 1\right)$ -- 1.3

$$\frac{D_N - H}{D - D_N} = \frac{F_3}{F_4} = \rho_2$$

$$H = D_N (1 + \rho_2) - \rho_2 D \qquad \text{-- 1.4}$$

From (1.3) and (1.4) $D_N = \frac{1 + \rho_2^2}{(1+\rho_2)^2} D = C_1 D$ -- 1.5

where $C_1 = \frac{1 + \rho_2^2}{(1+\rho_2)^2}$

Note: An equation same as 1.5, but with different symbols can be found in Kollmann and Cotē. (1968)

Substituting (1.5) into (1.4) $H = \left(\frac{1-\rho_2}{1+\rho_2}\right) D = \phi D$ -- 1.6

where $\phi = \frac{1-\rho_2}{1+\rho_2}$

Taking moments about the top fibre,

$$\text{ULTM} = \tfrac{1}{2} F_4B(D-D_N)\left\{D-\tfrac{1}{3}(D-D_N)\right\} - \tfrac{1}{2}F_3BH^2 - \tfrac{1}{2}F_3B(D_N - H)\left\{H + \tfrac{1}{3}(D_N - H)\right\}$$

The equation for ULTM reduces to

$$ULTM = C_2 F_4 \frac{BD^2}{6} \qquad -- 1.7$$

$$\text{where } C_2 = \frac{\rho_2}{(1+\rho_2)^4}(3 + 8\rho_2 + 6\rho_2^2 - \rho_2^4)$$

Table 1 shows the values of C_1, C_2 and $\emptyset$ for different values of ρ_2.

1.2.3 Plywood in compression and tension

The methods of calculating the strength and modulus of elasticity of plywood were probably first developed at the U.S Forest Product Laboratory. Liska (1942), Markwardt and Freas(1946) presented approximate methods. After conducting extensive investigations, Curry (1954) also has suggested equations for calculating the bending, tension, compression and shear strength of plywood. Plywood in a stressed-skin panel is mainly under the influence of compressive and tensile stresses. Curry suggested that the modulus of elasticity in tension and compression for the plywood may be assumed the same.

$$\text{Equivalent modulus of elasticity } E_C = E_T = \frac{\Sigma(Et)}{\Sigma t} \qquad -- 1.8$$

where E = modulus of elasticity of each element

t = thickness of each element

Tottenham (1958) also derived an expression for equivalent modulus of elasticity in a slightly different form, but the result is the same in both cases. For compression strength, Curry's equation (11A) as given below is found to be simple and appropriate for the plywood.

$$\text{Equivalent compression strength } f_c = \frac{1}{\Sigma t}[\Sigma(f_1 t_1) + \Sigma(f_2 t_2)] \qquad -- 1.9$$

where f_1 and t_1 are the strength and thickness of the parallel plies and f_2 and t_2 are the strength and thickness of the perpendicular plies.

To estimate the tension strength of plywood, the strength of the perpendicular plies can be ignored and Curry's simplified equation (16) may be adopted.

$$f_T = \frac{\Sigma(f_i t_i)}{\Sigma t} \qquad -- 1.10$$

1.3 Object and scope of present investigation

It is now an accepted fact that the design codes should be presented in a 'limit state' format. The publication of CP 110, code of practice for the structural use of concrete in 1972 has firmly established this new and logical trend. A draft code on structural steel has already been published and it is under discussion by the code users prior to its final acceptance. It is anticipated that the timber design code, CP 112 will eventually be brought into line with the others.

The two most important limit states are 'ultimate limit state' and 'serviceability limit state'; the former is related to the collapse and the latter to the excessive deformation. The behaviour related to collapse only is considered in this thesis.

As stated earlier, all previous work on stressed-skin panels is limited to the elastic analysis. Because of the recent change in direction adopted by the code writers, it is not only desirable but also essential to acquire more knowledge about the ultimate load behaviour of stressed-skin panels. This is the main object of this investigation.

The present investigation essentially consists of treating the single and double skin panels as a series of T beams and I beams respectively and finding the ultimate resisting moment. Plastic behaviour of timber and plywood in compression and the sudden brittle

failure they exhibit in tension have been considered. As the ultimate load of the panel is mainly influenced by the ultimate tensile stress of the rib, this area has now been subjected to further investigation in the case of the T section. It is now widely believed that the ultimate tensile strength of a timber beam is dependent upon the volume of the beam and the type of loading. It is also a fact that two similar timber beams of the same species with the same geometrical properties will not fail at the same load. Hence a statistical approach is essential to find a probable failure load. Weibull's (1939) statistical strength theory is found to be a very useful tool to tackle this problem. This theory has been applied to the tensile zone of the rib of the T sections to predict the ultimate tensile stress at a desired probability of failure.

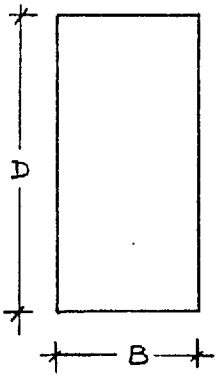
The scope of the present investigation can be brought into the following sub-headings.

1. Analyse the following panel sections as if the ultimate tensile stresses of the rib and the bottom flange are known.
   a) T section with non-layered flanges
   b) T section with layered flanges
   c) I section with non-layered flanges
   d) I section with layered flanges
2. Apply Weibull's statistical strength theory to the rib of the T section with non-layered and layered flange and predict the ultimate tensile stress and thereby derive ultimate resisting moment at a particular probability of failure.
3. Write computer programs.
   a) to cover the items 1 (a) to 1 (d)
   b) to cover item 2.
4. Do pilot tests on T beams and compare the results with the ultimate loads predicted using the available statistical strength data.

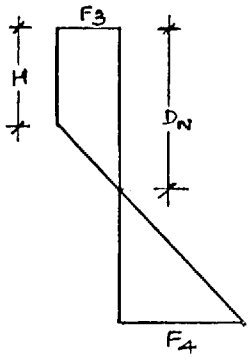
TABLE 1

Timber beam with rectangular cross section.

Coefficients at the ultimate load stage according to the relative magnitude of ultimate compressive and tensile stress.



Cross section



Stress diagram

$$\rho_2 = \frac{\text{Ult. compressive stress } (F_3)}{\text{Ult. tensile stress } (F_4)} \leq 1$$

$$D_N = C_1 D$$

where $C_1 = \dfrac{1+\rho_2^2}{(1+\rho_2)^2}$

$$H = \phi D$$

where $\phi = \dfrac{1-\rho_2}{1+\rho_2}$

$$ULTM = C_2 F_4 \frac{BD^2}{6}$$

where $C_2 = \dfrac{\rho_2}{(1+\rho_2)^4}(3+8\rho_2+6\rho_2^2-\rho_2^4)$

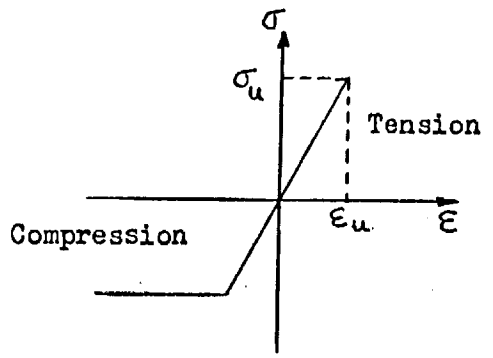
ρ_2	C_1	C_2	ϕ
0.1000	0.8347	0.2636	0.8182
0.2000	0.7222	0.4667	0.6667
0.3000	0.6450	0.6231	0.5385
0.4000	0.5918	0.7429	0.4286
0.5000	0.5556	0.8333	0.3333
0.6000	0.5313	0.9000	0.2500
0.7000	0.5156	0.9471	0.1765
0.8000	0.5062	0.9778	0.1111
0.9000	0.5014	0.9947	0.0526
1.0000	0.5000	1.0000	0.0000

CHAPTER 2

ANALYSIS OF T SECTION WITH NON-LAYERED FLANGE

2.1 Stress-strain relationships of the materials of flange and rib

Idealised stress-strain relationships in tension and in compression as shown in fig.2.1 have been assumed for the materials of flange and rib.



σ Stress

ε Strain

σ_u Ultimate tensile stress

ε_u Ultimate tensile strain

Unlimited compression strain is assumed.

Fig. 2.1 Idealised stress-strain relationships in tension and in compression.

The stress-strain relationships shown in fig. 2.1 is assumed to be valid for the layers of the layered material (eg. plywood) also.

2.2 Assumptions for T section in bending

1. Plane sections remain plane until the ultimate moment is reached.
2. Modulus of elasticity of flange is same throughout its depth.
3. Modulus of elasticity of rib is same throughout its depth.
4. No slip is allowed at the interface between flange and rib.
5. Local buckling of flange is not allowed.
6. Effect of Poisson's ratio is ignored.
7. Ultimate moment is reached when the extreme bottom fibre attains ultimate tensile stress.
8. Plastic deformation can take place in the compression zone only; not in the tension zone.

2.3 Modes of failure

When T sections with non-layered flange are tested in bending to failure, eight distinct modes of failure are possible. They are listed below in two groups according to the location of the neutral axis at the ultimate moment.

a) Neutral axis within the rib

Mode 1. Both flange and rib are in the elastic state.

Mode 2. Flange is partially plastic, but the rib is completely elastic.

Mode 3. Flange is completely elastic, but the rib is partially plastic.

Mode 4. Both flange and rib are partially plastic.

Mode 5. Flange is completely plastic, but the rib is completely elastic. In this mode $F_1 = \sigma_{12}$, which may or may not be equal to $\sigma_{21} \frac{E_1}{E_2}$.

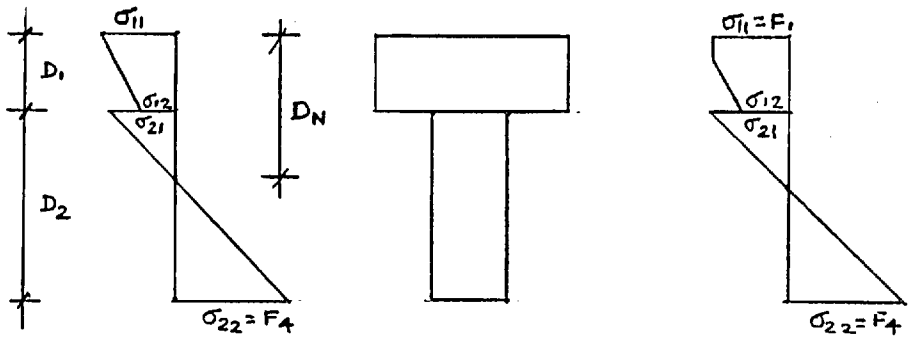
Mode 6. Flange is completely plastic and the rib is partially plastic.

b) Neutral axis within the flange or at the interface

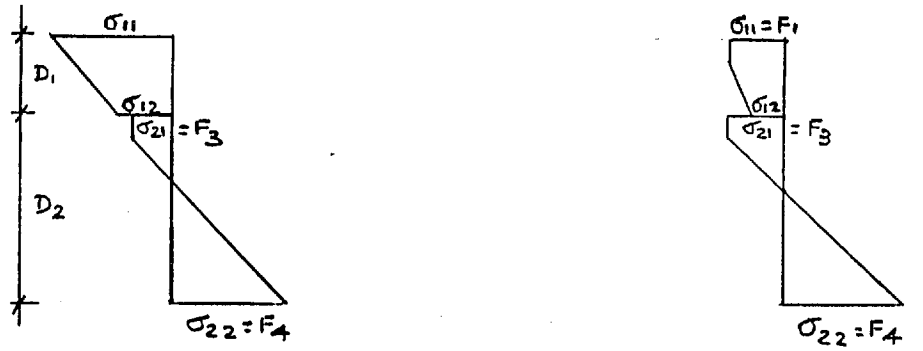
Mode 7. Both flange and rib are in the elastic state.

Mode 8. Flange is partially plastic, but the rib is completely elastic.

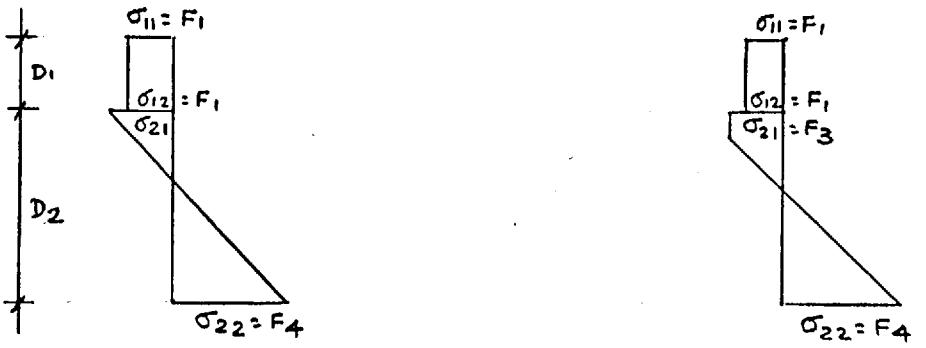
Typical stress diagrams related to the above modes of failure are shown in fig. 2.2 and the examples of the modes of failure are given in Table 2.



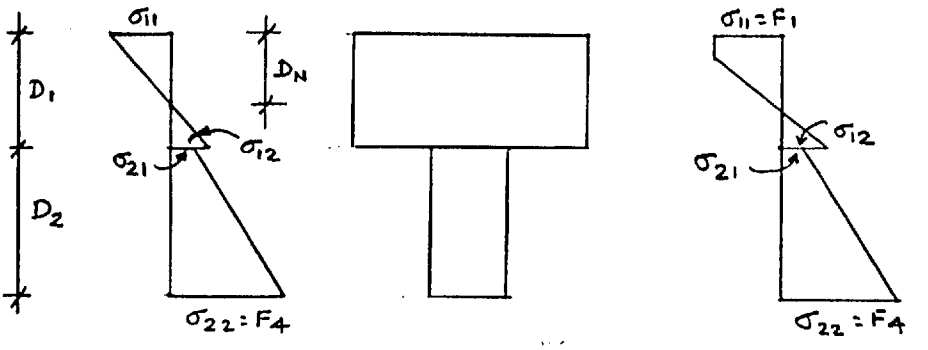
Mode 1 T section Mode 2



Mode 3 Mode 4



Mode 5 Mode 6



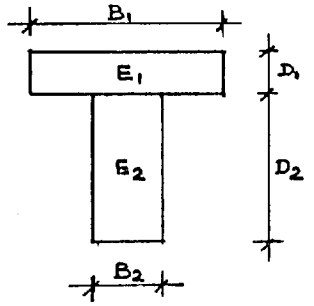
Mode 7 T section Mode 8

Fig. 2.2 Failure modes of T sections

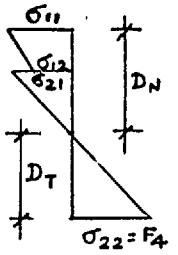
Typical stress diagrams

2.4 Derivation of governing equations

2.4.1 Failure mode 1



Cross section



Stress diagram

$$H_1 = 0 \qquad H_2 = 0$$

$$\sigma_{11} = \frac{F_4 D_N E_1}{D_T E_2} = \frac{F_4 D_N}{D_T \gamma}$$

$$\sigma_{12} = \frac{F_4 (D_N - D_1)}{D_T \gamma}$$

$$\sigma_{21} = \frac{F_4 (D_N - D_1)}{D_T}$$

$$D_N = \frac{\frac{1}{2}E_1 B_1 D_1^2 + E_2 B_2 D_2 (D_1 + \frac{1}{2}D_2)}{E_1 B_1 D_1 + E_2 B_2 D_2}$$

This reduces to $D_N = C_1 D_1$ 2.1

$$\text{where } C_1 = \frac{\frac{\beta}{\gamma} + \alpha(2+\alpha)}{2(\frac{\beta}{\gamma} + \alpha)}$$

Taking moments about the top fibre of the flange,

$$ULTM = \tfrac{1}{2}F_4 B_2 D_T (D_1 + D_2 - \tfrac{1}{3}D_T) - \tfrac{1}{2}(\sigma_{11} + \sigma_{12}) B_1 D_1^2 \frac{(\sigma_{11} + 2\sigma_{12})}{3(\sigma_{11} + \sigma_{12})} - \tfrac{1}{2}\sigma_{21} B_2 (D_N - D_1)\frac{(2D_1 + D_N)}{3}$$

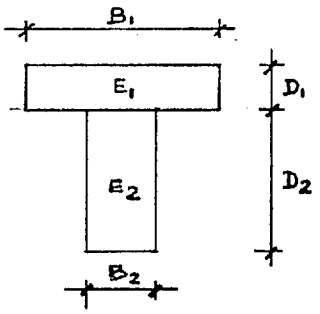
This reduces to

$$ULTM = C_2 F_4 \frac{B_2 D_2^2}{6} \qquad - 2.2$$

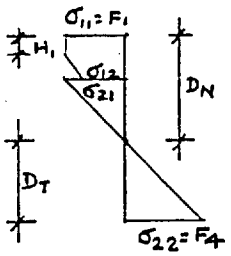
where

$$C_2 = \frac{(1+\alpha-C_1)^2\left[2(1+\alpha)+C_1\right] - (C_1-1)^2(2+C_1) - (3C_1-2)\frac{\beta}{\gamma}}{\alpha^2(1+\alpha-C_1)}$$

2.4.2 Failure mode 2



Cross section



Stress diagram

$$\sigma_{12} = \frac{F_4(D_N-D_1)E_1}{D_T E_2} = \frac{F_4(D_N-D_1)}{D_T \gamma}$$

$$\sigma_{21} = \frac{F_4(D_N-D_1)}{D_T}$$

$$H_2 = 0$$

$$\frac{D_N-H_1}{D_N-D_1} = \frac{F_1}{\sigma_{12}} = \frac{F_1 D_T \gamma}{F_4(D_N-D_1)} = \frac{\rho_1 D_T \gamma}{(D_N-D_1)}$$

$$\therefore \quad D_N-H_1 = \rho_1 D_T \gamma$$

$$H_1 = D_N - \rho_1 D_T \gamma \qquad - 2.3$$

$$\text{Total compression } C = -\left[F_1 B_1 H_1 + \tfrac{1}{2}(F_1+\sigma_{12})B_1(D_1-H_1) + \tfrac{1}{2}\sigma_{21}B_2(D_N-D_1)\right]$$

$$\text{Total tension } \quad T = +\tfrac{1}{2}F_4 B_2 D_T$$

For equilibrium $C + T = 0$ - 2.4

By substituting relevant values in (2.4) and rearranging,

$$AD_N^2 + BD_1D_N + C_3D_1^2 = 0 \qquad - 2.5$$

where $A = (\gamma\rho_1+1)^2$

$$B = -2\left[\gamma\rho_1(1+\alpha)(\gamma\rho_1+1)+1+\frac{\alpha}{\frac{\beta}{\gamma}}\right]$$

$$C_3 = (\gamma\rho_1)^2(1+\alpha)^2 + \frac{\alpha}{\frac{\beta}{\gamma}}(2+\alpha)+1$$

$$D_N = C_1 D_1 \qquad - 2.6$$

where $C_1 = \dfrac{-B-\sqrt{B^2-4AC_3}}{2A}$

Substituting (2.6) into (2.3) $H_1 = \phi_1 D_1$ - 2.7

where $\phi_1 = C_1(\gamma\rho_1+1) - \gamma\rho_1(1+\alpha)$

Taking moments about the top fibre of the flange,

$$ULTM = \tfrac{1}{2}F_4 B_2 D_T (D_1+D_2-\tfrac{1}{3}D_T) - \tfrac{1}{2}F_1 B_1 H_1^2 - \tfrac{1}{2}(F_1+\sigma_{i2})B_1(D_1-H_1)\left\{H_1+\frac{(F_1+2\sigma_{i2})(D_1-H_1)}{3(F_1+\sigma_{i2})}\right\}$$

$$- \tfrac{1}{2}\sigma_{2i}B_2(D_N-D_1)\left\{D_1+\tfrac{1}{3}(D_N-D_1)\right\}$$

This reduces to

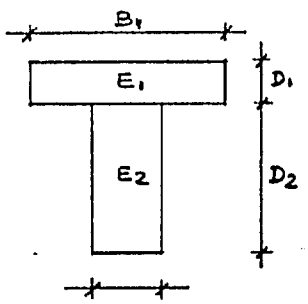
$$ULTM = C_2 F_4 \frac{B_2 D_2^2}{6} \qquad - 2.8$$

where,

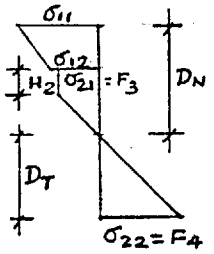
$$C_2 = \frac{1}{\alpha^2}\Big[(1+\alpha-C_1)\{2(1+\alpha)+C_1\} - 3\beta\rho_1\phi_1^2 - \beta\rho_1\frac{(1-\phi_1)}{(C_1-\phi_1)}\{\phi_1(3C_1-2-2\phi_1)$$

$$+3C_1-2\} - \frac{(C_1-1)^2(C_1+2)}{(1+\alpha-C_1)}\Big]$$

2.4.3 Failure mode 3



Cross section



Stress diagram

$$H_1 = 0$$

$$\sigma_{11} = \frac{F_4 D_N E_1}{D_T E_2} = \frac{F_4 D_N}{D_T \gamma}$$

$$\sigma_{12} = \frac{F_4 (D_N - D_1)}{D_T \gamma}$$

$$\frac{D_N - D_1 - H_2}{D_T} = \frac{F_3}{F_4} = \rho_2$$

$$H_2 = D_N - D_1 - \rho_2 D_T \qquad - 2.9$$

Total compression $C = -\left[\frac{1}{2}(\sigma_{11}+\sigma_{12})B_1 D_1 + F_3 B_2 H_2 + \frac{1}{2}F_3 B_2 (D_N - D_1 - H_2)\right]$

Total tension $T = + \frac{1}{2}F_4 B_2 D_T$

For equilibrium $C + T = 0$ - 2.10

By substituting relevant values in (2.10)and rearranging, the following equation is obtained.

$$AD_N^2 + BD_1 D_N + C_3 D_1^2 = 0 \qquad - 2.11$$

where $A = (1+\rho_2)^2$

$$B = -2\left[(1+\alpha) + \frac{\beta}{\gamma} + \rho_2\left\{1 + (1+\rho_2)(1+\alpha)\right\}\right]$$

$$C_3 = \frac{\beta}{\gamma} + (1+\alpha)^2 + \rho_2(1+\alpha)\left[2 + \rho_2(1+\alpha)\right]$$

$$D_N = C_1 D_1 \qquad - 2.12$$

where $C_1 = \dfrac{-B - \sqrt{B^2 - 4AC_3}}{2A}$

Substituting (2.12)into (2.9) $H_2 = \phi_2 D_2$ - 2.13

where $\phi_2 = \frac{1}{\alpha}\left[C_1 - 1 - \rho_2(1+\alpha - C_1)\right]$

Taking moments about the top fibre of the flange,

$$ULTM = \tfrac{1}{2}F_4 B_2 D_T (D_1 + D_2 - \tfrac{1}{3}D_T) - \tfrac{1}{2}(\sigma_{11}+\sigma_{12})B_1 D_1^2 \frac{(2\sigma_{12}+\sigma_{11})}{3(\sigma_{11}+\sigma_{12})}$$

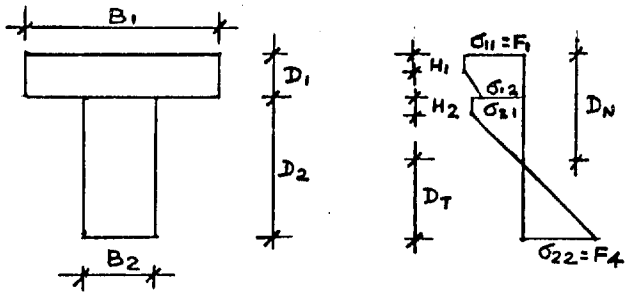
$$- F_3 B_2 H_2 (D_1 + \tfrac{1}{2}H_2) - \tfrac{1}{2}F_3 B_2 (D_N - D_1 - H_2)\tfrac{1}{3}(D_N + 2D_1 + 2H_2)$$

This reduces to $ULTM = C_2 F_4 \dfrac{B_2 D_2^2}{6}$ - 2.14

Where $C_2 = \frac{1}{\alpha^2}\Big[(1+\alpha-C_1)\left\{2(1+\alpha)+C_1\right\} - \rho_2\Big\{\frac{\beta(3C_1-2)}{\gamma}(C_1 - 1 - \phi_2\alpha)$

$$+ (\phi_2\alpha)^2 + C_1(C_1 + 1 + \phi_2\alpha) + 2(\phi_2\alpha - 1)\Big\}\Big]$$

2.4.4 Failure mode 4



Cross section Stress diagram

$$\sigma_{21} = F_3$$

$$\sigma_{12} = \frac{F_4(D_N-D_1)E_1}{D_T E_2} = \frac{F_4(D_N-D_1)}{D_T \gamma}$$

Comparing with modes (2) and (3)

$$H_1 = D_N - \rho_1 D_T \gamma \qquad - 2.15$$

$$H_2 = D_N - D_1 - \rho_2 D_T \qquad - 2.16$$

Total compression $C = -\left[F_1 B_1 H_1 + \frac{1}{2}(F_1+\sigma_{12})B_1(D_1-H_1) + F_3 B_2 H_2 + \frac{1}{2}F_3 B_2 (D_N-D_1-H_2)\right]$

Total tension $T = +\frac{1}{2}F_4 B_2 D_T$

For equilibrium $C + T = 0$ - 2.17

By substituting relevant values in (2.17) and rearranging,

$$AD_N^2 + BD_1 D_N + C_3 D_1^2 = 0 \qquad - 2.18$$

where,

$$A = (1+\rho_2)^2 + (\gamma\rho_1+1)^2 \frac{\beta}{\gamma}$$

$$B = -2\left[(1+\alpha) + \frac{\beta}{\gamma} + \rho_2\{1+(1+\rho_2)(1+\alpha)\}\right] - 2\left[\gamma\rho_1(1+\alpha)(\gamma\rho_1+1)\right]\frac{\beta}{\gamma}$$

$$C_3 = \frac{\beta}{\gamma} + (1+\alpha)^2 + \rho_2(1+\alpha)\{2+\rho_2(1+\alpha)\} + (\gamma\rho_1)^2(1+\alpha)^2\frac{\beta}{\gamma}$$

$$D_N = C_1 D_1 \qquad - 2.19$$

where $C_1 = \dfrac{-B-\sqrt{B^2-4AC_3}}{2A}$

Substituting (2.19) into (2.15) and (2.16)

$$H_1 = \phi_1 D_1 \qquad - 2.20$$

where $\phi_1 = C_1(\gamma\rho_1+1)-\gamma\rho_1(1+\alpha)$

$$H_2 = \phi_2 D_2 \qquad - 2.21$$

where $\phi_2 = \frac{1}{\alpha}\left[C_1-1-\rho_2(1+\alpha-C_1)\right]$

Taking moments about the top fibre of the flange,

$$ULTM = \tfrac{1}{2}F_4 B_2 D_T (D_1+D_2-\tfrac{1}{3}D_T)-\tfrac{1}{2}\sigma_{11}B_1 H_1^2-\tfrac{1}{2}(\sigma_{11}+2\sigma_{12})B_1(D_1-H_1)\left\{H_1+\frac{(\sigma_{11}+2\sigma_{12})(D_1-H_1)}{3(\sigma_{11}+\sigma_{12})}\right\}$$

$$-\sigma_{21}B_2H_2(D_1+\tfrac{1}{2}H_2)-\tfrac{1}{2}\sigma_{21}B_2(D_N-D_1-H_2)\tfrac{1}{3}(D_N+2D_1+2H_2) \qquad - 2.22$$

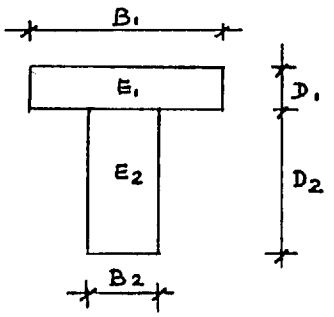
This reduces to $ULTM = C_2 F_4 \dfrac{B_2 D_2^2}{6}$ $\qquad - 2.22a$

where $C_2 = \frac{1}{\alpha^2}\Big[(1+\alpha-C_1)\left\{2(1+\alpha)+C_1\right\}$

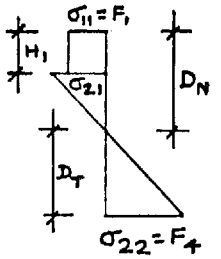
$$-\rho_2\left\{(\phi_2\alpha)^2+C_1(C_1+1+\phi_2\alpha)+2(\phi_2\alpha-1)\right\}$$

$$-3\beta\rho_1\phi_1^2-\beta\rho_1\frac{(1-\phi_1)}{(C_1-\phi_1)}\left\{\phi_1(3C_1-2-2\phi_1)+3C_1-2\right\}\Big]$$

2.4.5 Failure mode 5



Cross section



Stress diagram

$\sigma_{12} = F_1$

$\sigma_{21} = \dfrac{F_4(D_N - D_1)}{D_T}$

$H_1 = D_1$

Total compression $C = -\left[F_1 B_1 D_1 + \frac{1}{2} F_4 \dfrac{(D_N - D_1)}{D_T} B_2 (D_N - D_1)\right]$

Total tension $T = +\frac{1}{2} F_4 B_2 D_T$

For equilibrium $C + T = 0$ - 2.23

By substititing relevant values in (2.23) and rearranging,

$$D_N = C_1 D_1 \qquad - 2.24$$

where $C_1 = \dfrac{(1+\alpha)(\alpha - 2\rho_1\beta) + \alpha}{2(\alpha - \rho_1\beta)}$

Taking moments about the top fibre of the flange,

$$ULTM = \tfrac{1}{2} F_4 B_2 D_T (D_1 + D_2 - \tfrac{1}{3} D_T) - \tfrac{1}{2} F_1 B_1 D_1^2 - \tfrac{1}{2} \sigma_{21} B_2 (D_N - D_1) \left\{ D_1 + \tfrac{1}{3}(D_N - D_1) \right\}$$

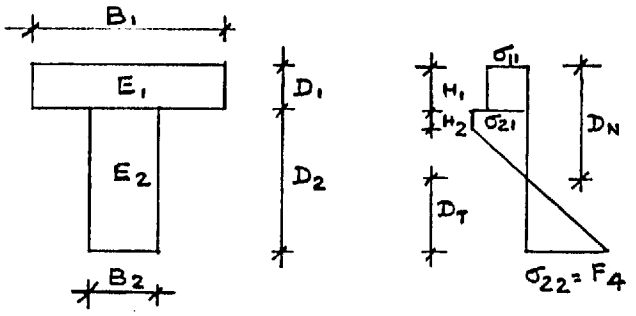
This reduces to

$$ULTM = C_2 F_4 \frac{B_2 D_2^2}{6} \qquad - 2.25$$

where $C_2 = \dfrac{1}{\alpha^2}\left[(1+\alpha - C_1)\left\{2(1+\alpha) + C_1\right\} - 3\rho_1\beta - \dfrac{(C_1 - 1)^2 (C_1 + 2)}{(1+\alpha - C_1)}\right]$

Note: It will be noticed that the values of E_1 and E_2 are not required for the derivation of the equations of this mode of failure.

2.4.6 Failure mode 6



Cross section Stress diagram

$H_1 = D_1$

$H_2 = D_N - D_1 - \rho_2 D_T$ - 2.26

(refer to mode 3)

Total compression $C = -\left[F_1 B_1 D_1 + F_3 B_2 H_2 + \frac{1}{2} F_3 B_2 (D_N - D_1 - H_2)\right]$

Total tension $T = +\frac{1}{2} F_4 B_2 D_T$

For equilibrium $C + T = 0$ - 2.27

By substituting relevant values in (2.27) and rearranging,

$$D_N = C_1 D_1 \qquad \text{- 2.28}$$

where $C_1 = \dfrac{(1+\alpha)(1+\rho_2^2) + 2\rho_2 - 2\rho_1\beta}{(1+\rho_2)^2}$

Substituting (2.28) into (2.26)

$$H_2 = \phi_2 D_2 \qquad \text{- 2.29}$$

where $\phi_2 = \dfrac{1 - \rho_2 - 2\rho_1 \frac{\beta}{\alpha}}{1+\rho_2}$

Note: It will be noticed that the values of E_1 & E_2 are not required for the derivation of the equations of this mode of failure.

Taking moments about the top fibre of the flange,

$$ULTM = \tfrac{1}{2}F_4B_2D_T(D_1+D_2-\tfrac{1}{3}D_T)-\tfrac{1}{2}F_1B_1D_1^2-F_3B_2H_2(D_1+\tfrac{1}{2}H_2)$$

$$- \tfrac{1}{2}F_3B_2(D_N-D_1-H_2)\tfrac{1}{3}(D_N+2D_1+2H_2)$$

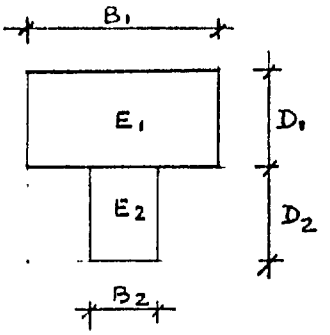
This reduces to

$$ULTM = C_2F_4\frac{B_2D_2^2}{6} \qquad - 2.30$$

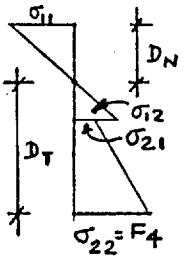
where $C_2 = \frac{1}{\alpha^2}\Big[(1+\alpha-C_1)\{2(1+\alpha)+C_1\}$

$$-\rho_2\{(\phi_2\alpha)^2+C_1(C_1+1+\phi_2\alpha)+2(\phi_2\alpha-1)\}-3\rho_1\beta\Big]$$

2.4.7 · Failure mode 7



Cross section



Stress diagram

$$H_1 = 0$$

$$\sigma_{11} = \frac{F_4 D_N E_1}{D_T E_2} = \frac{F_4 D_N}{D_T \gamma}$$

$$\sigma_{12} = \frac{\sigma_{11}(D_1 - D_N)}{D_N} = \frac{F_4(D_1 - D_N)}{D_T \gamma}$$

$$\sigma_{21} = \frac{F_4(D_1 - D_N)}{D_T}$$

$$D_N = \frac{\frac{1}{2}E_1 B_1 D_1^2 + E_2 B_2 D_2 (D_1 + \frac{1}{2}D_2)}{E_1 B_1 D_1 + E_2 B_2 D_2}$$

$$D_N = C_1 D_1 \qquad - 2.31$$

where $C_1 = \dfrac{\frac{\beta}{\gamma} + \alpha(2+\alpha)}{2(\frac{\beta}{\gamma} + \alpha)}$

Taking moments about the top fibre of the flange,

$$ULTM = \tfrac{1}{2}(F_4 + \sigma_{21}) B_2 D_2 \left\{ D_1 + \frac{(\sigma_{21} + 2F_4) D_2}{3(\sigma_{21} + F_4)} \right\} + \tfrac{1}{2}\sigma_{12} B_1 (D_1 - D_N) \tfrac{1}{3}(2D_1 + D_N) - \tfrac{1}{2}\sigma_{11} B_1 \frac{D_N^2}{3}$$

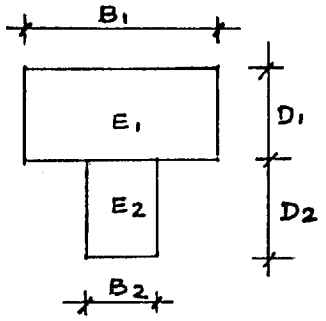
This reduces to

$$ULTM = C_2 F_4 \frac{B_2 D_2^2}{6} \qquad - 2.32$$

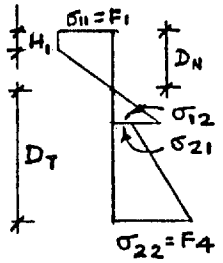
where

$$C_2 = \frac{1}{\alpha^2(1+\alpha-C_1)} \left[6\alpha(1+\alpha-C_1) - \alpha^2(3C_1 - 2\alpha) + \frac{\beta}{\gamma} \{(1-C_1)^2(2+C_1) - C_1^3\} \right]$$

2.4.8 Failure mode 8



Cross section



Stress diagram

$$\sigma_{12} = \frac{F_4(D_1-D_N)E_1}{D_T E_2} = \frac{F_4(D_1-D_N)}{D_T \gamma}$$

$$\sigma_{21} = \frac{F_4(D_1-D_N)}{D_T}$$

$$H_1 = D_N - \rho_1 D_T \gamma \qquad - 2.33$$

Total compression $C = -\left[F_1 B_1 H_1 + \frac{1}{2} F_1 B_1 (D_N - H_1)\right]$

Total tension $T = +\left[\frac{1}{2}(F_4 + \sigma_{21}) B_2 D_2 + \frac{1}{2} \sigma_{12} B_1 (D_1 - D_N)\right]$

For equilibrium $C + T = 0$ - 2.34

By substituting relevant values in (2.34) and rearranging,

$$AD_N^2 + BD_1 D_N + C_3 D_1^2 = 0 \qquad - 2.35$$

where $A = (\gamma \rho_1 + 1)^2$

$$B = -2\left[\gamma \rho_1 (1+\alpha)(\gamma \rho_1 + 1) + 1 + \frac{\alpha}{\beta/\gamma}\right]$$

$$C_3 = (\gamma \rho_1)^2 (1+\alpha)^2 + 1 + \frac{\alpha}{\beta/\gamma}(2+\alpha)$$

$$D_N = C_1 D_1 \qquad - 2.36$$

where $C_1 = \dfrac{-B - \sqrt{B^2 - 4AC_3}}{2A}$

Sustituting (2.36) into (2.33) $H_1 = \phi_1 D_1$ - 2.37

$$\text{where } \phi_1 = C_1(\gamma\rho_1+1)-\gamma\rho_1(1+\alpha)$$

Taking moments about the top fibre of the flange,

$$\text{ULTM} = \tfrac{1}{2}(F_4+\sigma_{21})B_2D_2\left\{ D_1+ \frac{(\sigma_{21}+2F_4)D_2}{3(\sigma_{21}+F_4)} \right\} +\tfrac{1}{2}\sigma_{12}B_1(D_1-D_N)\tfrac{1}{3}(2D_1+D_N)$$

$$- \tfrac{1}{2}\sigma_{11}B_1H_1^2- \tfrac{1}{2}\sigma_{11}B_1(D_N-H_1)\tfrac{1}{3}(2H_1+D_N) \quad \text{- 2.38}$$

This reduces to

$$\text{ULTM} = C_2F_4\,\frac{B_2D_2^2}{6} \quad \text{- 2.38 a}$$

$$\text{where } C_2 = \frac{1}{\alpha^2(1+\alpha-C_1)}\left[6\alpha(1+\alpha-C_1)-\alpha^2(3C_1-2\alpha)\right.$$

$$\left.+\frac{\beta}{\gamma}\left\{(1-C_1)^2(2+C_1)-\gamma\rho_1(C_1^2+\phi_1C_1+\phi_1^2)(1+\alpha-C_1)\right\}\right]$$

2.4.9 Essential conditions for various modes of failure

Mode	Conditions		
	(1) Based on the Position of N.A	(2) Based on the depth of yield penetration in flange	(3) Based on the depth of yield penetration in rib
1	$\alpha^2 > \frac{\beta}{\gamma}$	$c_1 \geq \frac{\gamma\rho_1(1+\alpha)}{\gamma\rho_1+1}$	$c_1 \geq \frac{\rho_2(1+\alpha)+1}{\rho_2+1}$
2	$c_1 > 1$	$\frac{\gamma\rho_1(1+\alpha)}{\gamma\rho_1+1} < c_1 < \frac{\gamma\rho_1(1+\alpha)+1}{\gamma\rho_1+1}$	$c_1 \geq \frac{\rho_2(1+\alpha)+1}{\rho_2+1}$
3	$c_1 > 1$	$c_1 \geq \frac{\gamma\rho_1(1+\alpha)}{\gamma\rho_1+1}$	$c_1 > \frac{\rho_2(1+\alpha)+1}{\rho_2+1}$
4	$c_1 > 1$	$\frac{\gamma\rho_1(1+\alpha)}{(\gamma\rho_1+1)} < c_1 < \frac{\gamma\rho_1(1+\alpha)+1}{\gamma\rho_1+1}$	$c_1 > \frac{\rho_2(1+\alpha)+1}{\rho_2+1}$
5	$\frac{\alpha}{\beta} > 2\rho_1$	$c_1 \leq \frac{\gamma\rho_1(1+\alpha)}{\gamma\rho_1+1}$	$c_1 \geq \frac{\rho_2(1+\alpha)+1}{\rho_2+1}$
6	$\frac{\alpha}{\beta} > \frac{2\rho_1}{1+\rho_2^2}$	$c_1 \leq \frac{\gamma\rho_1(1+\alpha)}{\gamma\rho_1+1}$	$\frac{\alpha}{\beta} > \frac{2\rho_1}{1-\rho_2}$
7	$\alpha^2 \geq \frac{\beta}{\gamma}$	$c_1 \geq \frac{\gamma\rho_1(1+\alpha)}{\gamma\rho_1+1}$	—
8	$c_1 \geq 1$	$c_1 > \frac{\gamma\rho_1(1+\alpha)}{\gamma\rho_1+1}$	—

2.5 Analysis of T sections using Computer

When the geometrical and mechanical properties of the flange and the rib are known, a T section can be analysed to find the mode of failure and ultimate resisting moment. Two procedures can be adopted.

2.5.1 Procedure 1

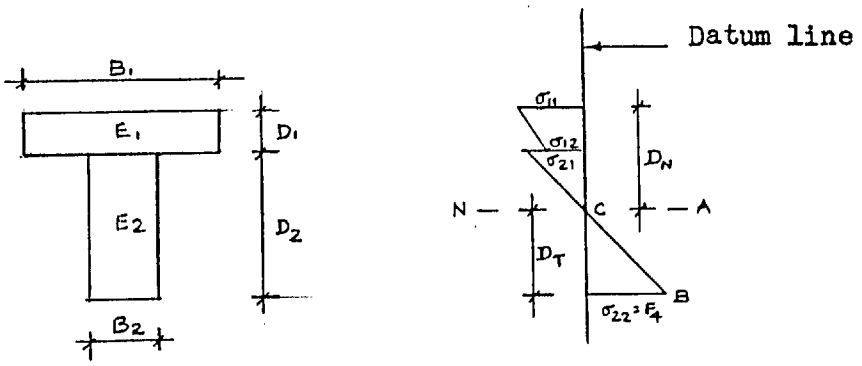
'Direct search method' is the basis of this procedure. Starting from mode 1, essential conditions for each mode can be tested. When all essential conditions for a particular mode are satisfied, detailed analysis of that mode can be made. A flow chart for this procedure is given in the chapter for computer programs (see chapter 7).

The disadvantage of direct search method is that almost all modes have to be tested to arrive at the correct mode. But this is not very serious in the case of a T section as there are only eight modes to be considered and the equations involved are small in numbers and not higher than second degree.

2.5.2 Procedure 2

This is an iteration procedure suitable for the computer.

Stage 1 Modes 1 to 6 are considered in this stage. The neutral axis is always within the rib.



Cross section Stress diagram

Fig. 2.3

Assume an arbitrary depth of neutral axis. Let C be the position of N.A on the datum line of the stress diagram.

Mark the magnitude of ultimate tensile stress of rib (F_4) on the stress diagram as shown. Join the points B & C and extend it to meet the interface. Now workout the stresses at various critical points.

$$\sigma_{11} = \frac{F_4 D_N E_1}{D_T E_2} \qquad - 2.39$$

If $\sigma_{11} \not> F_1$ $\qquad H_1 = 0.0$

If $\sigma_{11} > F_1$ assume $F = \sigma_{11}$ (as calculated above by equation 2.39)

Let H_1 be the depth at which stress is F_1

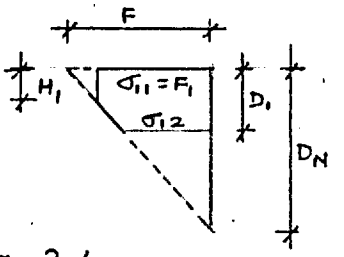


Fig. 2.4

$$\frac{D_N - H_1}{D_N} = \frac{F_1}{F}$$

$$\therefore \quad H_1 = D_N\left(1 - \frac{F_1}{F}\right) \qquad - 2.40$$

Maximum possible value of $\sigma_{11} = F_1$

Maximum possible value of $H_1 = D_1$

Refer to fig. 2.3

$$\sigma_{12} = \frac{F_4 (D_N - D_1) E_1}{D_T \quad E_2} \qquad - 2.41$$

If $\sigma_{12} > F_1$ assume $\sigma_{12} = F_1$

$$\sigma_{21} = \frac{F_4 (D_N - D_1)}{D_T} \qquad - 2.42$$

If $\sigma_{21} \not> F_3$ $\quad H_2 = 0.0$

If $\sigma_{21} > F_3$ assume $F_R = \sigma_{21}$ (as calculated by equation 2.42)

Refer to fig. 2.5

Let H_2 be the depth at which stress is F_3

$$H_2 = (D_N - D_1)\left(1 - \frac{F_3}{F_R}\right)$$

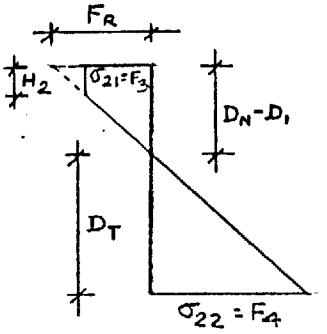
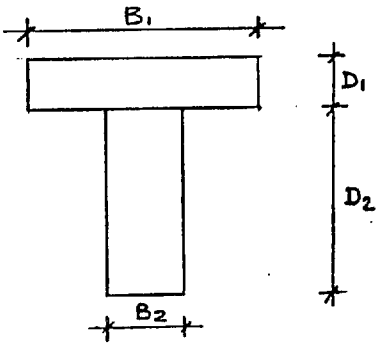


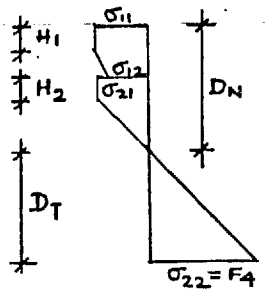
Fig. 2.5

Maximum possible value of $\sigma_{21} = F_3$

Most general form of the stress diagram for the whole section is as shown in fig. 2.6



Cross section



Stress diagram (general form)

Fig. 2.6

Total compression $C = -\left[\sigma_{11}B_1H_1 + \frac{1}{2}(\sigma_{11}+\sigma_{12})B_1(D_1-H_1) + \sigma_{21}B_2H_2 + \frac{1}{2}\sigma_{21}B_2(D_N-D_1-H_2)\right]$

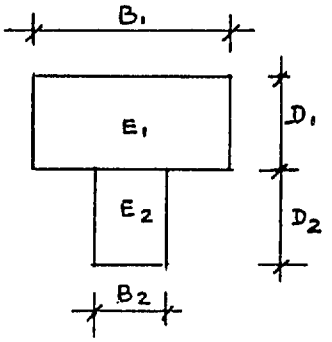
Total tension $T = + \frac{1}{2}F_4B_2D_T$

For equilibrium $C + T = 0$

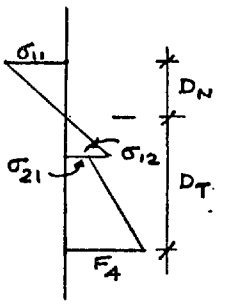
If the assumed value of D_N is not correct, the equilibrium condition will not be satisfied and the whole process has to be repeated with a new value of D_N.

An iteration procedure is adopted to find the value of D_N, so that $C + T \not> \epsilon$ where ϵ is an acceptable small error. The iteration procedure is given in Appendix 1.

Stage 2. Modes 7 & 8 are considered here. The neutral axis is within the flange or at the interface.



Cross section



Stress diagram

Fig. 2.7

Assume an arbitrary depth for N.A. which is within the flange as shown in fig. 2.7. Knowing the magnitude of F_4, the stresses σ_{11}, σ_{12} and σ_{21} can be calculated.

$$\sigma_{11} = \frac{F_4 D_N E_1}{D_T E_2} \qquad - 2.43$$

If $\sigma_{11} \not> F_1$ $\qquad H_1 = 0.0$

If $\sigma_{11} > F_1$ assume $F = \sigma_{11}$ (as calculated by equation 2.43)

Let H_1 be the depth at which stress is F_1

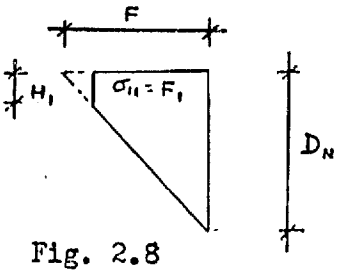


Fig. 2.8

$$\frac{D_N - H_1}{D_N} = \frac{F_1}{F}$$

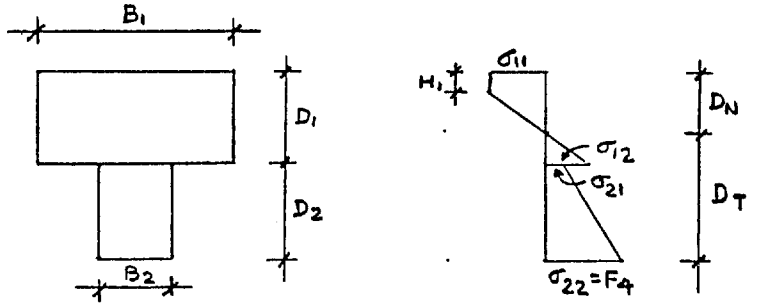
$$\therefore \quad H_1 = D_N\left(1 - \frac{F_1}{F}\right)$$

Maximum possible value of $\sigma_{11} = F_1$

$$\sigma_{12} = \frac{F_4(D_1 - D_N)E_1}{D_T E_2} \qquad - 2.44$$

$$\sigma_{21} = \frac{F_4(D_1 - D_N)}{D_T} \qquad - 2.45$$

The most general form of the stress diagram for the whole section is as shown in fig. 2.9



Cross section Stress diagram

Fig. 2.9

Total compression $C = -\left[\sigma_{11}B_1H_1 + \frac{1}{2}\sigma_{11}B_1(D_N-H_1)\right]$

Total tension $T = +\frac{1}{2}\sigma_{12}B_1(D_1-D_N)+\frac{1}{2}(F_4+\sigma_{21})B_2D_2$

For equilibrium $C + T = 0$

The equilibrium condition will not be satisfied if the assumed value of D_N is incorrect in which case the whole process has to be repeated with a new value of D_N. An iteration procedure as shown in Appendix 1 has been adopted to find the value of D_N, so that $C + T \not> \epsilon$ where ϵ is an acceptable error.

When the correct depth of neutral axis is located, the ultimate resisting moment of the section is calculated using the following equations.

a) When the N.A is within the rib

Equation 2.22 (see failure mode 4)

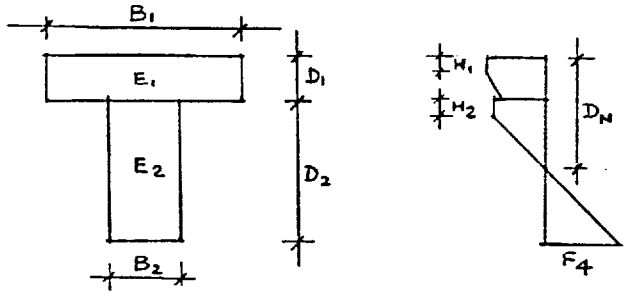
b) When the N.A is within the flange or at the interface

Equation 2.38 (see failure mode 8)

2.5.3 Examples: Typical examples of failure modes of T sections are given in Table 2.

TABLE 2

Typical examples of failure modes of T sections with non-layered flange.



The following properties are common for all cases.

Breadth of flange B_1 = 300.0 mm

Breadth of rib B_2 = 50.0 mm

Ult. tensile stress of rib, F_4 = 40.0 N/mm^2

Serial No.	D_1 (mm)	D_2 (mm)	E_1 (N/mm^2)	E_2 (N/mm^2)	F_1 (N/mm^2)	F_3 (N/mm^2)	D_N (mm)	H_1 (mm)	H_2 (mm)	Ult.RM (kN.m)	Failure Mode
1	10	100	8000	12000	20	21	44.29	0.00	0.00	5.177	1
2	10	100	8000	12000	16	22	44.73	5.57	0.00	5.131	2
3	10	100	8000	12000	20	19	44.32	0.00	3.12	5.175	3
4	10	100	8000	12000	16	20	44.75	5.60	2.12	5.130	4
5	10	100	8000	12000	14	24	46.71	10.00	0.00	5.117	5
6	10	100	8000	12000	14	20	46.89	10.00	5.33	4.929	6
7	20	40	12000	6000	26	20	14.29	0.00	0.00	1.933	7
8	20	40	12000	6000	24	20	14.29	0.58	0.00	1.932	8
9	20	40	8000	12000	20	20	20.00	0.00	0.00	1.600	7
10	20	40	8100	12000	12	20	20.00	2.22	0.00	1.597	8

Notes: 1. In serial numbers 1 to 6 the N.A. is within the rib.

2. In serial numbers 7 & 8 the N.A. is within the flange.

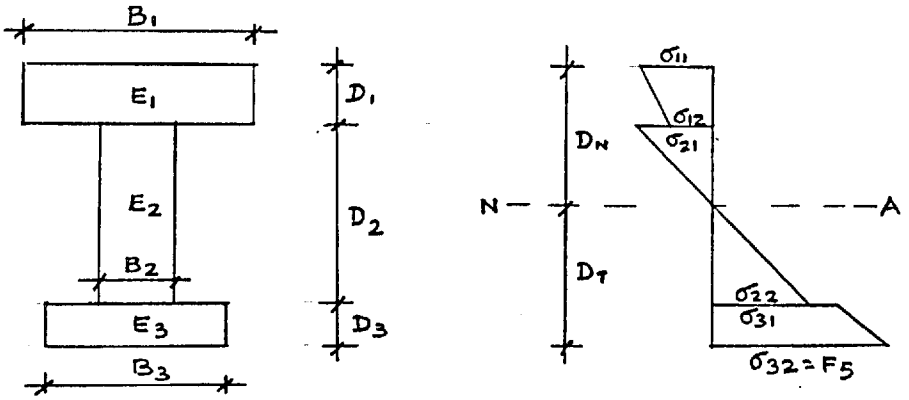
3. In serial numbers 9 & 10 the N.A. is on the interface.

CHAPTER 3

ANALYSIS OF I SECTION WITH NON-LAYERED FLANGES

3.1 Assumptions: Assumptions are same as those given in sections 2.1 and 2.2 for the T section.

3.2 Analysis: Iteration procedure is adopted for the analysis of the I section.



Cross section Fig. 3.1 Stress diagram

Mode 1 to mode 6 are only considered.

Neutral axis is always within the rib.

Assume an arbitrary depth of neutral axis. The stresses at vital points are worked out as follows.

$$\sigma_{11} = \frac{F_5 D_N E_1}{D_T E_3} \qquad - 3.1$$

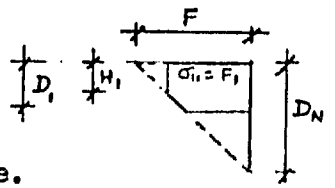


Fig.3.2

If $\sigma_{11} \not> F_1$ $\quad H_1 = 0.0$

If $\sigma_{11} > F_1$ $\quad$ assume $F = \sigma_{11}$ as calculated above.

Let H_1 be the depth at which stress is F_1

$$H_1 = D_N\left(1 - \frac{F_1}{F}\right) \qquad - 3.2$$

Maximum possible value of $\sigma_{11} = F_1$

Maximum possible value of $H_1 = D_1$

$$\sigma_{12} = \frac{F_5(D_N-D_1)E_1}{D_T E_3} \qquad - 3.3$$

If $\sigma_{12} > F_1$ assume $\sigma_{12} = F_1$

Refer to fig. 3.1

$$\sigma_{21} = \frac{F_5(D_N-D_1)E_2}{D_T E_3} \qquad - 3.4$$

If $\sigma_{21} \not> F_3 \quad H_2 = 0.0$

If $\sigma_{21} > F_3$ assume $F_R = \sigma_{21}$ as per (3.4)

$$H_2 = (D_N-D_1)(1-\frac{F_3}{F_R}) \qquad - 3.5$$

Also

$$H_2 < D_N-D_1$$

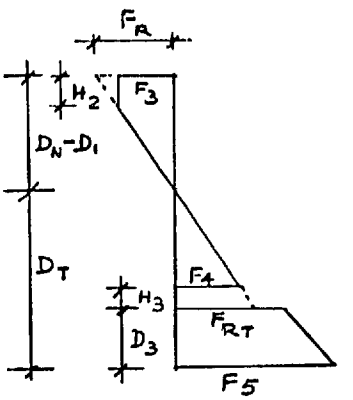


Fig. 3.3

Maximum possible value of $\sigma_{21} = F_3$

$$\sigma_{22} = \frac{F_5(D_T-D_3)E_2}{D_T E_3} \qquad - 3.6$$

If $\sigma_{22} \not> F_4 \qquad H_3 = 0.0$

If $\sigma_{22} > F_4$ assume $F_{RT} = \sigma_{22}$ as per (3.6)

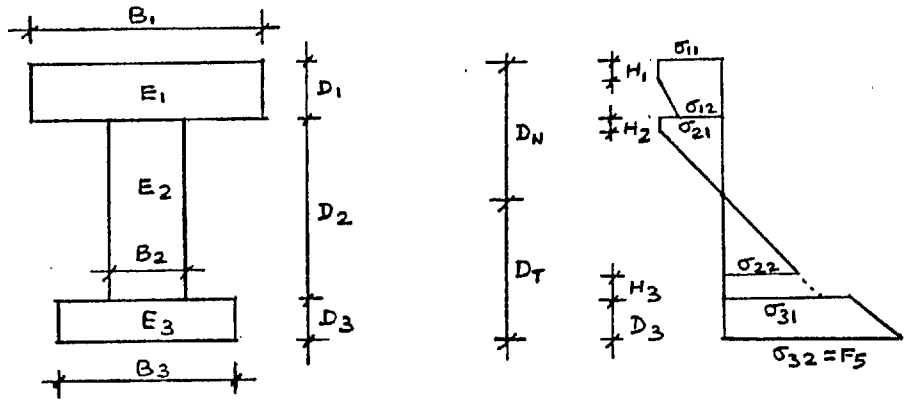
$$H_3 = (D_T-D_3)\ (1-\frac{F_4}{F_{RT}}) \qquad - 3.7$$

$$H_3 < D_T-D_3$$

Maximum possible value of $\sigma_{22} = F_4$

$$\sigma_{31} = \frac{F_5(D_T-D_3)}{D_T} \qquad - 3.8$$

Most general form of the stress diagram is shown below.



Cross section Stress diagram

Fig.3.4

From the general stress diagram,

Total compression $C = -\left[\sigma_{11}B_1H_1+\frac{1}{2}(\sigma_{11}+\sigma_{12})B_1(D_1-H_1)+\sigma_{21}B_2H_2+\frac{1}{2}\sigma_{21}B_2(D_N-D_1-H_2)\right]$

Total tension $T = +\left[\frac{1}{2}(F_5+\sigma_{31})B_3D_3+\frac{1}{2}B_2(D_T-D_3-H_3)\sigma_{22}\right]$

For equilibrium $C + T = 0$

The iteration procedure as described in appendix 1 is adopted to find the value of D_N so that $C+T \not> \varepsilon$, where ε is an acceptable small error.

Now the values of D_N, H_1, H_2, H_3 and stress at all important points are known.

Using the general stress diagram and taking the moments about the top fibre of the flange,

$$\begin{aligned}
ULTM = {} & \sigma_{31}B_3D_3(D_1+D_2+\tfrac{1}{2}D_3)+\tfrac{1}{2}(F_5-\sigma_{31})B_3D_3(D_1+D_2+\tfrac{2}{3}D_3) \\
& + \frac{\sigma_{22}}{2}B_2(D_T-D_3-H_3)\left\{D_N+\tfrac{2}{3}(D_T-D_3-H_3)\right\} \\
& - \tfrac{1}{2}\sigma_{11}B_1H_1^2-\sigma_{12}B_1(D_1-H_1)\left\{H_1+\tfrac{1}{2}(D_1-H_1)\right\} \\
& - \tfrac{1}{2}(\sigma_{11}-\sigma_{12})B_1(D_1-H_1)\left\{H_1+\tfrac{1}{3}(D_1-H_1)\right\}-\sigma_{21}B_2H_2(D_1+\tfrac{1}{2}H_2) \\
& - \tfrac{1}{2}\sigma_{21}B_2(D_N-D_1-H_2)\left\{D_1+H_2+\tfrac{1}{3}(D_N-D_1-H_2)\right\}
\end{aligned}$$

Failure modes

If $H_1 = 0$ and $H_2 = 0$ .. Mode 1

If $H_1 > 0$ and $H_2 = 0$, but $H_1 \neq D_1$ .. Mode 2

If $H_1 = 0$ and $H_2 > 0$ .. Mode 3

If $H_1 > 0$ and $H_2 > 0$, but $H_1 \neq D_1$ .. Mode 4

If $H_1 = D_1$ and $H_2 = 0$ .. Mode 5

If $H_1 = D_1$ and $H_2 > 0$ .. Mode 6

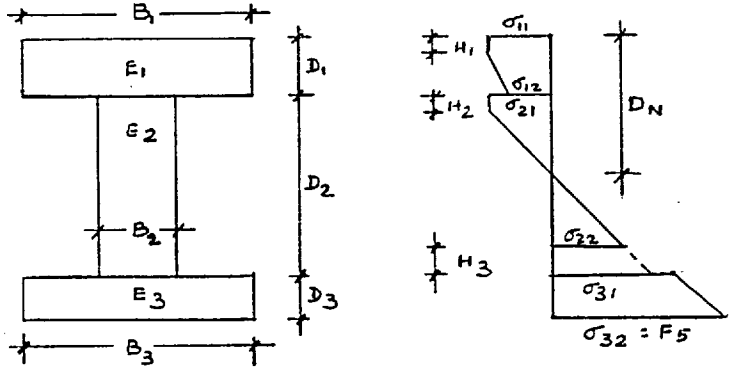
In the case of I sections there is a possibility at the ultimate load stage that a weak bottom flange breaks completely and offers no additional resistance; whereas the rib attains the ultimate tensile strength and provides more resisting moment than the I section. Computer program takes this into account and prints out the values associated with the higher resisting moment.

3.2.1 Examples

Typical examples of failure modes of I sections with non-layered flanges are given in Table 3.

TABLE 3

Typical examples of failure modes of I sections with non-layered flanges



The following properties are common for all cases.

B_1 = 300.0 mm
B_2 = 50.0 mm
B_3 = 300.0 mm
D_1 = 10.0 mm
D_2 = 100.0 mm
D_3 = 8.0 mm

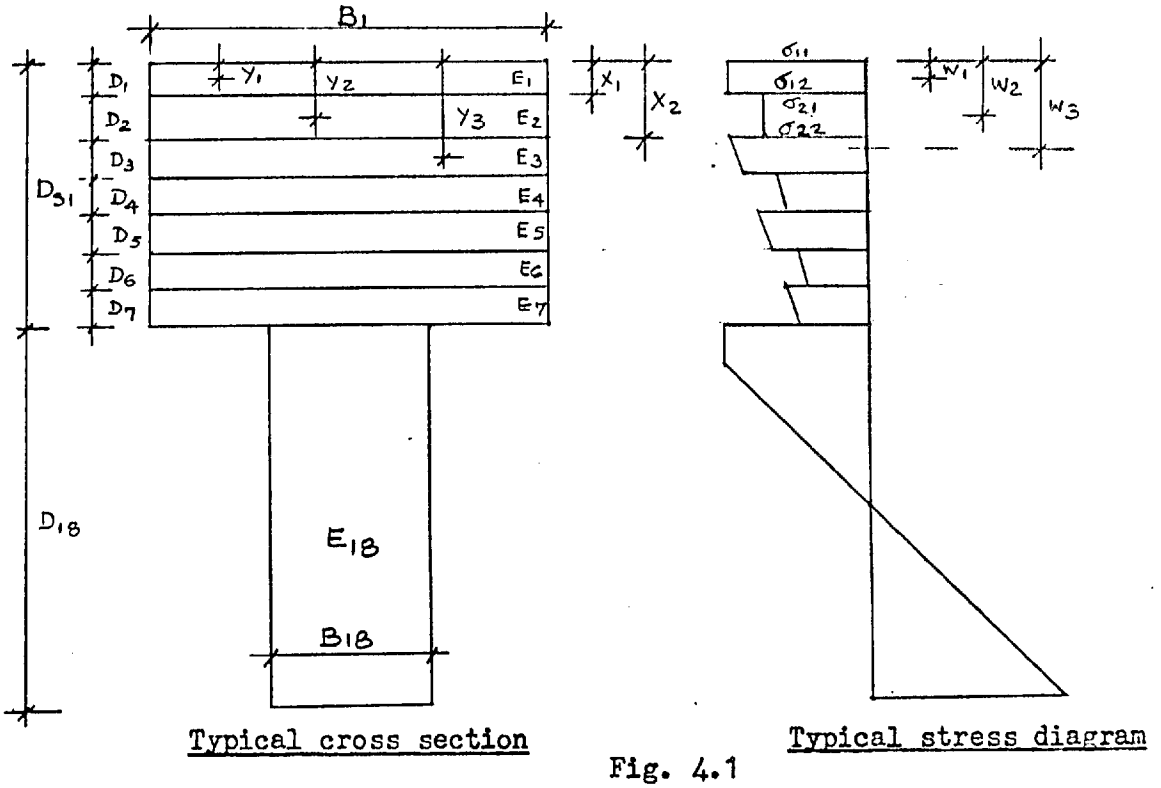
E_1 = 8000 N/mm^2
E_2 = 12000 N/mm^2
E_3 = 10000 N/mm^2

Serial No.	F_1 (N/mm^2)	F_3 (N/mm^2)	F_4 (N/mm^2)	F_5 (N/mm^2)	D_N (mm)	H_1 (mm)	H_2 (mm)	H_3 (mm)	Ult.RM (kN.m)	Failure Mode
1	20	22	22	20	59.78	0.00	0.00	0.00	6.627	1
2	15	22	22	20	60.17	5.95	0.00	0.00	6.587	2
3	21	19	22	20	59.82	0.00	3.75	0.00	6.624	3
4	15	20	22	20	60.19	5.99	2.01	0.00	6.586	4
5	10	27	25	20	66.17	10.00	0.00	0.00	5.977	5
6	10	19	25	20	67.15	10.00	17.54	0.00	5.861	6
7	15	19	18	20	57.91	1.57	0.33	7.02	6.096	4
8	30	30	40	5	44.29	0.00	0.00	0.00	5.177	1

Note: In the case of serial number 8, bottom flange will not provide any strength at the ultimate load.

CHAPTER 4

ANALYSIS OF T SECTION WITH LAYERED FLANGE



Typical cross section

Typical stress diagram

Fig. 4.1

4.1 Assumptions.

All assumptions, except assumption No. 2, listed under section 2.2 in Chapter 2 are valid in the case of T section with layered flange.

4.2 Additional assumptions.

In addition to the above, the following assumptions are also made for the layered flanges considered in this thesis.

1. $E_1 = E_3 = E_5 = E_i$ where i is an odd number $\neq N_1$

   $E_2 = E_4 = E_6 = E_j$ where j is an even number $\neq N_1$

2. Yield penetration in the flange reaches the full depth of a layer. This is a convenient approximation without much loss of accuracy as the thickness of the layers in a plywood flange is small when compared to the overall depth of the panel section.

4.3 Additional notation

The following additional notation is adopted in the case of the T sections with layered flanges. See fig. 4.1

$$x_1 = 0 + D_1 \qquad y_1 = 0 + \tfrac{1}{2} D_1 \qquad w_1 = 0 + \tfrac{1}{3} D_1 \frac{(\sigma_{11} + 2\,\sigma_{12})}{(\sigma_{11} + \sigma_{12})}$$

$$x_2 = x_1 + D_2 \qquad y_2 = x_1 + \tfrac{1}{2} D_2$$

$$w_2 = x_1 + \tfrac{1}{3} D_2 \frac{(\sigma_{21} + 2\,\sigma_{22})}{(\sigma_{21} + \sigma_{22})}$$

$$x_3 = x_2 + D_3 \qquad y_3 = x_2 + \tfrac{1}{2} D_3$$

------ ------- -------------

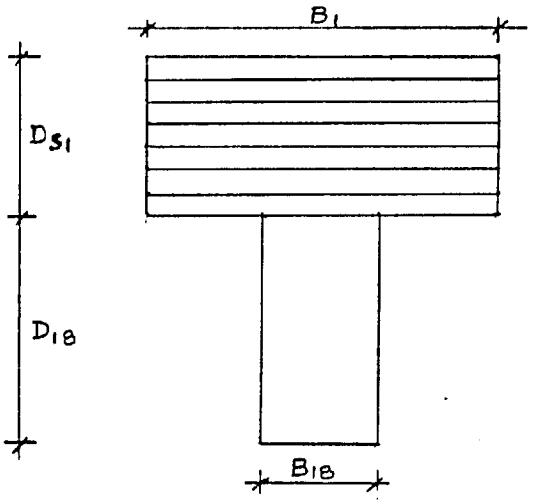
$$x_i = x_{i-1} + D_i \qquad y_j = x_{j-1} + \tfrac{1}{2} D_j \qquad w_k = x_{k-1} + \tfrac{1}{3} D_i \frac{(\sigma_{k1} + 2\,\sigma_{k2})}{(\sigma_{k1} + \sigma_{k2})}$$

------ ------- -------------

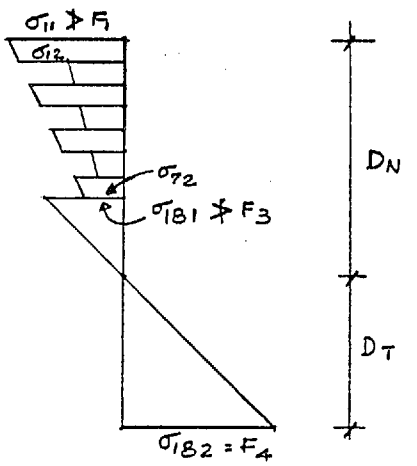
$$x_7 = x_6 + D_7 \qquad y_7 = x_6 + \tfrac{1}{2} D_7 \qquad w_7 = x_6 + \tfrac{1}{3} D_7 \frac{(\sigma_{71} + 2\,\sigma_{72})}{(\sigma_{71} + \sigma_{72})}$$

4.4 Derivation of governing equations

4.4.1 Failure mode 1



Cross section



Stress diagram

Note: For clarity seven layers are only shown in the flange. The stress diagram shows that the first layer is stronger than the second layer. But the analysis is also valid when first layer is weaker than the second layer. This condition is satisfied in all modes.

$$\sigma_{11} = \frac{F_4 D_N E_1}{D_T E_{18}}$$

$$\sigma_{11} = A_1 D_N E_1 \qquad \text{where} \quad A_1 = \frac{F_4}{D_T E_{18}}$$

$$\sigma_{12} = A_1 (D_N - x_1)\, E_1$$

$$\sigma_{21} = A_1 (D_N - x_1)\, E_2$$

$$\sigma_{22} = A_1 (D_N - x_2)\, E_2$$

- - - - - - - - - - - -

$$\sigma_{i1} = A_1 (D_N - x_{i-1})\, E_i$$

$$\sigma_{i2} = A_1 (D_N - x_i)\, E_i$$

$$\sigma_{18i} = \frac{F_4(D_N - D_{S1})}{D_T}$$

$$D_N = \frac{B_1 \sum_{i=1}^{N_1} E_i D_i y_i + B_{18} E_{18} D_{18} (D_{S1} + \frac{1}{2} D_{18})}{B_1 \sum_{i=1}^{N_1} E_i D_i + B_{18} E_{18} D_{18}} \qquad - 4.1$$

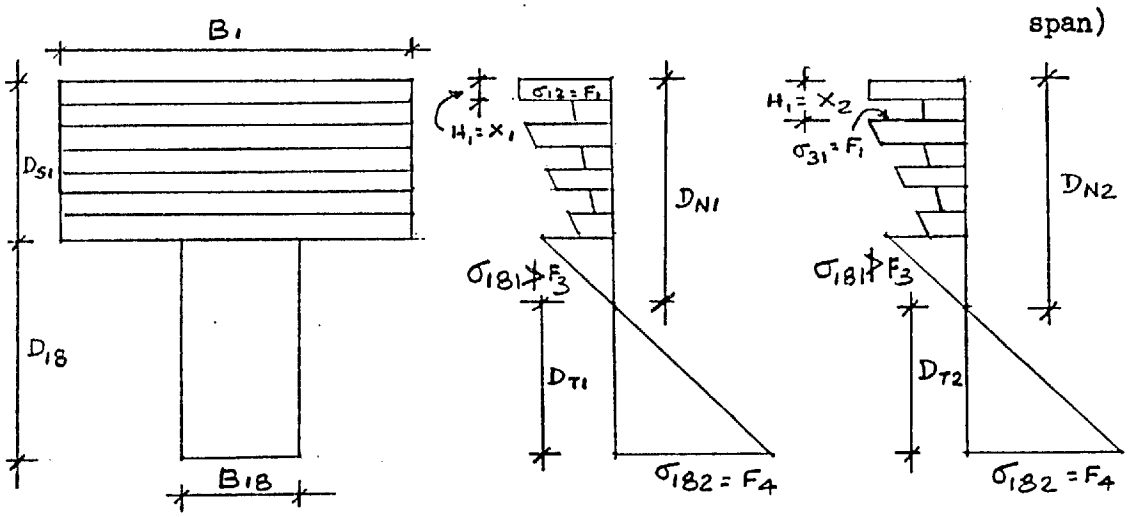
$$\text{ULTM} = \tfrac{1}{2} F_4 B_{18} D_T (D_{S1} + D_{18} - \tfrac{1}{3} D_T) - \tfrac{1}{2} B_1 \sum_{i=1}^{N_1} D_i (\sigma_{i1} + \sigma_{i2}) w_i$$

$$- \tfrac{1}{2} \sigma_{18i} B_{18} (D_N - D_{S1}) \frac{(2 D_{S1} + D_N)}{3} \qquad - 4.2$$

4.4.2 Failure mode 2

Incremental analysis: The routine is to check the equilibrium condition by assuming the increment of yield penetration layer by layer, considering strong layers only.

Case 1 $F_1 > F_2$ (Typical case with plywood when face grain parallel to span)



i = 1 $H_1 = x_1$ i = 2 $H_1 = x_2$

When i = 1 assume bottom edge of layer 1 is just plastic.

$$F_1 = \sigma_{12} = \frac{\sigma_{182}(D_N - x_1)\, E_1}{(D_{S1} + D_{18} - D_{N1})E_{18}}$$

$$\text{This reduces to } D_{N1} = \frac{(D_{S1} + D_{18})F_1 E_{18} + x_1 F_4 E_1}{F_1 E_{18} + F_4 E_1}$$

When i = 2 assume top edge of layer 3 is just plastic.

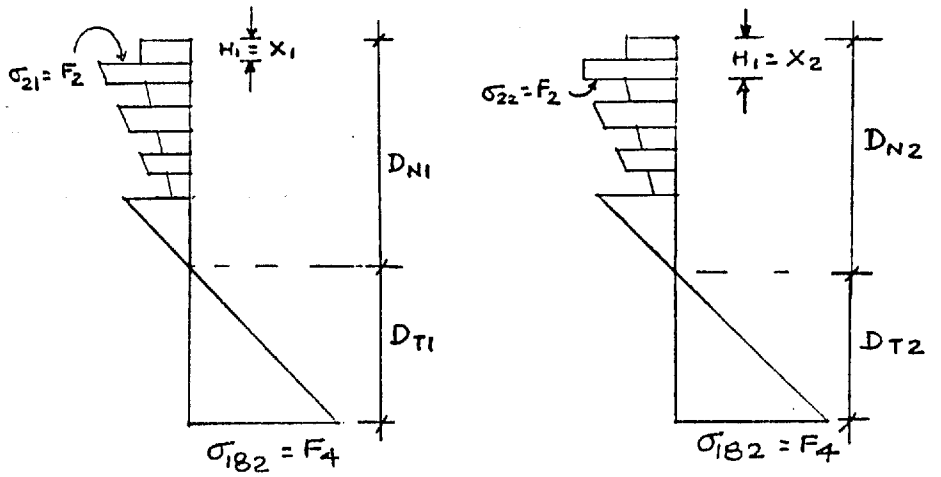
$$F_1 = \sigma_{31} = \frac{\sigma_{182}(D_N - x_2)\, E_1}{(D_{S1} + D_{18} - D_{N2})E_{18}}$$

$$\text{This reduces to } D_{N2} = \frac{(D_{S1} + D_{18})\, F_1\, E_{18} + x_2\, F_4\, E_1}{F_1\, E_{18} + F_4\, E_1}$$

General equation for D_N is as follows.

$$D_{Ni} = \frac{(D_{S1} + D_{18})F_1\, E_{18} + x_i\, F_4\, E_1}{F_1\, E_{18} + F_4\, E_1} \qquad - 4.3$$

Case. 2 $F_2 > F_1$ (Typical case with plywood when face grain perpendicular to span)



i = 1 $\quad H_1 = x_1$ $\qquad$ i = 2 $\quad H_1 = x_2$

When i = 1 Assume top edge of layer 2 is just plastic.

$$F_2 = \sigma_{21} = \frac{\sigma_{182}(D_N - x_1)E_2}{(D_{S1} + D_{18} - D_{N1})\,E_{18}}$$

$$\therefore \quad D_{N1} = \frac{(D_{S1} + D_{18})F_2\,E_{18} + x_1\,F_4\,E_2}{F_2\,E_{18} + F_4\,E_2}$$

When i = 2 Assume bottom edge of layer 2 is just plastic.

$$F_2 = \sigma_{22} = \frac{\sigma_{182}(D_N - x_2)\,E_2}{(D_{S1} + D_{18} - D_{N2})\,E_{18}}$$

$$\therefore \quad D_{N2} = \frac{(D_{S1} + D_{18})\,F_2\,E_{18} + x_2\,F_4\,E_2}{F_2\,E_{18} + F_4\,E_2}$$

General equation for D_N is as follows.

$$D_{Ni} = \frac{(D_{S1} + D_{18})\,F_2\,E_{18} + x_i\,F_4\,E_2}{F_2\,E_{18} + F_4\,E_2} \qquad - 4.4$$

Most general form of equations (4.3) and (4.4) will be

$$D_{Ni} = \frac{(D_{S1} + D_{18})\, F_j\, E_{18} + x_i\, F_4\, E_j}{F_j\, E_{18} + F_4\, E_j} \qquad \text{when } F_1 > F_2 \quad j = 1$$

$$F_2 > F_1 \quad j = 2$$

General equation for the stresses at the vital points of the layers can be written as follows.

For a particular value of i; i takes a value from 1 to N_1

$$\sigma_{k1} = A_1\, (D_{Ni} - x_{k-1})\, E_k$$

$$\sigma_{k2} = A_1\, (D_{Ni} - x_k)\, E_k \qquad \text{where } k \text{ takes the values 1 to } N_1$$

If k is odd and $\sigma_{k1} > F_1$ assume $\sigma_{k1} = \sigma_{k2} = F_1$

If k is even and $\sigma_{k1} > F_2$ assume $\sigma_{k1} = \sigma_{k2} = F_2$

$$A_1 = \frac{F_4}{D_{Ti}\, E_{18}} \qquad \text{and } x_0 = 0$$

General equation of total compression for a particular value of i is

$$C = -\left[\tfrac{1}{2} B_1 \sum_{k=1}^{N_1} (\sigma_{k1} + \sigma_{k2})\, D_k\right] - \tfrac{1}{2}\, \sigma_{18}\, B_{18} (D_{Ni} - D_{S1})$$

Total tension $T = + \tfrac{1}{2} F_4\, B_{18}\, D_{Ti}$

For equilibrium $C + T = 0$ - 4.5

As this value of i may not be correct,

assume $(C + T)_i =$ Error

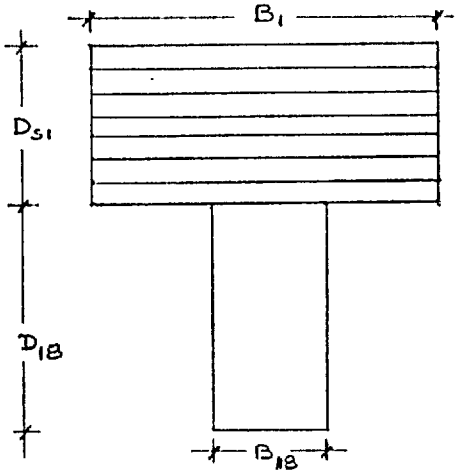
Now take the next value of i and repeat the whole process and find the error.

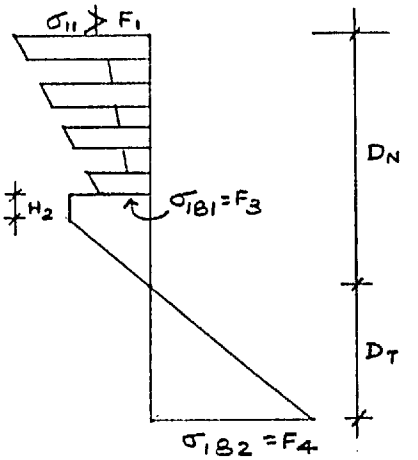
The value of i which gives the least error is adopted to calculate the final stresses and the Ultimate resisting moment. w_1, w_2 etc., take the same form as that for Mode 1. $D_N = D_{Ni}$

$$ULTM = \tfrac{1}{2} F_4\, B_{18}\, D_T (D_{S1} + D_{18} - \tfrac{1}{3} D_T) - \tfrac{1}{2} B_1 \sum_{k=1}^{N_1} D_k (\sigma_{k1} + \sigma_{k2})\, w_k$$

$$- \tfrac{1}{2}\, \sigma_{18}\, B_{18} (D_N - D_{S1})\, \tfrac{1}{3} (2\, D_{S1} + D_N)$$

4.4.3 Failure mode 3





$$\sigma_{11} = \frac{F_4 D_N E_1}{D_T E_{18}} = A_1 D_N E_1 \qquad \text{where } A_1 = \frac{F_4}{D_T E_{18}}$$

Refer to Mode 1. σ_{12}, σ_{21}, σ_{22} etc; can be written in the following general form.

$$\sigma_{i1} = A_1(D_N - x_{i-1})\, E_i$$

$$\sigma_{i2} = A_1(D_N - x_i)\, E_i$$

$$H_2 = D_N - D_{S1} - \frac{\sigma_{181}}{\sigma_{182}} D_T \qquad - 4.6$$

w_1, w_2 etc., take the same form as that as mode 1.

$$\text{Total compression } C = -\left[\left\{\tfrac{1}{2} B_1 \sum_{i=1}^{N_1} (\sigma_{i1}+\sigma_{i2}) D_i\right\} + \sigma_{181} H_2 B_{18} + \tfrac{1}{2}\sigma_{181} B_{18}(D_N - D_{S1} - H_2)\right]$$

$$\text{Total tension } T = + \tfrac{1}{2}\, \sigma_{182} B_{18} D_T$$

$$\text{For equilibrium } C + T = 0 \qquad - 4.7$$

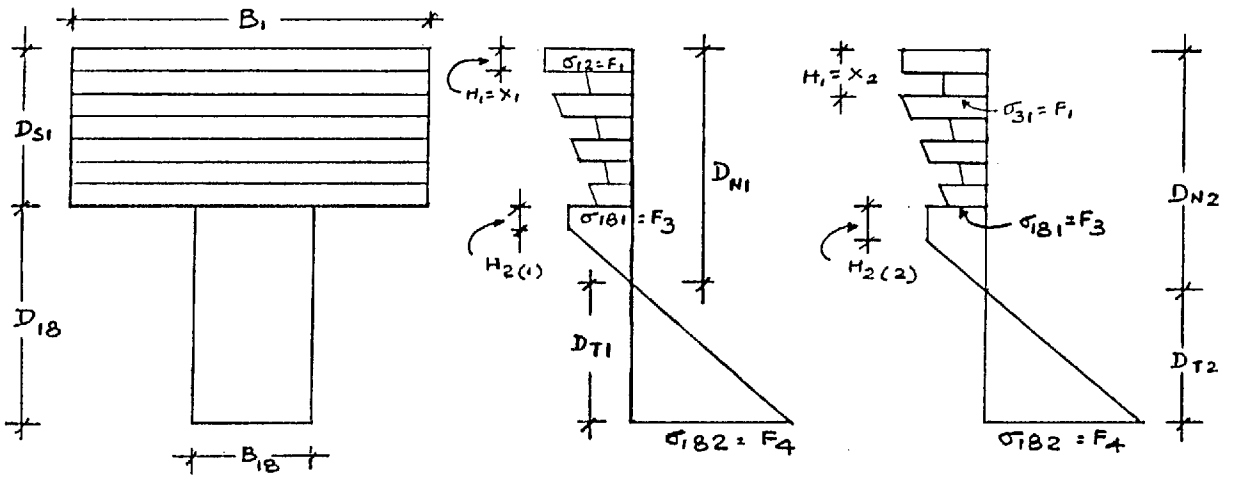
Using the equations (4.6) and (4.7) and assuming various values for D_N, the correct values of D_N and H_2 are found by iteration process.

$$\text{ULTM} = \tfrac{1}{2} F_4 B_{18} D_T (D_{S1} + D_{18} - \tfrac{1}{3} D_T) - \tfrac{1}{2} B_1 \sum_{i=1}^{N_1} D_i (\sigma_{i1} + \sigma_{i2}) w_i$$

$$- \sigma_{181} B_{18} H_2 (D_{S1} + \tfrac{1}{2} H_2) - \frac{\sigma_{181}}{6} B_{18} (D_N - D_{S1} - H_2)(2D_{S1} + 2H_2 + D_N)$$

4.4.4 Failure mode 4

Incremental Analysis



Assumptions same as mode 2.

Stress diagram for $F_2 > F_1$ can be constructed easily referring to mode 2.

Adopting the routine of mode 2, we get

$$D_{Ni} = \frac{(D_{S1} + D_{18})\, F_j\, E_{18} + x_i\, F_4\, E_j}{F_j\, E_{18} + F_4\, E_j}$$

when $F_1 > F_2$ $\quad j = 1$

$F_2 > F_1$ $\quad j = 2$

When i = 1

$$\frac{\sigma_{181}}{D_{N1} - D_{S1} - H_{2(1)}} = \frac{\sigma_{182}}{D_{S1} + D_{18} - D_{N1}}$$

$$H_{2(1)} = (D_{N1} - D_{S1})\left(1 + \frac{\sigma_{181}}{\sigma_{182}}\right) - D_{18}\,\frac{\sigma_{181}}{\sigma_{182}}$$

General equation for H_2 is as follows.

$$H_{2(i)} = (D_{Ni} - D_{S1})\left(1 + \frac{\sigma_{181}}{\sigma_{182}}\right) - D_{18}\,\frac{\sigma_{181}}{\sigma_{182}}$$

Total compression, using the routine of mode 2,

$$C = -\left[\left\{\tfrac{1}{2} B_1 \sum_{k=1}^{N_1} (\sigma_{k1} + \sigma_{k2}) D_k\right\} + B_{18} F_3 H_{2(i)} + \tfrac{1}{2} B_{18} F_3 \left\{ D_{Ni} - D_{S1} - H_{2(i)} \right\}\right]$$

Total tension $T = + \tfrac{1}{2} F_4 B_{18} D_{Ti}$

For equilibrium $C + T = 0$

As the assumed value of i may not be correct,

$$(C + T)_i = \text{error}$$

Starting from 1 increase the value of i to find that value which gives the least error. This value of i is adopted to calculate the final stresses and the ultimate resisting moment.

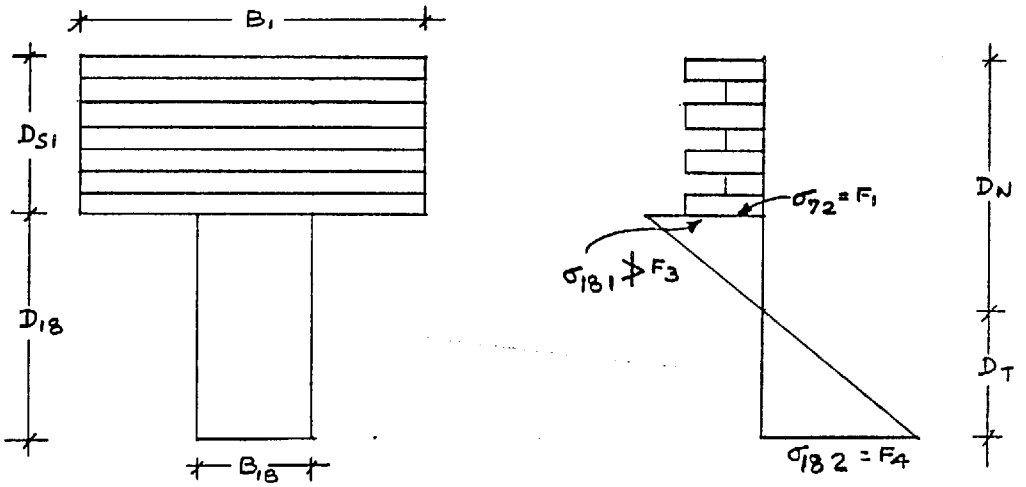
$$ULTM = \tfrac{1}{2} F_4 B_{18} D_{Ti} (D_{S1} + D_{18} - \tfrac{1}{3} D_{Ti}) - \tfrac{1}{2} B_1 \sum_{k=1}^{N_1} D_k (\sigma_{k1} + \sigma_{k2}) w_k$$

$$- F_3 B_{18} H_{2(i)} \left\{ D_{S1} + \tfrac{1}{2} H_{2(i)} \right\}$$

$$- \frac{F_3}{6} B_{18} \left\{ D_{Ni} - D_{S1} - H_{2(i)} \right\} \left\{ 2 D_{S1} + 2 H_{2(i)} + D_{Ni} \right\}$$

4.4.5 Failure mode 5

In this mode yield penetration covers full depth of flange, but rib is elastic.



$$\sigma_{181} = \frac{F_4 (D_N - D_{S1})}{D_T}$$

Total compression $C = -\left[C_1 + \frac{1}{2} \sigma_{181} B_{18}(D_N - D_{S1})\right]$

where $C_1 = \frac{1}{2} B_1 \sum_{k=1}^{N_1} (\sigma_{k1} + \sigma_{k2}) D_k$

Total tension $T = \frac{1}{2} F_4 B_{18} D_T$

For equilibrium $C + T = 0$ - 4.8

From equation (4.8) $D_N = \frac{A D_{S1}^2 + 2 C_1 B - AB^2}{2 (A D_{S1} - AB + C_1)}$ - 4.9

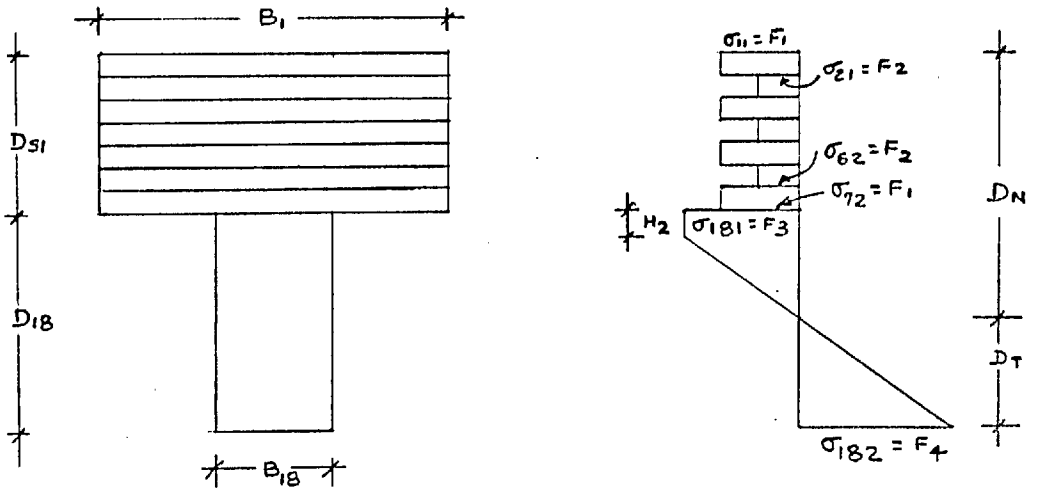
where $A = F_4 B_{18}$

$B = D_{S1} + D_{18}$

$$ULTM = \frac{1}{2} F_4 B_{18} D_T(D_{S1} + D_{18} - \frac{1}{3} D_T) - \frac{1}{2} B_1 \sum_{k=1}^{N_1} D_k(\sigma_{k1} + \sigma_{k2}) w_k$$

$$- \frac{1}{2} \sigma_{181} B_{18}(D_N - D_{S1}) \frac{1}{3} (2 D_{S1} + D_N)$$

4.4.6 Failure mode 6



$$D_N - D_{S1} - H_2 = \frac{\sigma_{181}}{\sigma_{182}} (D_{S1} + D_{18} - D_N) = A_2(D_{S1} + D_{18} - D_N)$$

$$\text{where } A_2 = \frac{\sigma_{181}}{\sigma_{182}}$$

$$H_2 = D_N - D_{S1} - A_2(D_{S1} + D_{18} - D_N) \qquad - 4.10$$

$$\text{Total compression } C = -\left[A_1 + \sigma_{181}\, B_{18}\, H_2 + \sigma_{182}\, B_{18}(D_N - D_{S1} - H_2)\right]$$

$$\text{where } A_1 = B_1 \left[\sigma_{11}\,(D_1+D_3+D_5+D_7)+\sigma_{21}(D_2+D_4+D_6)\right]$$

$$\text{Total tension } T = + \tfrac{1}{2} F_4\, B_{18}(D_{S1} + D_{18} - D_N)$$

$$\text{For equilibrium } C + T = 0 \qquad - 4.11$$

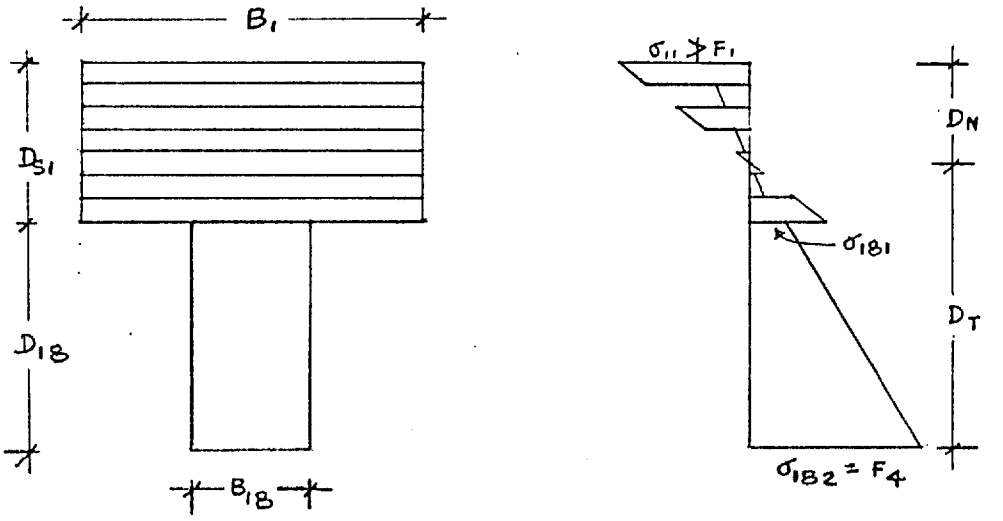
From 4.11

$$D_N = \frac{F_4\, B_{18}(D_{S1} + D_{18}) + F_3\, B_{18}(2\, D_{S1} + A_2\, D_{S1} + A_2\, D_{18}) - 2\, A_1}{B_{18}\left[F_3(2 + A_2) + F_4\right]} \qquad - 4.12$$

$$\text{ULTM} = \tfrac{1}{2} F_4\, B_{18}\, D_T(D_{S1} + D_{18} - \tfrac{1}{3} D_T) - \tfrac{1}{2} B_1 \sum_{k=1}^{N_1} D_k(\sigma_{k1} + \sigma_{k2})\, w_k$$

$$- F_3\, B_{18}\, H_2(D_{S1} + \tfrac{1}{2} H_2) - \frac{F_3}{6} B_{18}(D_N - D_{S1} - H_2)(2\, D_{S1} + 2\, H_2 + D_N)$$

4.4.7 Failure mode 7



$$D_N = \frac{B_1 \sum_{i=1}^{N_1} E_i D_i y_i + B_{18} E_{18} D_{18}(D_{S1} + \frac{1}{2} D_{18})}{B_1 \sum_{i=1}^{N_1} E_i D_i + B_{18} E_{18} D_{18}} \qquad - 4.13$$

$$\sigma_{11} = A_1 E_1 D_N \qquad \text{where } A_1 = \frac{F_4}{E_{18} D_T}$$

$$\sigma_{12} = A_1 E_1 (D_N - x_1)$$

$$\sigma_{21} = A_1 E_2 (D_N - x_1)$$

$$\sigma_{22} = A_1 E_2 (D_N - x_2)$$

The general equations for the stresses at various levels in the flange are as follows.

$$\sigma_{j1} = A_1 E_j (D_N - x_{j-1})$$

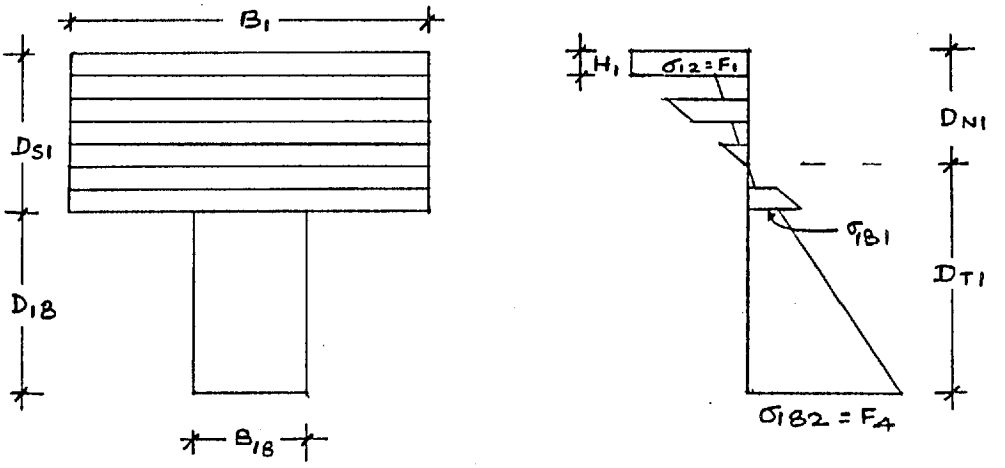
$$\sigma_{j1} = A_1 E_j (D_N - x_j)$$

where j takes a value from 1 to N_1 and $x_0 = 0$

$$\sigma_{181} = \sigma_{182} \frac{(D_{S1} - D_N)}{D_T}$$

$$ULTM = \sigma_{181} B_{18} D_{18} (D_{S1} + \tfrac{1}{2} D_{18}) + \tfrac{1}{2} (F_4 - \sigma_{181}) B_{18} D_{18} (D_{S1} + \tfrac{2}{3} D_{18}) - \tfrac{1}{2} B_1 \left[\sum_{i=1}^{N_1} (\sigma_{i1} + \sigma_{i2}) D_i w_i \right]$$

4.4.8 Failure mode 8



Refer to mode 2.

According to the value of i, D_N takes the following general form.

$$D_{Ni} = \frac{(D_{S1} + D_{18})\, E_{18}\, F_j + x_i\, F_4\, E_j}{F_j\, E_{18} + F_4\, E_j}$$

when $F_1 > F_2$ $\quad j = 1$

$F_2 > F_1$ $\quad j = 2$

$$\sigma_{181} = \frac{F_4(D_{S1} - D_{N1})}{D_T}$$

General form of $(C + T)_i$ is

$$(C + T)_i = -\frac{B_1}{2} \sum_{k=1}^{N_1} (\sigma_{k1} + \sigma_{k2}) D_k + \tfrac{1}{2}(F_4 + \sigma_{181}) B_{18}\, D_{18} = \text{error}$$

The value of i which gives the least error is adopted to calculate the final stresses and ultimate resisting moment.

$$\text{ULTM} = \sigma_{181}\, B_{18} D_{18} (D_{S1} + \tfrac{1}{2} D_{18}) + \tfrac{1}{2}(F_4 - \sigma_{181}) B_{18} D_{18} (D_{S1} + \tfrac{2}{3} D_{18})$$

$$- \tfrac{1}{2} B_1 \left[\sum_{k=1}^{N_1} (\sigma_{k1} + \sigma_{k2})\, D_k\, w_k \right]$$

4.5 Analysis of T sections with layered flange using computer.

4.5.1 Procedure 1. 'Direct search method' can be adopted for analysing a T section with layered flange. Starting from mode 1, each mode can be examined to arrive at that particular mode which satisfies the equilibrium condition, $C + T = 0$ or $C + T = \epsilon$ where ϵ is a small acceptable error. Based on the position of neutral axis and the depth of yield penetration in the flange and rib, the mode of failure can be ascertained.

a) Neutral axis within the rib

$H_1 = 0$ and $H_2 = 0$ .. Mode 1

$H_1 > 0$ and $H_2 = 0$, but $H_1 \neq D_{S1}$ .. Mode 2

$H_1 = 0$ and $H_2 > 0$ .. Mode 3

$H_1 > 0$ and $H_2 > 0$, but $H_1 \neq D_{S1}$ .. Mode 4

$H_1 = D_{S1}$ and $H_2 = 0$ .. Mode 5

$H_1 = D_{S1}$ and $H_2 > 0$ .. Mode 6

b) Neutral axis within the flange or at the interface

$H_1 = 0$ and $H_2 = 0$ .. Mode 7

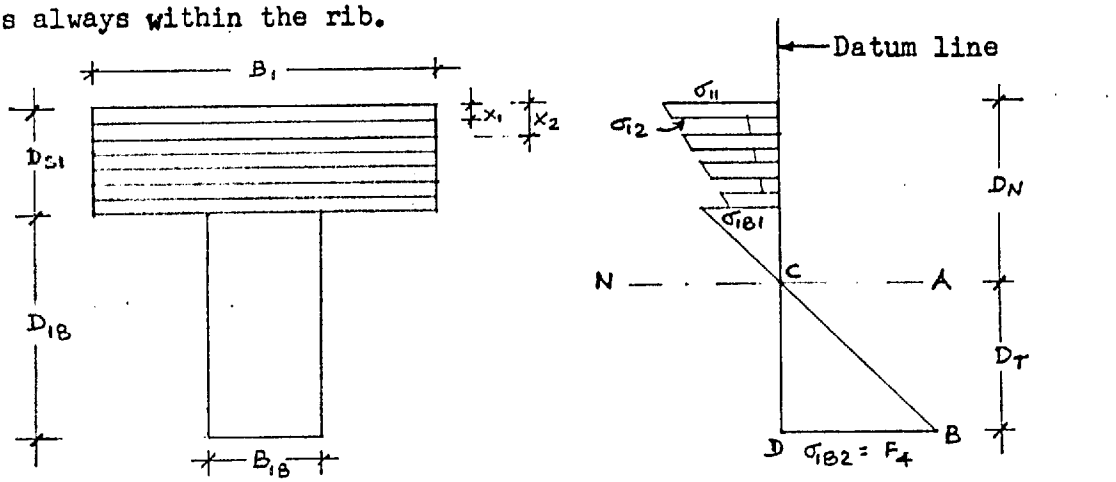
$H_1 > 0$ and $H_2 = 0$ .. Mode 8

The 'Direct search method' is not recommended in the case of sections with layered flanges because of the wastage of computer time. To arrive at the correct solution it is necessary to evaluate and compare many trial solutions in each mode.

4.5.2 Procedure 2

The sections are analysed using the same iteration procedure that was used in the case of non-layered flanges.

Stage 1 Modes 1 to 6 are considered in this stage. The neutral axis is always within the rib.



Cross section Fig. 4.2 Stress diagram

Assume an arbitrary depth of neutral axis. Let C be the position of N.A on the datum line of the stress diagram and BD represent the magnitude of the ultimate tensile stress of rib (F_4).

The stresses at the vital points can be worked out as follows.

$$\sigma_{11} = A_1 D_N E_1 \qquad \text{where } A_1 = \frac{F_4}{D_T E_{18}} \qquad - 4.14$$

If $\sigma_{11} \not> F_1$ $\qquad H_1 = 0.0$

The general equations for the stresses at various positions are as follows.

$$\sigma_{j1} = A_1 (D_N - x_{j-1}) E_j \qquad - 4.15$$

$$\sigma_{j2} = A_1 (D_N - x_j) E_j \qquad - 4.16$$

where j takes a value from 1 to N_1 and $x_0 = 0$

If $\sigma_{j1} > F_s$, $\sigma_{j1} = F_s$ where s = 1 if j is odd; s = 2 if j is even.

The basic assumption is that the yield penetration extends to the full depth of a layer.

$\therefore$ if $\sigma_{j1} = F_s$ then $\sigma_{j2} = F_s$

and $H_1 = x_j$

Stresses at various levels are shown in fig. 4.3

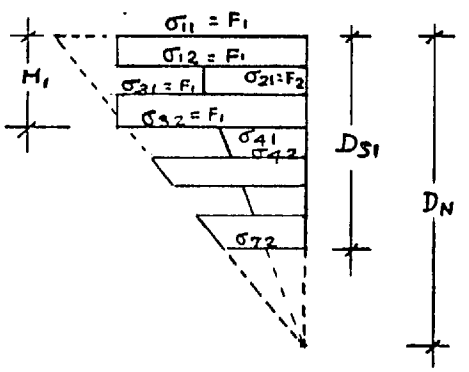


Fig. 4.3

Refer to fig. 4.2

$$\sigma_{181} = \frac{F_4(D_N - D_{S1})}{D_T} \qquad - 4.17$$

If $\sigma_{181} \not> F_3$ $H_2 = 0.0$

If $\sigma_{181} > F_3$, assume $F_R = \sigma_{181}$ as calculated above (equation 4.17).

Refer to fig. 4.4

Let H_2 be the depth at which stress is F_3

$$H_2 = (D_N - D_{S1})(1 - \frac{F_3}{F_R})$$

Also $H_2 < D_N - D_{S1}$

Maximum possible value of $\sigma_{181} = F_3$

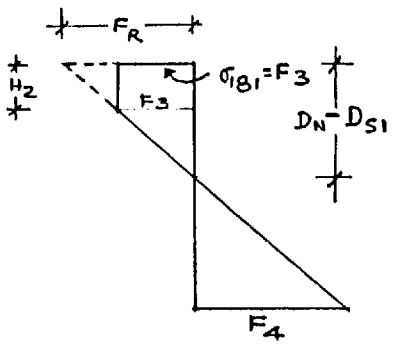
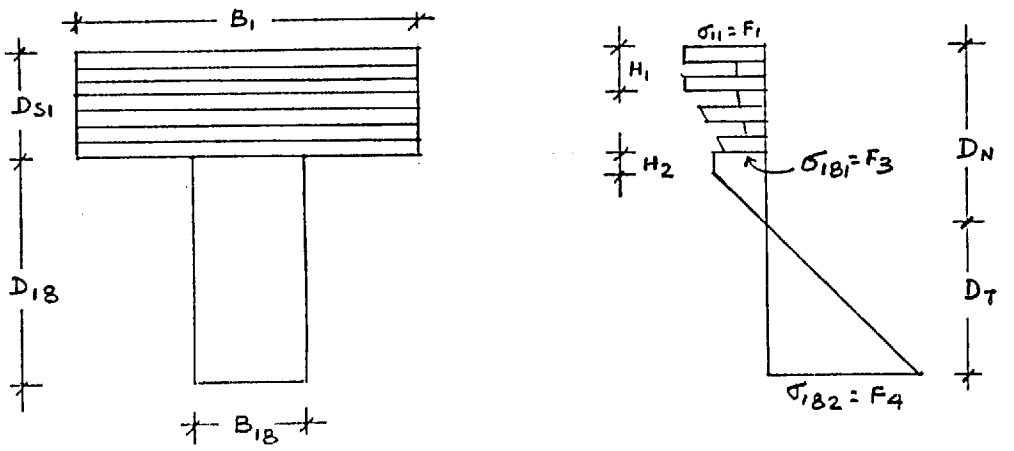


Fig. 4.4

Stress diagram for the rib is shown in fig. 4.4

Most general form of the stress diagram for the whole section is as shown below.



Cross section Stress diagram

Fig.4.5

Total compression $C = -\left[\left\{\frac{1}{2} B_1 \sum_{k=1}^{N_1} (\sigma_{k1} + \sigma_{k2})\, D_k\right\} + B_{18}\, \sigma_{181}\, H_2 + \frac{1}{2} B_{18}\, \sigma_{181} (D_N - D_{S1} - H_2)\right]$

Total tension $T = + \frac{1}{2} F_4\, B_{18}\, D_T$

For equilibrium $C + T = 0$ - 4.18

As the assumed value of D_N may not be correct,

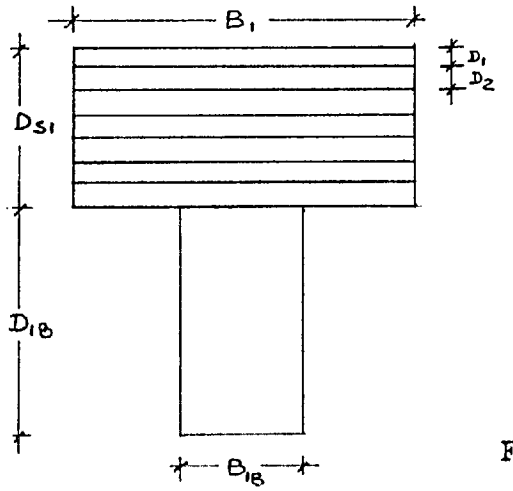
$$C + T = \text{error}$$

By adopting the iteration procedure explained earlier, the value of D_N which gives the acceptable error is found.

$$ULTM = \frac{1}{2} F_4\, B_{18}\, D_T (D_{S1} + D_{18} - \frac{1}{3} D_T) - \frac{1}{2} B_1 \sum_{k=1}^{N_1} D_k (\sigma_{k1} + \sigma_{k2})\, w_k$$

$$- \sigma_{181}\, B_{18} H_2 (D_{S1} + \frac{1}{2} H_2) - \frac{\sigma_{181}}{6} B_{18} (D_N - D_{S1} - H_2)(2 D_{S1} + 2 H_2 + D_N)$$

Stage 2. Modes 7 & 8 are considered here. The neutral axis is within the flange or at the interface.



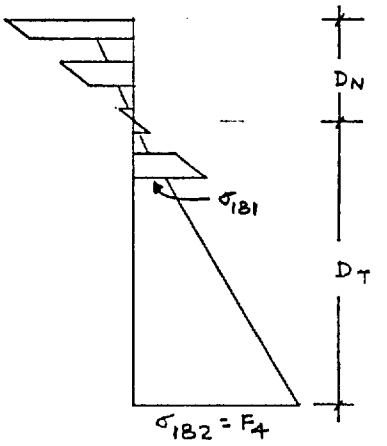


Fig. 4.6

Assume an arbitrary depth for N.A which is within the flange as shown in fig. 4.6. Knowing the magnitude of F_4, the stresses at various levels in the flange can be calculated using the equations 4.15 and 4.16. Using the same procedure that was adopted in stage 1, the depth of yield penetration in the flange also can be found.

Stresses at various levels are shown in fig. 4.7

$$\sigma_{181} = \sigma_{182} \frac{(D_{S1} - D_N)}{D_T}$$

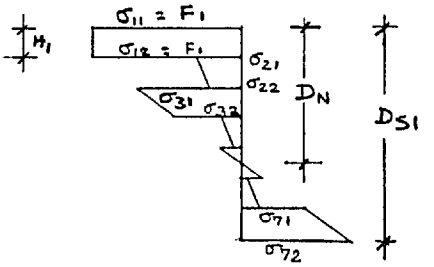


Fig. 4.7

The most general form of the stress diagram is as shown in fig. 4.8

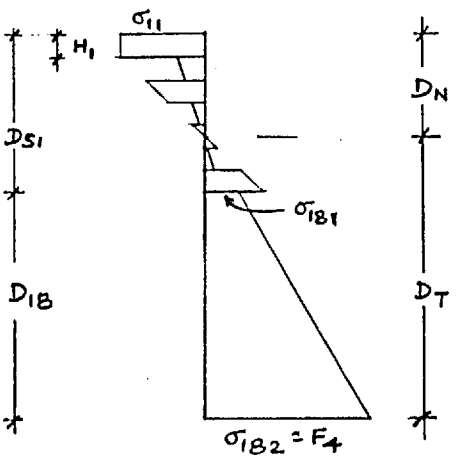


Fig. 4.8

$$C + T = -\left[\tfrac{1}{2} B_1 \sum_{k=1}^{N_1} (\sigma_{k1} + \sigma_{k2}) D_k\right] + \tfrac{1}{2} (\sigma_{181} + \sigma_{182}) B_{18} D_{18} = \text{error}$$

Using the iteration procedure, the value of D_N which gives the acceptable error is found.

$$\text{ULTM} = \tfrac{1}{2} (\sigma_{181} + \sigma_{182}) B_{18} D_{18} \left[D_{S1} + \tfrac{1}{3} D_{18} \frac{(\sigma_{181} + 2\sigma_{182})}{(\sigma_{181} + \sigma_{182})}\right]$$

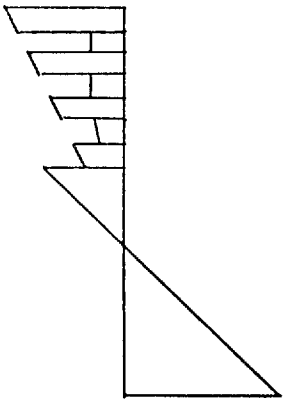
$$- \tfrac{1}{2} B_1 \sum_{k=1}^{N_1} D_k (\sigma_{k1} + \sigma_{k2}) w_k$$

4.5.3 Examples

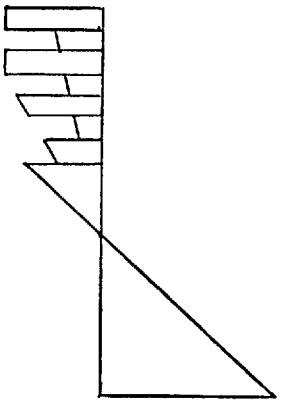
Typical examples of failure modes of T sections with layered flanges are given in Tables 4 and 4A.

The relationship of the mechanical properties of the components with the ultimate resisting moment of the T sections is examined in Table 5. It has been established that the ultimate resisting moment is very sensitive to the ultimate tensile strength of the rib.

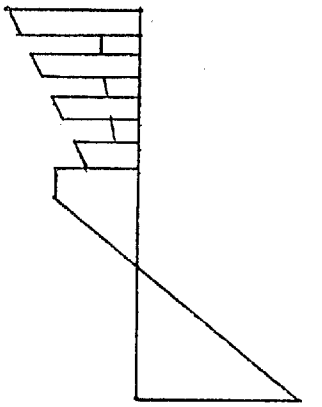
In the case of the sections with layered flanges, the following typical alternative stress diagrams are possible according to the modulus of elasticity and compressive strength of the layers. Stress levels in the stronger layers only are considered to specify the mode numbers. However, stresses in both (strong and weak) layers have been used to calculate the ultimate resisting moment.



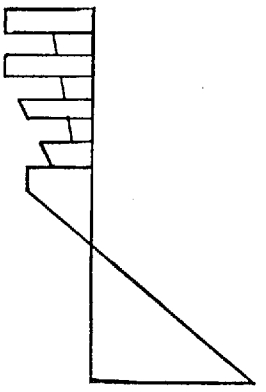
Mode 1 a



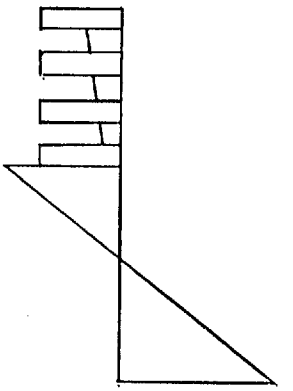
Mode 2 a



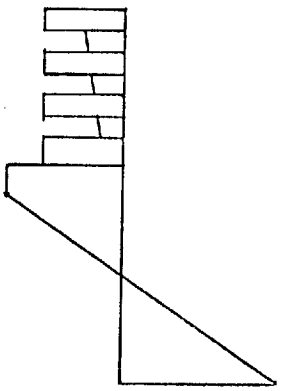
Mode 3 a



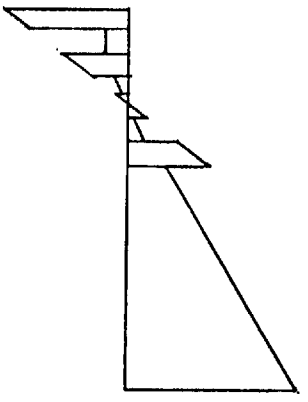
Mode 4 a



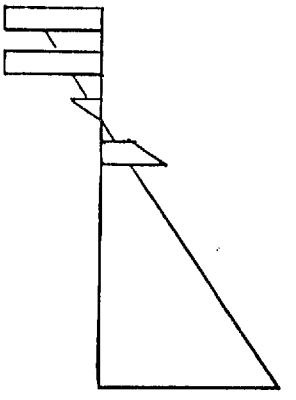
Mode 5 a



Mode 6 a



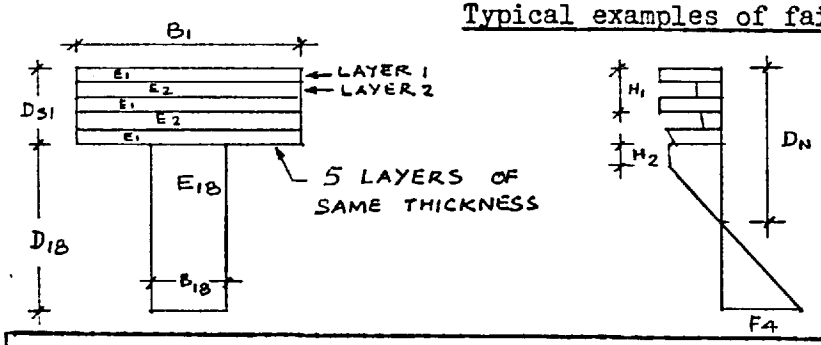
Mode 7 a



Mode 8 a

TABLE - 4

Typical examples of failure modes of T section with layered flange. Layer 1 stronger than layer 2.



The following properties are common for all cases.

Breadth of flange B_1 = 300.0 mm

Breadth of rib B_{18} = 50.0 mm

Ult. tensile stress of rib F_4 = 40.0 N/mm^2

Serial No.	D_{S1} (mm)	D_{18} (mm)	E_1 (N/mm^2)	E_2 (N/mm^2)	E_{18} (N/mm^2)	F_1 (N/mm^2)	F_2 (N/mm^2)	F_3 (N/mm^2)	D_N (mm)	H_1 (mm)	H_2 (mm)	Ult.RM (kN.m)	Failure Mode
1	10	100	12900	650	12000	30.8	3.8	21.0	42.28	0.00	0.00	5.180	1
2	10	100	12900	650	12000	24.6	3.1	22.0	45.11	6.00	0.00	5.096	2
3	10	100	12900	650	12000	30.8	3.8	19.0	44.32	0.00	3.12	5.178	3
4	10	100	12900	650	12000	24.6	3.1	20.0	45.12	6.00	2.68	5.095	4
5	10	100	12900	650	12000	21.6	2.6	24.0	47.25	10.00	0.00	4.891	5
6	10	100	12900	650	12000	21.6	2.6	20.0	47.49	10.00	6.24	4.872	6
7	20	40	19350	975	6000	40.6	4.1	20.0	14.29	0.00	0.00	2.036	7
8	20	40	19350	975	6000	34.0	9.0	20.0	14.39	4.00	0.00	2.021	8
9	20	40	12900	650	12000	30.8	3.8	20.0	20.00	0.00	0.00	1.639	7
10	20	40	13060	660	12000	19.2	1.2	20.0	20.00	4.00	0.00	1.636	8

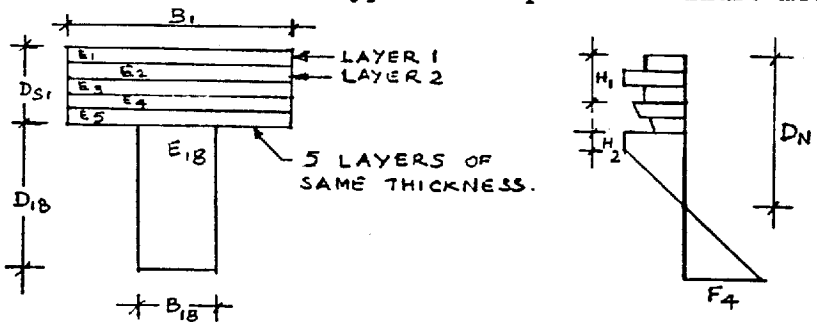
Notes: 1. In serial numbers 1 to 6 the N.A is within the rib.

2. In serial numbers 7 & 8 the N.A is within the flange.

3. In serial numbers 9 & 10 the N.A is on the interface.

TABLE 4A

Typical examples of failure modes of T section with layered flange . (Layer 2 is stronger than layer 1)



The following properties are common for all cases.

Breadth of flange B_1 = 300.0 mm

Breadth of rib B_{18} = 50.0 mm

Ult. tensile stress of rib F_4 = 40.0 N/mm^2

Serial No.	D_{S1} (mm)	D_{18} (mm)	E_1 (N/mm^2)	E_2 (N/mm^2)	E_{18} (N/mm^2)	F_1 (N/mm^2)	F_2 (N/mm^2)	F_3 (N/mm^2)	D_N (mm)	H_1 (mm)	H_2 (mm)	Ult.RM (kN.m)	Failure Mode
1	10	100	650	12900	12000	2.0	35.0	30.0	48.05	0.00	0.00	4.816	1
2	10	100	650	12900	12000	1.5	31.0	30.0	48.13	6.00	0.00	4.807	2
3	10	100	650	12900	12000	2.0	35.0	23.0	48.07	0.00	2.47	4.815	3
4	10	100	650	12900	12000	1.5	31.0	23.0	48.16	6.00	2.61	4.805	4
5	10	100	650	12900	12000	1.5	20.0	30.0	52.29	10.00	0.00	4.357	5
6	10	100	650	12900	12000	1.5	20.0	28.0	52.32	10.00	1.95	4.354	6
7	15	40	975	19350	6000	3.0	45.0	28.0	12.64	0.00	0.00	1.502	7
8	15	40	975	19350	6000	1.0	33.0	28.0	13.17	9.00	0.00	1.470	8
9	15	40	650	12900	12000	3.0	45.0	28.0	15.00	0.00	0.00	1.424	7
10	15	40	660	13060	12000	1.9	28.9	28.0	15.00	6.00	0.00	1.422	8

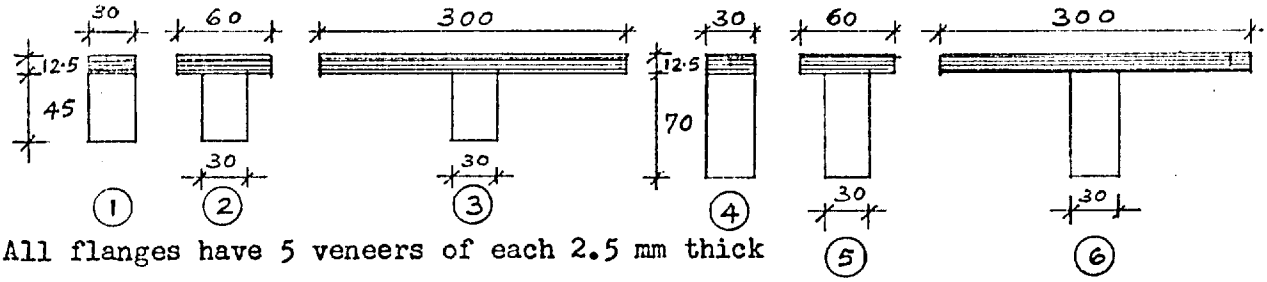
Notes: 1. In serial numbers 1 to 6 the N.A. is within the rib.

2. In serial numbers 7 & 8 the N.A. is within the flange.

3. In serial numbers 9 & 10 the N.A. is on the interface.

TABLE 5

Relationship of the mechanical properties of the components with the ultimate resisting moment of the T section



All flanges have 5 veneers of each 2.5 mm thick

Grain direction : Veneers 1, 3 & 5 parallel to the span

Veneers 2 & 4 perpendicular to the span

Mechanical properties of the flange and rib

Douglas fir flange

E ∥ to the grain, E_1	= 10500 N/mm^2	(published value)*
E ⊥ to the grain, E_2	= 350 "	(assumed value)
Compression ∥ to the grain, F_1	= 48 "	(published value)*
Compression ⊥ to the grain, F_2	= 12 "	(assumed value)

Redwood rib

E ∥ to the grain, E_{18}	= 10000 "	(published value)*
Compression ∥ to the grain, F_3	= 45 "	(published value)*
Tension ∥ to the grain, F_4	= 83 "	(published value for modulus of rupture)*

Effect on the resisting moment when one of the properties is changed by ± 30%

Model	Variation of the property %	Mechanical property						
		E_1	E_2	E_{18}	F_1	F_2	F_3	F_4
		Effect on the resisting moment (%)						
1	- 30 + 30	0	- 0.38 + 0.38	+ 0.48 - 0.28	- 8.32 + 7.84	- 0.10 0	- 6.79 + 2.77	- 21.22 + 14.72
2	- 30 + 30	- 1.37 0	- 0.38 + 0.38	+ 0.53 - 0.99	-11.35 + 8.07	0	- 2.06 + 0.15	- 23.15 + 15.76
3	- 30 + 30	- 5.11 + 3.56	- 0.05 + 0.10	+ 4.86 - 3.81	0	0	0	- 30.01 + 30.01
4	- 30 + 30	0	- 0.18 + 0.23	+ 0.36 - 0.14	- 5.80 + 5.71	0	- 9.39 + 4.85	- 21.38 + 14.83
5	- 30 + 30	0	- 0.27 + 0.30	+ 0.45 - 0.19	- 8.89 + 8.36	0	- 5.26 + 1.89	- 22.35 + 15.36
6	- 30 + 30	- 5.53 + 3.72	- 0.10 + 0.10	+ 5.07 - 4.11	- 1.10 0	0	0	- 30.00 + 29.97

Ultimate tensile stress of the rib (F_4) is the most critical property.

* Reference: PRL(1974). Strength properties of timber.

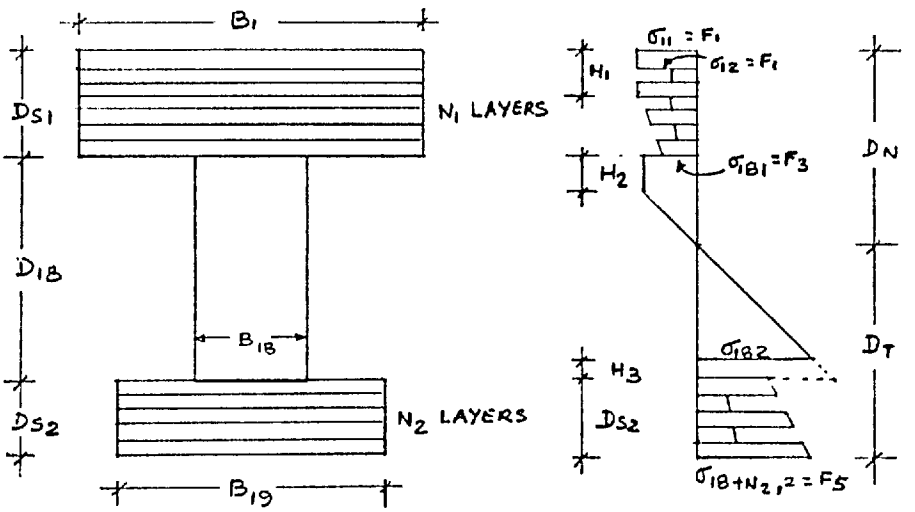
4.6 Analysis of I sections with layered flanges.

Procedure 2 is only adopted to analyse I section.

Let C + T = error

As in the case of T section, the value of D_N which gives an error which is within the acceptable limits is found by iteration.

Most general form of the stress diagram is as shown below.



Cross section Stress diagram

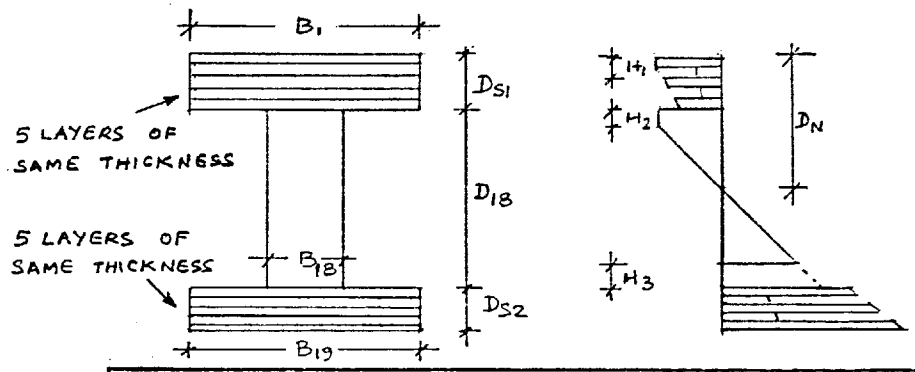
$$ULTM = \frac{B_{19}}{2}\sum_{j=19}^{18+N_2} D_j(\sigma_{j1} + \sigma_{j2})w_j + \frac{\sigma_{182}}{6} B_{18}(D_{S1} + D_{18} - D_N - H_3)$$
$$(2\,D_{S1} + 2\,D_{18} + D_N - 2\,H_3)$$
$$- \frac{B_1}{2}\sum_{k=1}^{N_1} D_k(\sigma_{k1} + \sigma_{k2})\,w_k - \sigma_{181}\,B_{18}H_2(D_{S1} + \frac{H_2}{2})$$
$$- \frac{\sigma_{181}}{6} B_{18}(D_N - D_{S1} - H_2)(2\,D_{S1} + 2\,H_2 + D_N)$$

4.6.1 Examples

Typical examples of failure modes of I sections with layered flanges are given in Table 6.

TABLE 6

Typical examples of failure modes of I sections with layered flanges



The following properties are common for all cases.

B_1	= 300.0 mm	E_1	= 12900 N/mm^2
B_{18}	= 50.0 mm	E_2	= 650 N/mm^2
B_{19}	= 300.0 mm	E_{18}	= 12000 N/mm^2
D_{S1}	= 10.0 mm	E_{19}	= 16120 N/mm^2
D_{18}	= 100.0 mm	E_{20}	= 820 N/mm^2
D_{S2}	= 8.0 mm		

Serial No.	F_1 (N/mm^2)	F_2 (N/mm^2)	F_3 (N/mm^2)	F_4 (N/mm^2)	F_5 (N/mm^2)	F_6 (N/mm^2)	D_N (mm)	H_1 (mm)	H_2 (mm)	H_3 (mm)	Ult.RM (kN.m)	Failure Mode
1	30.8	3.8	22.0	22.0	30.8	3.8	59.78	0.00	0.00	0.00	6.334	1
2	23.2	2.7	22.0	22.0	30.8	3.8	60.17	6.00	0.00	0.00	6.295	2
3	32.4	3.9	19.0	22.0	30.8	3.8	59.78	0.00	1.54	0.00	6.333	3
4	23.2	2.7	19.0	22.0	30.8	3.8	60.19	6.00	2.28	0.00	6.294	4
5	15.4	1.9	27.0	25.0	30.8	3.8	65.86	10.00	0.00	0.00	5.745	5
6	15.4	1.9	19.0	25.0	30.8	3.8	63.08	10.00	7.57	0.00	5.199	6
7	23.2	2.7	19.0	18.0	30.8	3.8	58.60	2.00	0.00	4.77	5.968	2
8	46.2	5.7	30.0	40.0	7.6	1.1	44.29	0.00	0.00	0.00	5.180	1

Note: In the case of serial number 8, bottom flange will not provide any strength at the ultimate load.

CHAPTER 5

STATISTICAL ANALYSIS OF SIZE EFFECT

5.1 Introduction

When timber specimens of the same species without any visible strength-reducing characteristics such as knots, cross grain etc., are tested in tension or in bending, it is noticed that their strength (ultimate stress) reduces with the increase of volume. This phenomenon has been of interest to many research workers. Newlin and Trayer (1924) suggested an empirical formula to relate the depth and strength of timber beams. According to Bohannan (1966) "in 1947, Dawley and Youngquist re-evaluated the strength-depth theory for wood beams and developed a new relationship". Other well known investigators of the depth-strength relationship were Freas and Selbo (1954), Beghtel and Norris (1959). But the application of Weibull's (1939) statistical theory of the strength of materials enabled a theoretical solution to be found for the size effect problem. Bohannan (1966), Barrett (1974), Barrett, Foschi and Fox (1975), Foschi and Barrett (1976) are well known for tackling the size effect problem with the aid of Weibull's theory.

5.2 Weakest link theory

The weakest link theory assumes that the strength of a specimen is analogous to the strength of a chain. In this theory, an element of the volume is considered as a link and the specimen as the chain. The strength of a chain is equal to the strength of its weakest link. Hence, by analogy, it is assumed that when the maximum stress in the specimen is equal to the failure stress of the weakest element, failure of the specimen will occur. This assumption is considered to be appropriate for a material which shows brittle-type failure in which propagation of failure is possible without additional load being applied, but in the case of a ductile material the possibility is that the stress will redistribute after the failure of a small volume element and complete failure will not occur until additional loads are applied.

5.3 Weibull's statistical strength theory

Weibull's statistical strength theory is founded on the weakest link theory. It assumes that there is a greater probability that a region of low strength will occur in a member of large volume than in a member of small volume. This region of low strength is assumed to cause complete failure of the member. In other words, the strength of a brittle material decreases with increasing specimen volume.

Statistical strength theory can be elaborated further. Any solid is an assembly of a very large quantity of primary elements, each of which is to some degree responsible for the strength of the solid as a whole. Since the mechanical properties of the primary elements are random in nature, the properties of a big enough volume containing a large number of these elements may be predicted by using probabilistic methods, if the distribution laws of the primary elements are known.

5.4 Brittle Fracture

In the theory of brittle fracture, the interaction of the primary elements in the brittle body is ignored by assuming that the strength of the solid is determined entirely by the strength of the weakest primary element. According to this theory, brittle fracture depends on the local stress at a point where the most dangerous structural defect occurs. In applying the theory to bending members, both the magnitude and the location of the stresses must be considered.

5.5 Material types

According to Barrett (1974), three material types considered by Johnson are as follows:

1. Perfectly brittle: Material in which total failure occurs when fracture occurs at weakest point.
2. Perfectly plastic: Failure by ductile yielding; failure occurs when

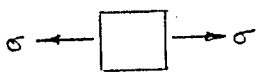
maximum load capacity of any cross section is exceeded.

3. Brittle material that do not follow the weakest-link concept; maximum load bearing capacity does not necessarily coincide with fracture of weakest element.

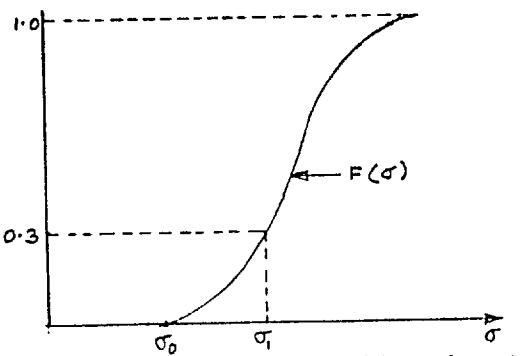
A timber member subjected to the tensile stress can be considered as perfectly brittle. Based on this assumption Weibull's statistical strength theory is applied to the tensile zone in the ribs to predict the ultimate resisting moment of the stressed skin panels of this thesis.

5.6 Development of statistical strength theory

It is customary to neglect the material variability observed in tests of similar specimens of some material like steel and the strength is often represented by a single average value. But when the variability is large, as in the case of timber in tension, the strength can be more precisely described by a " cumulative distribution function". Using the chain analogy, the effect of the number of elementary volumes can be calculated using the cumulative distribution function for the elementary volume.



Element



Cumulative distribution function for elementary volumes

F (σ) gives the probability that the strength is less than or equal to σ ; therefore 1 - F(σ) gives the probability of the strength being greater than σ. For example, as shown in the figure, probability of strength less than or equal to σ_1, is 0.3 and the probability of strength greater than σ_1, is 0.7

It has been shown by Foschi (1979) that,

$F(\sigma)$ = prob. (strength $\leq \sigma$) = prob. of failure at $\sigma = P_f(\sigma)$

Prob. of survival $P_s = 1 - F(\sigma)$

For a volume which contains n elements,

probability of all surviving $P_s = \left[1 - F(\sigma) \right]^n$

Using Newton's Binomial theorem,

$$[1- F]^n = \sum_{r=0}^{n} \frac{n!}{r!\ (n-r)!} F^r (-1)^r$$

$$= \sum_{r=0}^{n} \frac{n!}{(n-r)!} \frac{1}{n^r} \frac{(nF)^r}{r!} (-1)^r$$

$$= \sum_{r=0}^{n} \frac{n(n-1)(n-2)....(n-r+1)}{n^r} \frac{(nF)^r}{r!} (-1)^r$$

$$= \sum_{r=0}^{n} (1 - \frac{1}{n})(1 - \frac{2}{n}).... \left\{ 1 - \frac{(r-1)}{n} \right\} \frac{(nF)^r}{r!} (-1)^r$$

For large n

$$[1 - F]^n = \sum_{r=0}^{n} \left\{ 1 - O(\frac{1}{n}) \right\} \frac{(nF)^r}{r!} (-1)^r$$

As $n \longrightarrow \infty$

$$[1 - F]^n \simeq \sum_{r=0}^{n} \frac{(nF)^r}{r!} (-1)^r = e^{-nF}$$

Replacing F by $F(\sigma)$,

$$P_s = \left[1 - F(\sigma) \right]^n \approx e^{-nF(\sigma)}$$

Prob. of failure $P_f = 1 - P_s = 1 - e^{-nF(\sigma)}$

When n is large $F(\sigma)$ is near minimum.

$$\therefore \quad F(\sigma) \simeq C(\sigma - \sigma_0)^k$$

where k is a material constant which influences the fit of distribution function $F(\sigma)$,

σ_0 is the minimum strength and C is a scale factor.

$$\therefore \quad P_f = 1 - e^{-n\,C(\sigma - \sigma_0)^k} \qquad - 5.1$$

Equation (5.1) represents Weibull 3 parameter distribution.

If $\sigma_0 = 0$, equation (5.1) becomes Weibull 2 parameter distribution.

5.7 Non-uniform stress

When a beam is subjected to bending, it is under the influence of non-uniform stress. For this thesis we are specially interested in this state of stress in the body.

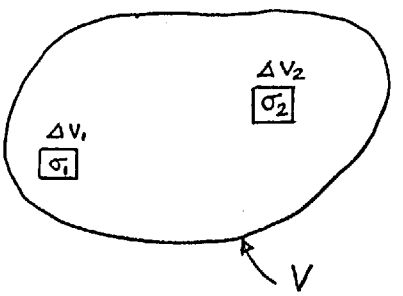
If the number of defects per unit volume is λ and $n_1, n_2, \ldots$ are the number of defects in $\Delta V_1, \Delta V_2, \ldots$ respectively,

$$n_1 = \lambda\, \Delta V_1$$

$$n_2 = \lambda\, \Delta V_2$$

$$\therefore \quad P_{s1} = e^{-\lambda(\sigma_1 - \sigma_0)^k\, \Delta V_1}$$

$$P_{s2} = e^{-\lambda(\sigma_2 - \sigma_0)^k\, \Delta V_2}$$



Probability of survival of V = probability that all ΔV_i survive.

$$P_s = P_{s1} \times P_{s2} \times \ldots\ldots = e^{-\lambda(\sigma_1-\sigma_0)^k \Delta V_1} \times e^{-\lambda(\sigma_2-\sigma_0)^k \Delta V_2} \times \ldots$$

$$= e^{-\Sigma\lambda(\sigma_i-\sigma_0)^k \Delta V_i}$$

In the limit $\Delta V_i \longrightarrow 0$

$$P_s = e^{-\int_V \lambda(\sigma-\sigma_0)^k dv}$$

$$P_s = e^{-\int_v \left(\frac{\sigma-\sigma_0}{m}\right)^k dv} \qquad \text{where } \left(\frac{1}{m}\right)^k = \lambda$$

$$P_f = 1 - e^{-\int_V \left(\frac{\sigma-\sigma_0}{m}\right)^k dv} \qquad - 5.2$$

where σ_0, m and k are material constants.

Note: The expression derived by Weibull is as follows:

Probability of rupture $S = 1 - e^{-B} = 1 - e^{-\int n(\sigma)dv}$

where $n(\sigma)$ is the function of tensile stress σ

For Weibull 2 parameter distribution $\sigma_0 = 0$

Equation (5.2) becomes $P_f = 1 - e^{-\int_v \left(\frac{\sigma}{m}\right)^k dv}$ - 5.3

Two parameter distribution is adopted throughout this thesis.

5.8 Comparison of two volumes at same probability of failure P_f

Let us consider volume V under stress σ and unit volume V^* under uniform stress K_0 at same probability of failure.

$$P_f = 1 - e^{-\int_v \left(\frac{\sigma}{m}\right)^k} \qquad = 1 - e^{-\left(\frac{K_0}{m}\right)^k V^*}$$

$$\therefore \quad \int_v \left(\frac{\sigma}{m}\right)^k dv = \left(\frac{K_o}{m}\right)^k V^*$$

Eliminating constant m from both sides and putting $V^* = 1$

$$\int_v \sigma^k \, dv = K_0^{\,k} \qquad - 5.4$$

We can define K_0 as the strength of unit volume in tension.

A method of finding the material constants k and K_0 from the experimental results is given later in this chapter.

5.9 Tensile stress at a particular probability of failure

$$P_f = 1 - e^{-\left(\frac{\sigma}{m}\right)^k V} \qquad - 5.5$$

$$\therefore \quad \left(\frac{\sigma}{m}\right)^k V = - \ln(1 - P_f)$$

For V = 1 (unit volume), $\sigma = K_0$

$$\left(\frac{K_0}{m}\right)^k = - \ln (1 - P_f)$$

$$K_0 = m \left[- \ln (1 - P_f)\right]^{\frac{1}{k}} \qquad - 5.6$$

Note: It is customary to represent the strength of a material by a " characteristic strength ". The characteristic strength is frequently defined as the ultimate strength below which not more than 5% of the test results fall and this is the value used in this thesis. Therefore at characteristic strength, the probability of failure is 0.05.

If our aim is to find the stress at the probability of failure 0.05 (or probability of survival 0.95) ,

$$K_{0(0.95)} = m \left[- \ln (0.95)\right]^{\frac{1}{k}} \qquad - 5.7$$

From (5.6) & (5.7) $K_0 = K_{0(0.95)} \left[\frac{\ln(1-P_f)}{\ln(0.95)}\right]^{\frac{1}{k}}$

By rearranging,

$$\ln(1 - P_f) = \left[\ln(0.95)\right]\left[\frac{K_0}{K_{0(0.95)}}\right]^k$$

$$1 - P_f = e^{\left[\ln(0.95)\right]\left[\frac{K_o}{K_o(0.95)}\right]^k}$$

$$1 - P_f = 0.95^{\left[\frac{K_o}{K_o(0.95)}\right]^k}$$

$$P_f = 1 - 0.95^{\left[\frac{K_o}{K_o(0.95)}\right]^k} \qquad - 5.8$$

If $K_{0(0.50)}$ (i.e. the mean value) and k are known from test results, $K_{0(0.95)}$ can be calculated from (5.5)

Consider mean stress value (when $P_f = 0.5$) for unit volume.

Equation (5.5) becomes

$$0.5 = 1 - e^{-\left[\frac{K_{0(0.5)}}{m}\right]^k}$$

$$m = \frac{K_{0(0.5)}}{\left[-\ln(0.5)\right]^{\frac{1}{k}}} \qquad - 5.9$$

Again using equation (5.5) for a survival probability of 0.95 for unit volume ,

$$0.05 = 1 - e^{-\left[\frac{K_{0(0.95)}}{m}\right]^k} \qquad - 5.10$$

Substituting (5.9) in (5.10) and rearranging,

$$K_{0(0.95)} = K_{0(0.5)} \left[\frac{\ln(0.95)}{\ln(0.50)}\right]^{\frac{1}{k}} \qquad - 5.11$$

For any probability of survival P_s equation (5.8) can be written in the general form.

$$P_f = 1 - P_s^{\left[\frac{K_o}{K_{0(P_s)}}\right]^k} \qquad - 5.12$$

$$\text{where } K_{0(P_s)} = K_{0(0.5)} \left[\frac{\ln(P_s)}{\ln(0.5)}\right]^{\frac{1}{k}}$$

Using equation (5.12), the tensile stress at a particular probability of failure can be found by the following iteration procedure.

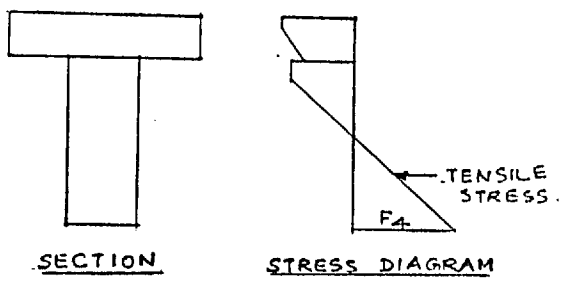
1. Assume an arbitrary stress and find K_0 from $\int_v \sigma^k \, dv = K_0^k$

2. Calculate P_f from the equation (5.12). If the calculated value is not equal to the assumed value, try with other values of stress until the correct P_f is attained. The stress corresponding to the correct value of P_f is the one which we are seeking.

5.10 Application of Weibull's theory to predict the ultimate resisting moment of a T beam in bending.

The basic assumption of the analysis of T section is that 'failure occurs when the extreme bottom fibre attains the ultimate tensile stress'. When the tensile stress of the extreme bottom fibre with a particular probability of failure is known, the resisting moment can be calculated using the methods described in the analysis of T sections. As explained in the previous section (5.9), the tensile stress at a particular probability of failure can be predicted using Weibull's theory. Now it is possible to set up a procedure to calculate the ultimate resisting moment of the section at a particular probability of failure.

1) Assume an arbitrary ultimate tensile (F_4) at the extreme bottom fibre.



2) Draw the stress diagram at the critical section using the known geometrical and mechanical properties so that it satisfies the equilibrium condition, total compression = total tension.

Now the stress at any point of the beam can be calculated according to the type of loading.

3) Integrating the tensile stress, find K_0 from $\int_v \sigma^k dv = K_0^k$ where k is known from the experiments.

4) Calculate P_f from equation (5.12). If the calculated value is not the assumed value, try with other values of stress F_4 until the required P_f is attained. An iteration procedure can be adopted to find F_4.

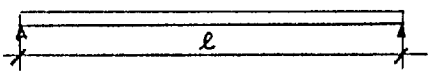
5) Using the ultimate tensile stress F_4 which corresponds to the correct

value of P_f derive the ultimate resisting moment.

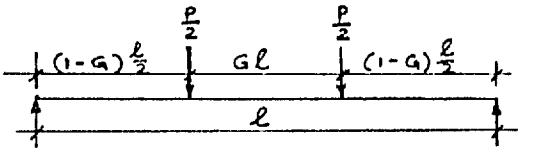
The same procedure can be used for T beam with non-layered flange or layered flange.

5.11 Method of Development of an Expression for $\int_v \sigma^k dv$ in the tension zone.

In the previous sections we have seen that the evaluation of the integral $\int_v \sigma^k dv$ is an essential routine in the analysis using Weibull's theory. For this thesis two loading cases are considered.



1. Uniformly distributed load



2. Two point loads symmetrically placed

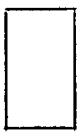
Three cross-sections are considered for the analysis.

They are a) Rectangle b) T section with non-layered flange

c) T section with layered flange.

5.11.1 Rectangular section with uniformly distributed load

Two types of failure are possible.



Cross section



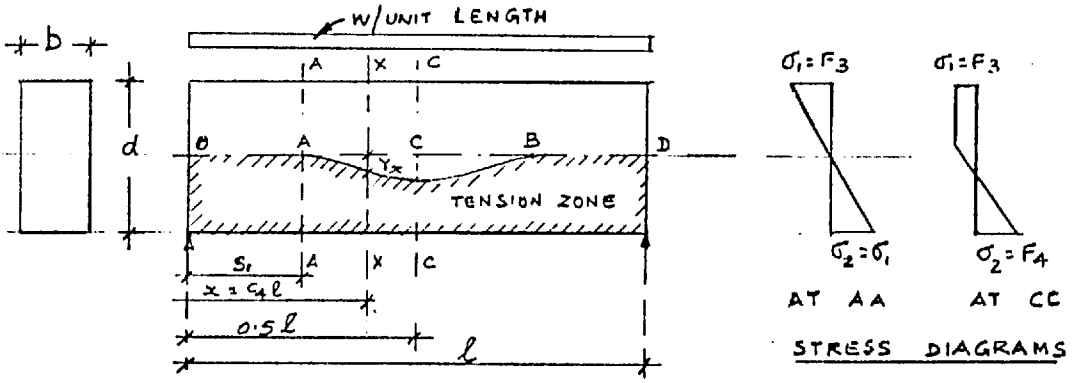
Stress diagrams

Type 1 (when $F_3 \geq F_4$)

Type 2 (when $F_3 < F_4$)

Type 1 failure can be considered as a special case of type 2.

Analysis of type 2 failure.



The first step is to find the boundaries of the tension zone.

The position where the N.A deviates from mid-depth is located as follows.

At section C C

$$M_c = \frac{wl^2}{8} = C_2 F_4 \frac{bd^2}{6} \quad \text{where } C_2 = \frac{\rho_2 (3+8\rho_2+6\rho_2^2-\rho_2^4)}{(1+\rho_2)^4} \quad \text{and } \rho_2 = \frac{F_3}{F_4}$$

$$w = \frac{4}{3} C_2 F_4 \frac{bd^2}{l^2} \qquad - 5.13$$

At section A A

$$M_A = \tfrac{1}{2} wls_1 - \tfrac{1}{2} w s_1^2 = F_3 \frac{bd^2}{6} = \rho_2 F_4 \frac{bd^2}{6}$$

$$\therefore \quad ls_1 - s_1^2 = \tfrac{1}{3} \frac{\rho_2 F_4}{w} bd^2$$

Substituting for w from (5.13)

$$ls_1 - s_1^2 = \tfrac{1}{4} \rho_2 \frac{l^2}{C_2}$$

$$s_1^2 - ls_1 + Cl^2 = 0 \qquad \text{where } C = \tfrac{1}{4} \frac{\rho_2}{C_2}$$

$$s_1 = C_3 l \qquad - 5.14$$

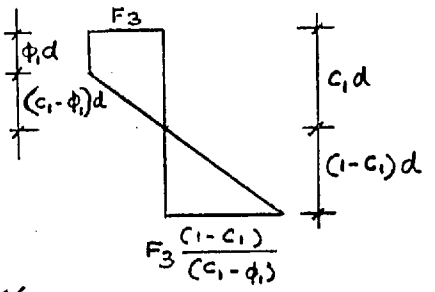
$$\text{where } C_3 = \frac{1 \pm \sqrt{1 - 4C}}{2}$$

To find the depth of N.A at $x = C_4 l$, between A and B

$$M_x = \tfrac{1}{2} wlx - \tfrac{1}{2} wx^2 = \tfrac{1}{2} wl^2 (C_4 - C_4^2)$$

$$\text{But } w = \frac{4}{3} C_2 F_4 \frac{bd^2}{l^2} = \frac{4}{3} C_2 \frac{F_3}{\rho_2} \frac{bd^2}{l^2}$$

$$\therefore \quad M_x = F_3 \frac{bd^2}{6} 4 \frac{C_2}{\rho_2} (C_4 - C_4^2) \qquad - 5.15$$



For equilibrium

Total compression = Total tension

From equilibrium equation

$$C_1 = \frac{\phi_1^2 + 1}{2} \qquad - 5.16$$

or

$$\phi_1 = \sqrt{2\,C_1 - 1}$$

Resisting moment (RM_x) from stress diagram

$$(RM_x) = F_3 \frac{bd^2}{6} \left[\frac{(1-C_1)^2(2+C_1)}{(C_1 - \phi_1)} - 3\phi_1^2 - (C_1-\phi_1)(2\phi_1 + C_1) \right] \qquad - 5.17$$

$$M_x = (RM_x)$$

$$\frac{4\,C_2}{\rho_2} (C_4 - C_4^2) = \frac{(\phi_1^3 + 2 - 3C_1)}{(C_1 - \phi_1)}$$

This reduces to $2\phi_1^3 - (3+K_1)\,\phi_1^2 + 2K_1\,\phi_1 + (1 - K_1) = 0 \qquad - 5.18$

$$\text{where } K_1 = \frac{4\,C_2}{\rho_2} (C_4 - C_4^2)$$

Using the equation (5.18) the value of ϕ_1 can be found by iteration for any particular value of C_4. Knowing the value of ϕ_1 the value of C_1 can be derived from equation (5.16)

Maximum tensile stress at C_4 1, between A and B = $F_3 \frac{(1- C_1)}{(C_1-\phi_1)}$

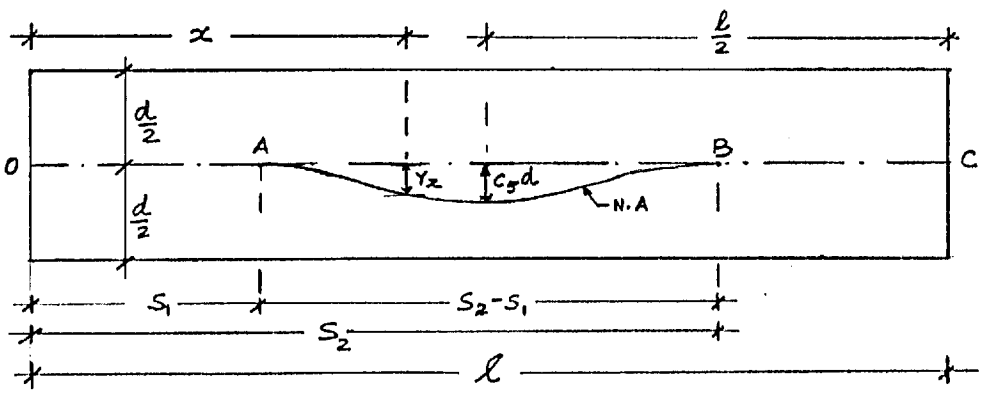
Maximum value of ϕ_1 (at $\frac{1}{2}$) = $\frac{1-\rho_2}{1+\rho_2}$

Maximum value of C_1 (at $\frac{1}{2}$) = $\frac{1 + \rho_2^2}{(1+ \rho_2)^2}$

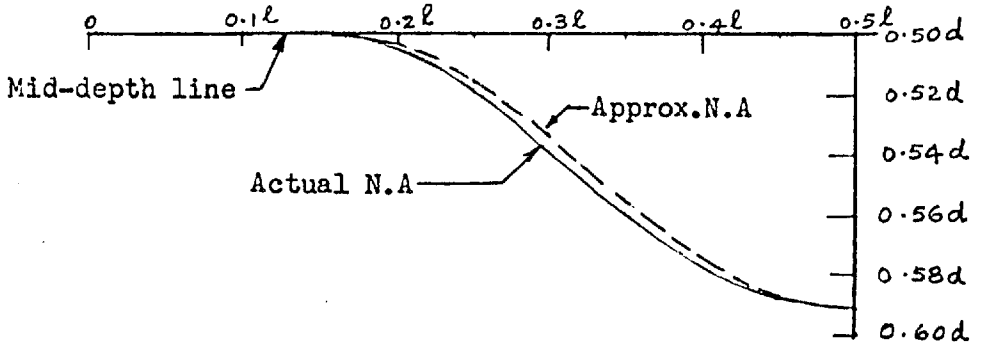
To trace the locus of the neutral axis, the equation (5.18) has to be solved. In this particular case we may have to resort to a trial and error method to get the solution. Because of the high consumption of computer time, this method is unsuitable when the solutions are required at many locations. In order to evaluate $\int \sigma^k dv$ using the numerical integration technique, the values of Y_x are required at various locations.

Alternatively, the location of the N.A may be described by a suitable approx. equation. The locations A and B where the N.A deviates from mid-depth and the magnitude of maximum deviation $C_5 d$ at midspan can be easily found. Using this information the following equation is formulated and it is found to be a good approximation.

$$Y_x = C_5\, d \sin^2 \left\{ \frac{\pi (x - S_1)}{(S_2 - S_1)} \right\}$$



The following sketch shows the actual position of the N.A and the position given by the approximate equation. It will be noticed that the position given by the equation is very close to the actual position. A typical ratio of $\frac{F_3}{F_4} = 0.4$ is chosen for the example. Different scales are adopted for span and depth for better clarity.



Relative positions of approximate and actual neutral axis

Calculation of integral $\int_v \sigma^k dv$

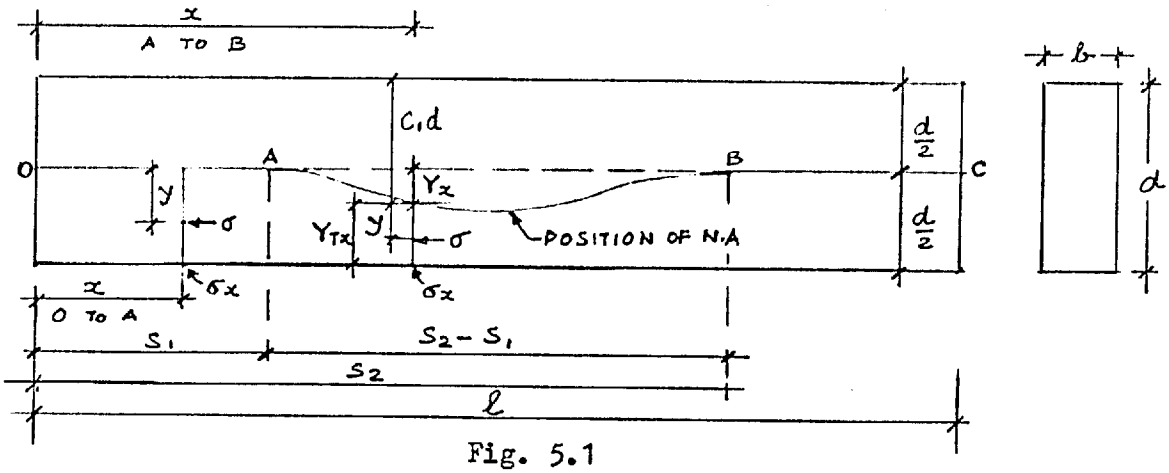
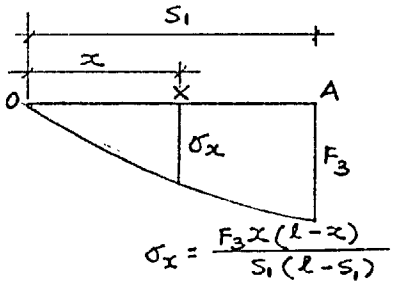
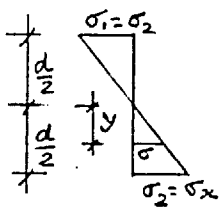


Fig. 5.1

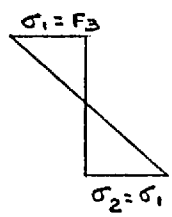
From 0 to A

B.M diagram from 0 to A is part of a parabola. As the material is elastic in this region and the section modulus is constant, the variation of maximum stress σ_x also is represented by a parabola.





AT X



AT A

Variation of max. tensile stress

Let σ be the tensile stress at a depth y from the N.A

$$\sigma = \sigma_x \frac{2y}{d} \qquad \text{but } \sigma_x = F_3 \frac{x(1-x)}{S_1(1-S_1)} \qquad \sigma = \frac{2F_3x(1-x)y}{S_1(1-S_1)d}$$

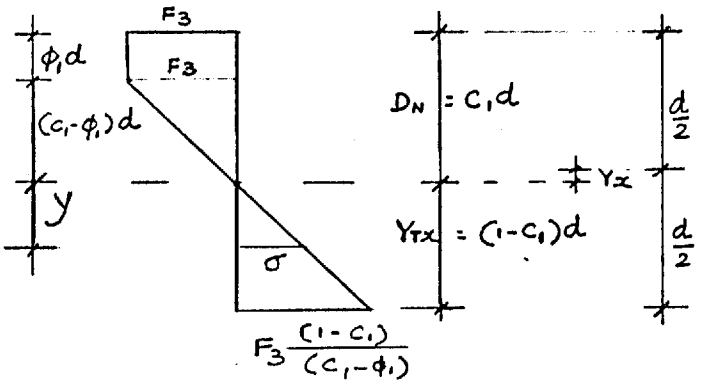
Integral from 0 to A and B to C

$$\int_v \sigma^k dv = 2\int_{x=0}^{S_1}\int_{y=0}^{\frac{d}{2}}\int_{z=0}^{b}\left[\frac{2F_3}{S_1(1-S_1)d}\right]^k \left[x(1-x)y\right]^k dz\, dy\, dx$$

$$= 2b\left[\frac{2F_3}{S_1(1-S_1)d}\right]^k \int_0^{S_1}\int_0^{\frac{d}{2}}\left[x(1-x)y\right]^k dy\, dx \qquad - 5.19$$

$$= 2b\left[\frac{2F_3}{S_1(1-S_1)d}\right]^k I_1 \qquad - 5.20$$

From A to B



$$C_1 d = \frac{d}{2} + Y_x = d\left[\frac{1}{2} + C_5 \sin^2\left\{\frac{\pi(x - S_1)}{(S_2 - S_1)}\right\}\right] = (1 - G_1)d$$

$$Y_{Tx} = \frac{d}{2} - Y_x = d\left[\frac{1}{2} - C_5 \sin^2\left\{\frac{\pi(x - S_1)}{(S_2 - S_1)}\right\}\right] = G_1 d$$

$\therefore C_1 = 1 - G_1$ where $G_1 = \frac{1}{2} - C_5 \sin^2\left\{\frac{\pi(x-S_1)}{(S_2-S_1)}\right\}$

$C_1 - \phi_1 = 1 - G_1 - \sqrt{1 - 2G_1}$ $\quad\because\quad \phi_1 = \sqrt{2C_1 - 1}$

$$\therefore \quad \sigma = \frac{F_3 y}{(C_1 - \phi_1)d} = \frac{F_3 y}{d(1 - G_1 - \sqrt{1-2G_1})}$$

$$\int_v \sigma^k \, dv = b\left(\frac{F_3}{d}\right)^k \int_{x=S_1}^{S_2} \int_{y=0}^{Y_{Tx}} \left[\frac{y}{(1-G_1-\sqrt{1-2G_1})}\right]^k dy \, dx$$

$$= b\left(\frac{F_3}{d}\right)^k I_2 \qquad - 5.21$$

Total integral from 0 to C

$$\int_v \sigma^k \, dv = 2b\left[\frac{2F_3}{S_1(1-S_1)d}\right]^k I_1 + b\left[\frac{F_3}{d}\right]^k I_2 \qquad - 5.22$$

I_1 and I_2 are evaluated by Gauss Quadrature technique.(Appendix 3)

Failure Type 1 Equation (5.19) can be modified to represent this failure.

Replace F_3 by F_4 and S_1 by $\frac{1}{2}$

Integral for total volume

$$\int_v \sigma^k \, dv = 2b\left[\frac{2F_4}{\frac{1}{2}(1-\frac{1}{2})d}\right]^k \int_{x=0}^{\frac{\ell}{2}} \int_{y=0}^{\frac{d}{2}} \left[x(1-x)y\right]^k dy \, dx$$

$$= 2b\left[\frac{8F_4}{l^2 d}\right]^k I_3 \qquad - 5.23$$

5.11.2 Rectangular section with two equal point loads symmetrically placed about centre of span. Distance between loads = Gl.

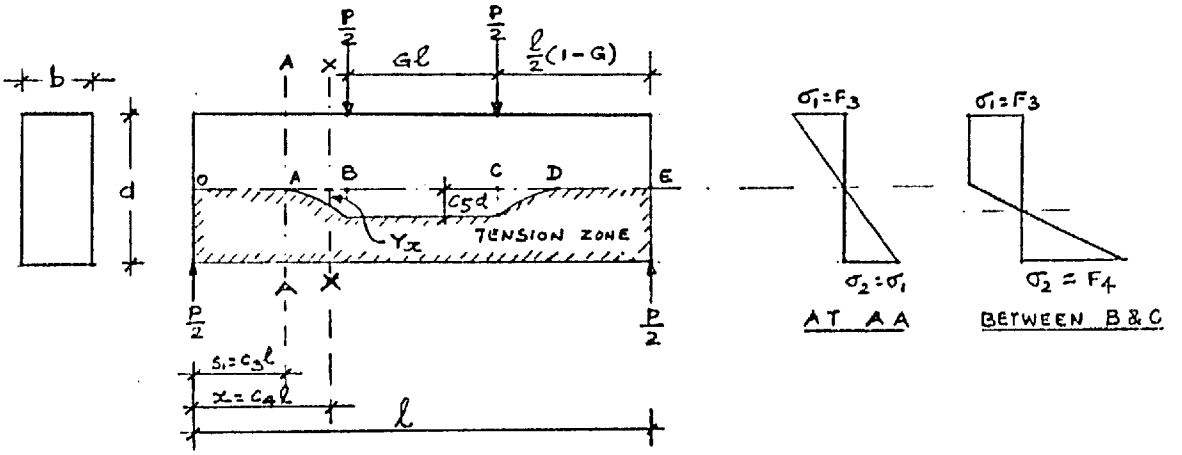


Fig. 5.2

To find the position where N.A deviates from Mid-depth

At B

$$M_B = \frac{P}{2}\frac{l}{2}(1-G) = \frac{Pl}{4}(1-G) = C_2 F_4 \frac{bd^2}{6}$$

$$\text{where } C_2 = \frac{\rho_2(3+8\rho_2+6\rho_2^2-\rho_2^4)}{(1+\rho_2)^4}$$

$$\text{and } \rho_2 = \frac{F_3}{F_4}$$

$$\therefore \quad P = C_2 F_4 \frac{bd^2 4}{6l(1-G)} \qquad - 5.24$$

At A

$$M_A = \tfrac{1}{2} PS_1 = \frac{F_3 bd^2}{6} = \rho_2 F_4 \frac{bd^2}{6}$$

$$\therefore \quad S_1 = \frac{2}{P}\rho_2 \frac{F_4 bd^2}{6}$$

Substituting for P from (5.24) $\qquad S_1 = C_3 l \qquad - 5.25$

$$\text{where } C_3 = \frac{\rho_2(1-G)}{2C_2}$$

To find the depth of N.A at $x = C_4 l$, between A and B

$$M_x = \tfrac{1}{2} Px = C_2 F_4 \frac{bd^2\, 2x}{6l(1-G)} = F_3 \frac{bd^2}{6} \frac{C_4}{C_3}$$

Using equation (5.17) for $R M_x$ and making $(R M_x) = M_x$

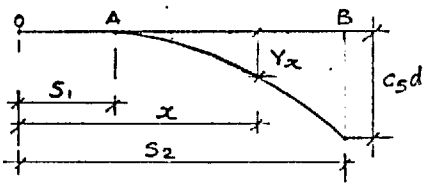
We get $2 \phi_1^3 - (3+K_2) \phi_1^2 + 2 K_2 \phi_1 + (1-K_2) = 0$ - 5.26

where $K_2 = \frac{C_4}{C_3}$ and $\phi_1 = \sqrt{2 C_1 - 1}$

For a particular value of G, the value of C_1 can be obtained by solving equation (5.26) for any value of C_4.

Alternatively, the locus of the N.A can be represented exactly by the following parabolic curve.

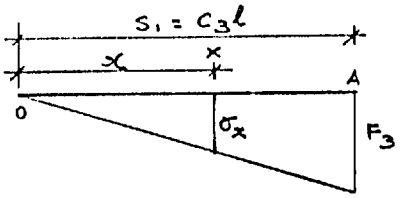
$$Y_x = C_5 d \left[1 - \frac{(S_2 - x)(S_2 + x - 2 S_1)}{(S_2 - S_1)^2} \right]$$

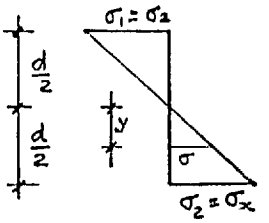


Calculation of Integral $\int_v \sigma^k \, dv$

From O to A

The variation of maximum stress O and A is as shown below.





Variation of max. tensile stress

AT X

$$\sigma_x = F_3 \frac{x}{S_1} \qquad \sigma = \sigma_x \frac{2y}{d} = \frac{2 F_3}{S_1 d} xy$$

Integral from O to A and D to E

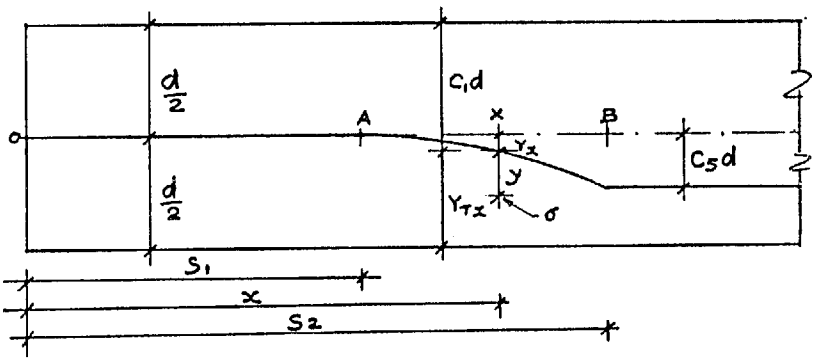
$$\int_v \sigma^k \, dv = 2 \int_{x=o}^{S_1} \int_{y=o}^{\frac{d}{2}} \int_{z=o}^{b} \left(\frac{2 F_3}{S_1 d} \right)^k (xy)^k \, dz \, dy \, dx$$

$$= 2 b \left(\frac{2 F_3}{S_1 d} \right)^k \int_o^{S_1} \int_o^{\frac{d}{2}} (xy)^k \, dy \, dx$$

$$= 2 b \left(\frac{2 F_3}{S_1 d} \right)^k \left(\frac{d}{2} \right)^{k+1} \left(\frac{1}{k+1} \right) S_1^{k+1} \left(\frac{1}{k+1} \right)$$

$$= \frac{bd \, S_1}{(k+1)^2} F_3^k \qquad - 5.27$$

From A to B



Following the same procedure adopted for the uniformly distributed load,

$C_1 d = \frac{d}{2} + Y_x = (1 - G_2) d$

$Y_{Tx} = \frac{d}{2} - Y_x = G_2 \, d$

where $Y_x = C_5 \, d \left[1 - \frac{(S_2 - x)(S_2 + x - 2S_1)}{(S_2 - S_1)^2} \right]$

$C_1 = 1 - G_2$

$G_2 = \frac{1}{2} - \frac{Y_x}{d}$

$C_1 - \phi_1 = 1 - G_2 - \sqrt{1 - 2 G_2}$

$$\sigma = \frac{F_3 \, y}{(C_1 - \phi_1) d} = \frac{F_3 \, y}{d(1 - G_2 - \sqrt{1 - 2 G_2})}$$

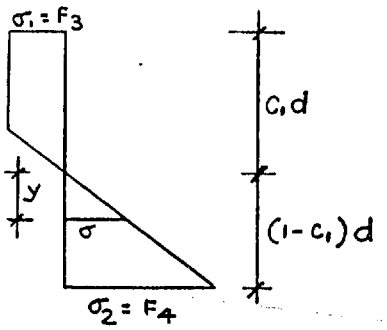
Integral from A to B and C to D

$$\int_v \sigma^k \, dv = 2\, b \left(\frac{F_3}{d}\right)^k \int_{x=S_1}^{S_2} \int_{y=0}^{Y_{Tx}} \left[\frac{y}{(1-G_2-\sqrt{1-2\,G_2})}\right]^k dy\, dx$$

$$= 2\, b \left(\frac{F_3}{d}\right)^k I_4 \qquad - 5.28$$

From B to C

In this region maximum tensile stress is constant and is equal to F_4



$$\sigma = \frac{F_4}{(1-C_1)} \cdot \frac{y}{d}$$

Integral from B to C

$$\int_v \sigma^k \, dv = Glb \left[\frac{F_4}{(1-C_1)d}\right]^k \int_o^{(1-C_1)d} y^k \, dy$$

$$= Gbdl\, F_4^{\,k} \, \frac{(1-C_1)}{(k+1)} \qquad - 5.29$$

Total integral from O to E

$$\int_v \sigma^k \, dv = \frac{bd\, S_1}{(k+1)^2} F_3^{\,k} + 2\, b \left(\frac{F_3}{d}\right)^k I_4 + Gbdl\, F_4^{\,k} \, \frac{(1-C_1)}{(k+1)} \qquad - 5.30$$

Integral I_4 is evaluated by Gauss Quadrature technique.

Failure Type 1

Zones A B and C D do not exist in this failure.

Replace S_1 by $\frac{1}{2}(1-G)$ and F_3 by F_4 in equation (5.27)

$C_1 = 0.5$ in equation (5.29)

Total integral from O to E

$$\int_v \sigma^k \, dv = \tfrac{1}{2} \frac{bdl\,(1-G)}{(k+1)^2} \; F_4^k + \tfrac{1}{2} \frac{Gbdl}{(k+1)} \; F_4^k$$

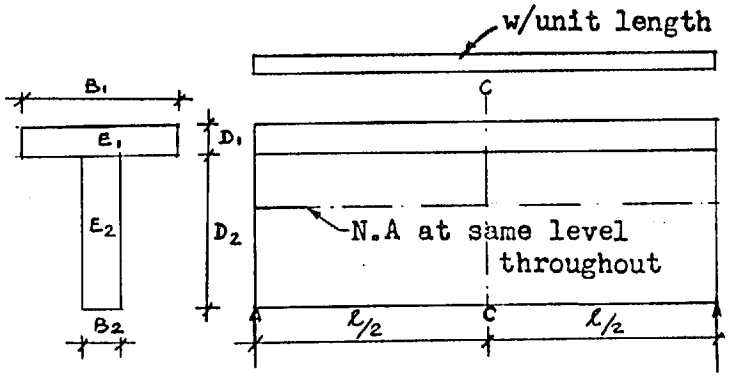
$$= \tfrac{1}{2} \frac{bdl\, F_4^k}{(k+1)^2} \; (1 + Gk) \qquad - 5.31$$

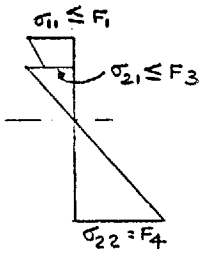
5.11.3 T section with Non-layered Flange T section with neutral axis within the rib only is considered in this thesis.

Uniformly distributed load

Two types of failure are possible.

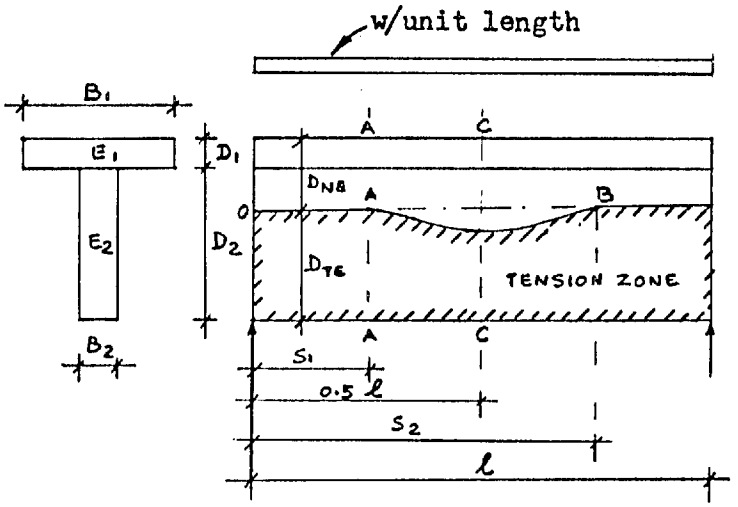
Failure type 1 Elastic failure

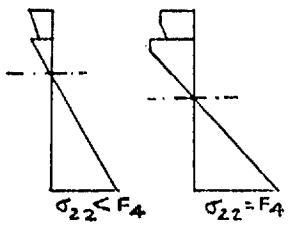




Stress diagram at C C

Failure type 2 Elasto-plastic failure





At A A At C C

Typical stress diagrams

Fig. 5.3

As in the previous occasion failure type 1 can be considered as a special case of failure type 2.

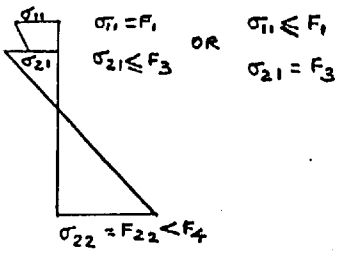
To find the position where N.A deviates from constant depth

If the values of F_1, F_3, F_4 and E_1 and E_2 are known the ultimate resisting moment (at C C) can be calculated. Let this be U and is equal to $\frac{wl^2}{8}$

$$w = \frac{8U}{l^2} \qquad - 5.32$$

Elastic N.A = $D_{NE} = C_1 D_1$ where $C_1 = \frac{\beta/\gamma + \alpha(2+\alpha)}{2(\beta/\gamma + \alpha)}$

By trial and error method stress diagram at A A can be drawn so that none of the stresses exceeds the ultimate value, but at least one attains the ultimate limit.



At A A

Let $\sigma_{22} = F_{22}$

Resisting moment R M_A (from stress diagram) = $C_{2E} \frac{B_2 D_2^2}{6} F_{22}$ - 5.33

where $C_{2E} = \frac{(1+\alpha-C_1)^2\{2(1+\alpha)+C_1\} - (C_1-1)^2(2+C_1) - (3C_1-2)\frac{\beta}{\gamma}}{\alpha^2(1+\alpha-C_1)}$

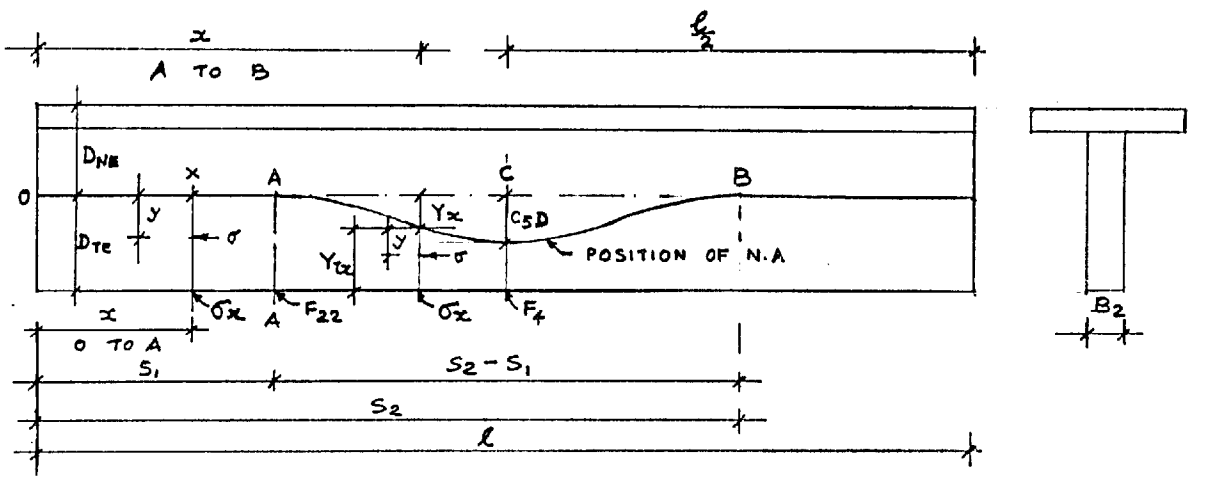
Bending moment B $M_A = \frac{1}{2} wlS_1 - \frac{1}{2} wS_1^2$ - 5.34

As $(R\ M_A) = (B\ M_A)$, we get $S_1 = + \frac{W_1 - \sqrt{W_1^2 - 2w(R\ M_A)}}{w}$ - 5.35

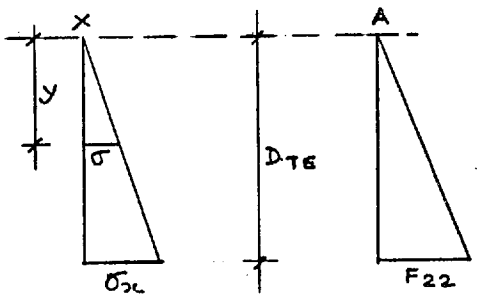
where $W_1 = \frac{1}{2} wl$

As in the case of the rectangular section, the locus of the N.A between A and B is represented by an approximate equation. With the aid of the equilibrium equation (total compression = total tension) the depth of N.A at C C can be found by trial and error method. Now the boundary of tensile zone is completely known.

Calculation of Integral $\int_v \sigma^k \, dv$

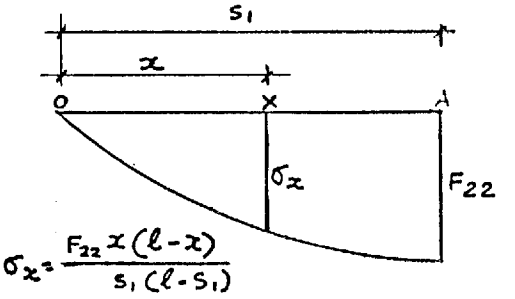


From 0 to A



At X At A

Stress diagrams in tension zone



Variation of max. tensile stress

$$\sigma = \frac{\sigma_x\, y}{D_{TE}} = \frac{F_{22}\, x(1-x)}{S_1(1-S_1)} \frac{y}{D_{TE}} = \frac{F_{22}\, x(1-x)y}{S_1(1-S_1)D_{TE}}$$

where F_{22} is the maximum tensile stress at section A A.

Integral from O to A and B to D

$$\int_v \sigma^k \, dv = 2 \int_{x=0}^{S_1} \int_{y=0}^{D_{TE}} \int_{z=0}^{B_2} \left[\frac{F_{22}}{S_1(1-S_1)D_{TE}} x(1-x)y \right]^k dz \, dy \, dx$$

$$= 2 \, B_2 \left[\frac{F_{22}}{S_1(1-S_1)D_{TE}} \right]^k \int_0^{S_1} \int_0^{D_{TE}} \left[x(1-x)y \right]^k dy \, dx$$

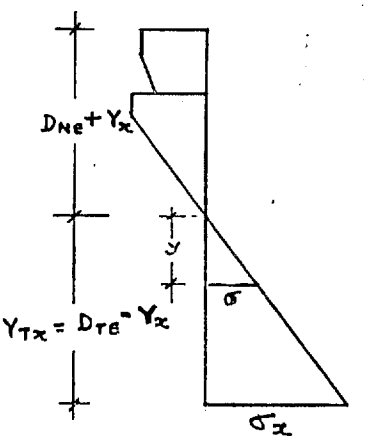
$$= 2 \, B_2 \left[\frac{F_{22}}{S_1(1-S_1)D_{TE}} \right]^k I_5 \qquad - 5.36$$

From A to B

$$Y_x = C_5 \, D \sin^2 \left\{ \frac{\pi (x - S_1)}{(S_2 - S_1)} \right\}$$

Where $C_5 \, D$ = depth of N.A at C C – (depth of elastic N.A)

Now σ_x can be calculated to satisfy the equilibrium equation. But to simplify the calculations the variation of σ_x from (A) to (B) is assumed as parabolic.



$$\sigma_x = F_{22} + \frac{4(F_4 - F_{22})(x - S_1)(1 - S_1 - x)}{(1 - 2S_1)^2}$$

$$\sigma = \frac{\sigma_x \, Y}{(D_{TE} - Y_x)}$$

$$\int_v \sigma^k \, dv = B_2 \int_{x=S_1}^{S_2} \int_{y=0}^{Y_{Tx}} \left[\frac{\sigma_x}{D_{TE} - Y_x} \right]^k dy \, dx = B_2 \, I_6 \qquad - 5.37$$

Total integral from O to D

$$\int_v \sigma^k \, dv = 2 B_2 \left[\frac{F_{22}}{S(1-S_1)D_{TE}} \right]^k I_5 + B_2 I_6 \qquad - 5.38$$

Integral I_5 and I_6 are evaluated by Gauss Quadrature Technique.

Failure Type 1

Equation (5.36) can be modified to represent this failure.

Zone A B does not exist here.

Replace F_{22} by F_4 and S_1 by $\frac{1}{2}$

Total integral from O to D

$$\int_v \sigma^k \, dv = 2 B_2 \left[\frac{4 F_4}{1^2 D_{TE}} \right]^k I_7 \qquad - 5.39$$

Integral I_7 is evaluated by Gauss Quadrature technique.

5.11.4 Two equal point loads symmetrically placed about centre of span

Distance between loads = Gl

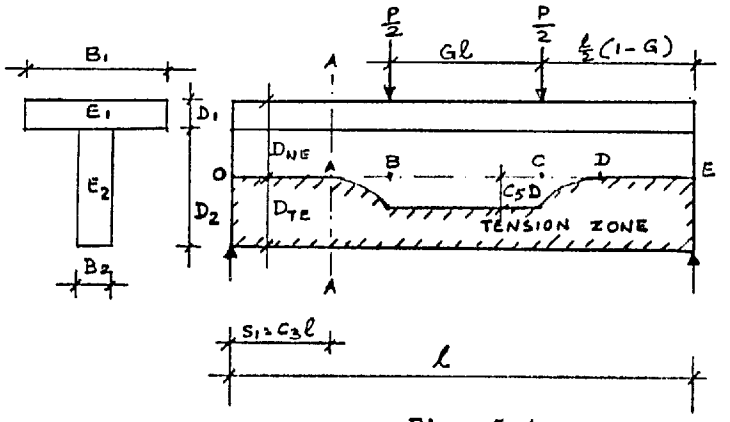
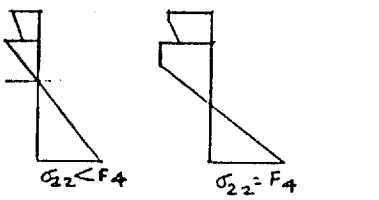


Fig. 5.4



At A A Between B & C

Typical stress diagrams

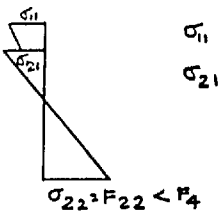
To find the position where N.A deviates from constant depth

If the values of F_1, F_3, F_4, E_1 & E_2 are known the ultimate resisting moment (moment between B and C) can be calculated. Let this be U and is equal to $\frac{1}{4}$ Pl (1-G)

$$\therefore \quad P = \frac{4U}{l(1-G)} \qquad - 5.40$$

Elastic N.A = $D_{NE} = C_1 D_1$ where $C_1 = \dfrac{\frac{\beta}{\gamma} + \alpha(2+\alpha)}{2\left(\frac{\beta}{\gamma} + \alpha\right)}$

By trial and error method stress diagram at A A can be drawn so that none of the stresses exceed the ultimate value, but at least one attains the ultimate limit.



$\sigma_{11} = F_1$ OR $\sigma_{11} \leq F_1$

$\sigma_{21} \leq F_3$ $\sigma_{21} = F_3$

At A A

Let $\sigma_{22} = F_{22}$

Resisting moment R M_A (from stress diagram) = $C_{2E} \dfrac{B_2 D_2^2}{6} F_{22}$ - 5.41

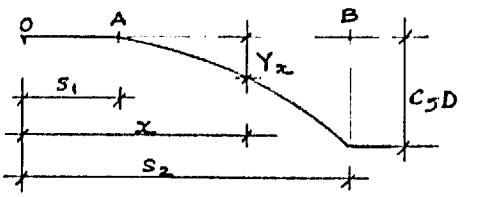
where C_{2E} is same as in equation 5.33

$$BM_A = \tfrac{1}{2} PS_1 = \frac{2\,U}{1(1-G)}\,S_1 \qquad - 5.42$$

$$\text{As}\left(RM_A\right)=\left(BM_A\right) \text{ we get } S_1 = \left(RM_A\right)\frac{1(1-G)}{2\,U} \qquad - 5.43$$

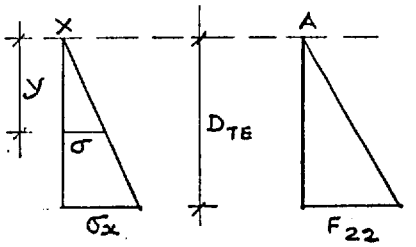
As in the case of rectangular section, the locus of N.A between A & B can be described by a parabolic equation.

$$Y_x = C_5\,D\left[\,1 - \frac{(S_2-x)(S_2+x-2S_1)}{(S_2-S_1)^2}\,\right]$$



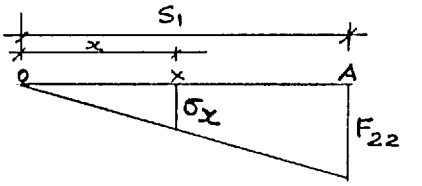
Calculation of Integral $\int_v \sigma^k\,dv$

From O to A



At X At A

Stress diagrams in tension zone



Variation of max. tensile stress

$$\sigma = \frac{\sigma_x\,y}{D_{TE}} = \frac{F_{22}\,xy}{S_1\,D_{TE}}$$

Integral from O to A and D to E

$$\int_v \sigma^k\,dv = 2\int_{x=0}^{S_1}\int_{y=0}^{D_{TE}}\int_{z=0}^{B_2}\left[\frac{F_{22}\,xy}{S_1\,D_{TE}}\right]^k dz\,dy\,dx$$

$$= 2\,B_2\left[\frac{F_{22}}{S_1\,D_{TE}}\right]^k\int_0^{S_1}\int_0^{D_{TE}}(xy)^k\,dy\,dx$$

$$= \frac{2\,B_2\,S_1\,D_{TE}}{(k+1)^2}\,F_{22}^{\,k} \qquad - 5.44$$

From A to B

$$Y_x = C_5 D \left[1 - \frac{(S_2 - x)(S_2 + x - 2S_1)}{(S_2 - S_1)^2} \right]$$

$$Y_{Tx} = D_{TE} - Y_x$$

Linear variation of stress from F_{22} to F_4 has been assumed. This is a good approximation.

$$\sigma_x = F_{22} + (F_4 - F_{22}) \frac{(x - S_1)}{(S_2 - S_1)} = F_{22} \left[1 - \frac{(R_1 - 1)(x - S_1)}{(S_2 - S_1)} \right]$$

where $R_1 = \frac{F_4}{F_{22}}$

$$\sigma = \frac{\sigma_x y}{Y_{Tx}} = F_{22} \left[1 + (R_1 - 1) \frac{(x - S_1)}{(S_2 - S_1)} \right] \frac{y}{Y_{Tx}}$$

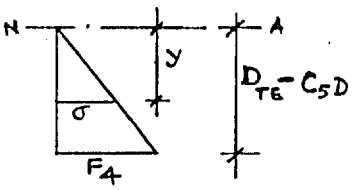
Integral from A to B & C to D

$$\int_v \sigma^k \, dv = 2 \int_{x=S_1}^{S_2} \int_{y=0}^{Y_{Tx}} \int_{z=0}^{B_2} \left[F_{22} \left\{ 1 + \frac{(R_1 - 1)(x - S_1)}{(S_2 - S_1)} \right\} \frac{y}{Y_{Tx}} \right]^k dz \, dy \, dx$$

$$= 2 B_2 (F_{22})^k \int_{S_1}^{S_2} \int_{0}^{Y_{Tx}} \left[\left\{ 1 + \frac{(R_1 - 1)(x - S_1)}{(S_2 - S_1)} \right\} \frac{y}{Y_{Tx}} \right]^k dy \, dx$$

$$= 2 B_2 (F_{22})^k I_8 \qquad - 5.45$$

From B to C



$$\sigma = \frac{F_4 y}{(D_{TE} - C_5 D)}$$

Integral from B to C

$$\int_v \sigma^k \, dv = \int_{x=0}^{Gl} \int_{y=0}^{D_{TE}-C_5D} \int_{z=0}^{B_2} \left(\frac{F_4 \, y}{D_{TE} - C_5 D} \right)^k dz \, dy \, dx$$

$$= B_2 \, Gl \left(\frac{F_4}{D_{TE} - C_5 D} \right)^k \int_0^{D_{TE}-C_5D} y^k \, dy$$

$$= B_2 \, Gl \, \frac{F_4^k \, (D_{TE} - C_5 D)}{(k+1)} \qquad - 5.46$$

Total integral from O to E

$$\int_v \sigma^k \, dv = \frac{2 \, B_2 \, S_1 \, D_{TE}}{(k+1)^2} \, F_{22}^k + 2 \, B_2 (F_{22})^k \, I_8 + B_2 Gl \frac{F_4^k}{(k+1)} (D_{TE} - C_5 D) \qquad - 5.47$$

Integral I_8 is evaluated by Gauss Quadrature Technique.

Failure Type 1

Zones A B & C D do not exist in this failure.

Replace S_1 by $\frac{1}{2}l\,(1-G)$ and F_{22} by F_4 in equation (5.44)

$C_5D = 0$ in equation (5.46)

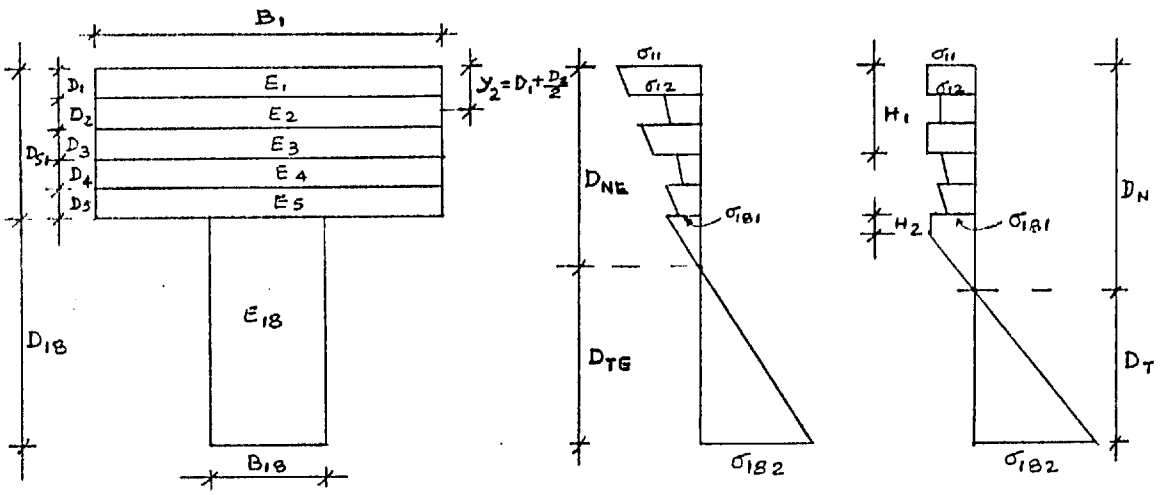
Total integral from O to E

$$\int_v \sigma^k \, dv = \frac{B_2 l (1 - G) D_{TE}}{(k+1)^2} \, F_4^k + \frac{B_2 \, Gl \, F_4^k \, D_{TE}}{(k+1)}$$

$$= \frac{B_2 l \, D_{TE} \, F_4^k \, (1 + Gk)}{(k+1)^2} \qquad - 5.48$$

5.11.5 T section with layered flange

The procedure for analysis is same as that of T section with non-layered flange. The following equations are relevant to the T section with layered flange.



Typical stress diagrams

Fig. 5.5

Depth of elastic N.A

$$D_{NE} = \frac{\sum_{i=1}^{n} B_1 E_i D_i Y_i + B_{18} E_{18} D_{18} (D_{S1} + \frac{D_{18}}{2})}{\sum_{i=1}^{n} B_1 E_i D_i + B_{18} E_{18} D_{18}} \qquad - 5.49$$

where n is the number of layers.

Taking moments about the extreme top fibre, the resisting moment at any section along the span can be calculated from stress diagram.

$$RM_x = \tfrac{1}{2}\sigma_{182} B_{18} D_T (D_N + \tfrac{2}{3}D_T) - \sigma_{181} B_{18} H_2 (D_{S1} + \tfrac{1}{2}H_2)$$

$$- \tfrac{1}{2}\sigma_{181} B_{18} (D_N - D_{S1} - H_2) \frac{(2D_{S1} + 2H_2 + D_N)}{3} - \sum_{i=1}^{n} B_1 \tfrac{1}{2}(\sigma_{i1} + \sigma_{i2}) D_i w_i \qquad - 5.50$$

With the aid of this additional information, the T section with a layered flange is analysed. All other assumptions are the same for both layered and non-layered flanged section. The procedures for finding the boundaries of the tension zone and the calculation of $\int_v \sigma^k \, dv$ for the tensile stresses are the same as that of T section with non-layered flange. As the neutral axis is within the rib, the resulting equations for the integral $\int_v \sigma^k \, dv$ are the same even though the numerical values are different. They are summarised as follows:

Loading case	Failure type	Relevant equation for $\int_v \sigma^k \, dv$
Uniformly distributed load	1	5.39
Uniformly distributed load	2	5.38
Two point loads symmetrically placed	1	5.48
Two point loads symmetrically placed	2	5.47

5.12 Derivation of the values of k and K_0 from test results

We have already seen that when rectangular timber beams are tested to failure in bending, there are two possible modes of failure.

1) Elastic failure. 2) Elasto-plastic failure.

5.12.1 Elastic failure

Let the loading arrangement be as shown below.

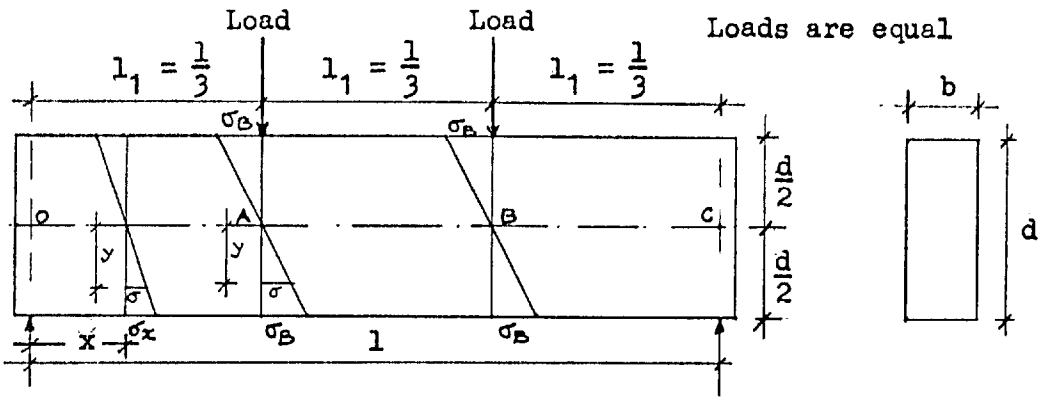


Fig. 5.6

σ_B is the ultimate tensile stress at failure.

$$I = \int_v \sigma^k \, dv = K_0^k$$

The integral I is evaluated using the following steps.

Step.1 From O to A

$$\sigma_x = \sigma_B \frac{x}{l_1} \qquad \sigma = \sigma_x \frac{2y}{d} = \sigma_B \frac{2xy}{l_1 d}$$

$$\int_v \sigma^k \, dv = \int_{x=0}^{l_1} \int_{y=0}^{\frac{d}{2}} \int_{z=0}^{b} \sigma^k \, dz \, dy \, dx$$

$$= \sigma_B^k \left(\frac{2}{d}\right)^k \left(\frac{1}{l_1}\right)^k \, b \int_0^{l_1} \int_0^{\frac{d}{2}} (xy)^k \, dy \, dx$$

$$= \sigma_B^k \left(\frac{2}{d}\right)^k \left(\frac{1}{l_1}\right)^k \, b \left(\frac{d}{2}\right)^{k+1} \frac{1}{(k+1)} \quad \frac{l_1^{k+1}}{(k+1)}$$

$$\int_v \sigma^k \, dv = \sigma_B^k \, \frac{d}{2} \, l_1 \, \frac{b}{(k+1)^2} = \frac{\sigma_B^k \, V}{2(1+k)^2} \qquad \text{where } V = bdl_1$$

Integral from O to A + B to C

$$\int_v \sigma^k \, dv = 2 \, \frac{\sigma_B^k \, V}{2(1+k)^2} = \frac{\sigma_B^k \, V}{(1+k)^2} \qquad - 5.51$$

Step 2. From A to B

Bending moment is constant in this region.

$$\sigma = \sigma_B \, \frac{2y}{d}$$

$$\int_v \sigma^k \, dv = \sigma_B^k \, (\tfrac{2}{d})^k \, bl_1 \int_o^{\frac{d}{2}} y^k \, dy$$

$$= \sigma_B^k \, (\tfrac{2}{d})^k \, \frac{bl_1}{(k+1)} \, (\tfrac{d}{2})^{k+1} = \sigma_B^k \, \frac{bdl_1}{2\,(k+1)} = \frac{\sigma_B^k \, V}{2(k+1)}$$

$$\int_v \sigma^k \, dv = \frac{\sigma_B^k \, V}{2(k+1)} \qquad - 5.52$$

Total integral from O to C

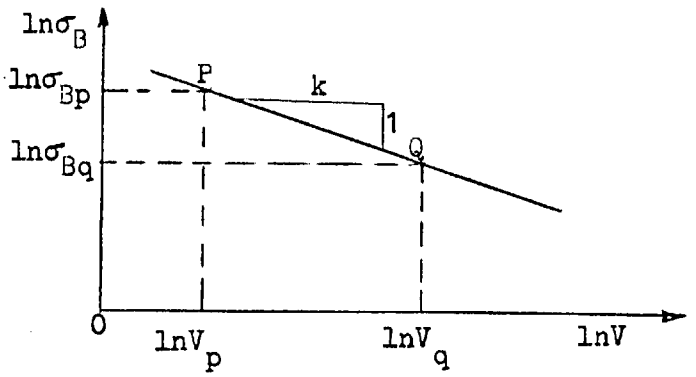
$$\int_v \sigma^k \, dv = \frac{\sigma_B^k \, V}{(1+k)^2} + \frac{\sigma_B^k \, V}{2(1+k)} = \sigma_B^k \, V \, \frac{(k+3)}{2(k+1)^2}$$

$$\sigma_B^k \, V \, \frac{(k+3)}{2(k+1)^2} = K_O^k$$

$$\sigma_B = \left\{ \frac{2(k+1)^2}{(k+3)} \right\}^{\frac{1}{k}} \frac{K_O}{V^{\frac{1}{k}}} \qquad - 5.53$$

$$\ln \sigma_B = \ln \left[\left\{ \frac{2(k+1)^2}{(k+3)} \right\}^{\frac{1}{k}} K_O \right] - \frac{1}{k} \ln V \qquad - 5.54$$

After testing different volumes, if the ultimate tensile stresses are σ_{B1}, σ_{B2}, σ_{B3}, σ_{B4}, ... for volumes V_1, V_2, V_3, V_4, ... respectively a graph can be plotted with lnV on the abscissa and ln σ_B on the ordinate. From the slope of the resulting line the value of k is found. Now using the equation (5.59) the value of K_0 can be found. For each volume several specimens are to be tested and the mean value of σ_B is used to plot the graph. By using the mean value of σ_B we get the value of K_0 at 50% probability of failure which will be denoted as K_0. (0.50)



Let P ($\ln V_p$, $\ln\sigma_{Bp}$) and Q ($\ln V_q$, $\ln\sigma_{Bq}$) be two points on the graph to represent volumes V_p and V_q.

Equation 5.54 can be written as follows:

$$\ln\sigma_B = a - \frac{1}{k}\ln V \qquad - 5.55$$

$$\text{where } a = \ln\left[\left\{\frac{2(k+1)^2}{(k+3)}\right\}^{\frac{1}{k}} K_0\right]$$

$$\therefore \ln\sigma_{Bp} = a - \frac{1}{k}\ln V_p \qquad - 5.56$$

$$\ln\sigma_{Bq} = a - \frac{1}{k}\ln V_q \qquad - 5.57$$

From equations (5.56) and (5.57)

$$k = \frac{\ln V_q - \ln V_p}{\ln\sigma_{Bp} - \ln\sigma_{Bq}} \qquad - 5.58$$

From equation (5.53)

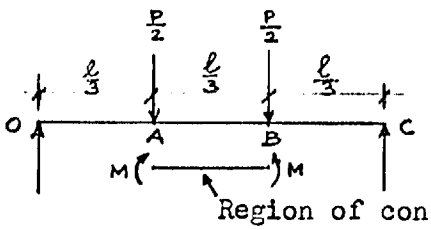
$$K_0 = \sigma_{Bq}\left[\frac{V_q(k+3)}{2(k+1)^2}\right]^{\frac{1}{k}} \qquad - 5.59$$

5.12.2 Approximate determination of k and K_0

Integration becomes much easier if the middle third volume (volume with constant moment) is only considered. This is particularly revelant when elasto-plastic failure is analysed. The error involved is found as follows.

To find the error in estimating the values of k and K_0 in mode 1 when the region A to B only is considered.

Case 1. For region A to B



$$\int_v \sigma^k \, dv = \frac{\sigma_B^k \, V}{2(k+1)} = K_0^k$$

$$\sigma_B = \left\{ 2\,(k+1) \right\}^{\frac{1}{k}} \frac{k_0}{V^{\frac{1}{k}}} = A_1 \frac{K_0}{V^{\frac{1}{k}}}$$

$$\ln\sigma_B = \ln \left[A_1 K_0 \right] - \frac{1}{k} \ln V \qquad - 5.60$$

Case 2. For full length of the beam O to C

$$\int_v \sigma^k \, dv = \sigma_B^k \, \frac{(k+3)}{2(k+1)^2} \, V = K_0^k$$

$$\sigma_B = \left\{ \frac{2(k+1)^2}{(k+3)} \right\}^{\frac{1}{k}} \frac{K_0}{V^{\frac{1}{k}}} = A_2 \frac{K_0}{V^{\frac{1}{k}}}$$

$$\ln\sigma_B = \ln \left[A_2 K_0 \right] - \frac{1}{k} \ln V \qquad - 5.61$$

It will be noticed that the value of k is not affected. however, the value of K_0 is different for case 1 and case 2.

Values of A_1 and A_2 are given in the following table for some typical values of k. Enough test data are not available to estimate the values of k appropriate for tension parallel to the grain. However, Barrett's (1974) Table 5 for tension perpendicular to the grain of Douglas fir shows that the value of k ranges from 2.9 to 6.69 for commercial material and 3.61 to 10.45 for clear material. The mean values for commercial and clear material are 4.04 and 6.35 respectively.

k	A_1	A_2	% error in A_1
3	2.0000	1.7472	+ 14.47
4	1.7793	1.6348	+ 8.78
5	1.6438	1.5518	+ 5.93
6	1.5525	1.4888	+ 4.28
7	1.4860	1.4394	+ 3.24
8	1.4352	1.3996	+ 2.54
9	1.3950	1.3670	+ 2.05
10	1.3622	1.3396	+ 1.69
11	1.3350	1.3164	+ 1.41
12	1.3117	1.2964	+ 1.20
13	1.2922	1.2790	+ 1.03
14	1.2750	1.2636	+ 0.90

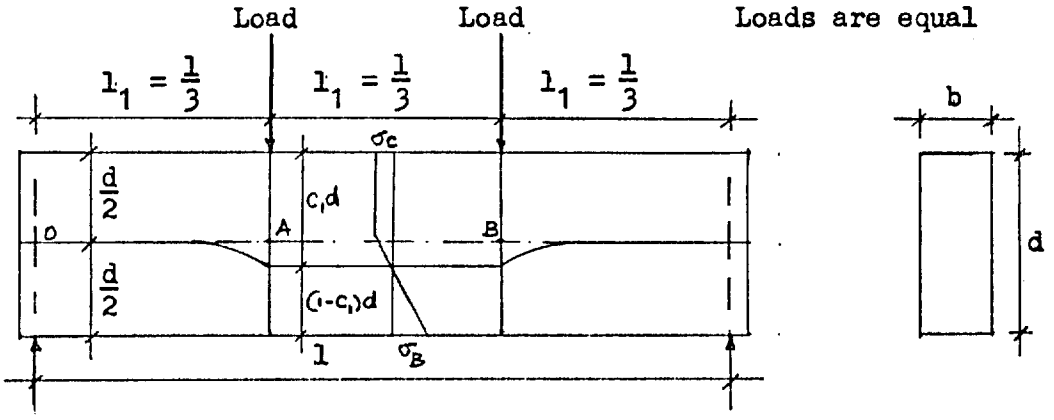
$$A_1 = \left\{2(k+1)\right\}^{\frac{1}{k}}$$

$$A_2 = \left[\frac{2(k+1)^2}{(k+3)}\right]^{\frac{1}{k}}$$

In the most general form $\sigma_B = A^* \frac{K_0}{V^{\frac{1}{k}}}$ or $K_0 = \sigma_B \frac{V}{A^*}^{\frac{1}{k}}$

K_0 is inversely proportional to A^*. From this we can infer that when the region A to B is only considered, a slightly lower value of K_0 is obtained.

5.12.3 Elasto-plastic failure Approximate determination of k and K_0



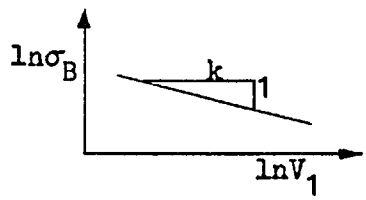
Ultimate resisting moment can be found from the bending test. By testing small specimens from compression zone of region AB, the ultimate compressive stress σ_c also can be found. Knowing the values of the ultimate resisting moment and the ultimate compressive stress, the values of the ultimate tensile stress σ_B and the coefficient C_1 can be derived. Without loosing much accuracy and without involving in complicated integration, values of k and K_0 can be estimated as follows by considering the volume between A & B only (see section 5.12.2).

$$\int_v \sigma_B^k \, dv = V_1(1-C_1) \frac{\sigma_B^k}{(k+1)} = K_0^k \qquad \text{where } V_1 = bdl_1$$

$$\therefore \quad \sigma_B^k = \left(\frac{k+1}{1-C_1}\right) \frac{K_0^k}{V_1}$$

$$\sigma_B = \left(\frac{k+1}{1-C_1}\right)^{\frac{1}{k}} \frac{K_0}{V_1^{\frac{1}{k}}}$$

$$\ln\sigma_B = \ln\left\{\left(\frac{k+1}{1-C_1}\right)^{\frac{1}{k}} K_0\right\} - \frac{1}{k} \ln V_1 \qquad - 5.62$$



Plot $\ln\sigma_B$ against the corresponding value of $\ln V_1$ as shown above. From the slope of the resulting line, value of k is obtained. From equation (5.62) value of K_0 can be calculated.

5.13 Solutions for typical examples using Weibull's theory

With the aid of computer programs PNT and PLT, several beams with non-layered and layered flanges were analysed.

Table 7 shows the probability of failure of a T beam at different levels of bending moment.

The relationship of flange breadth with the ultimate resisting moment and the ultimate tensile stress attained by the extreme bottom fibre of the rib is given in Table 8. As anticipated, the increase in flange width results in an increase in the ultimate resisting moment. However, it is noticed that the ultimate tensile stress attained by the rib is reduced with the increase of flange width. This can be explained as follows. When the flange width is increased, the neutral axis is shifted nearer to the flange and thereby the volume of the rib which is under tensile stress is increased. From Weibull's theory we know that there is a greater probability that a region of low strength will occur in a large volume than in a small volume. This is why the ultimate tensile stress is decreased with the increase of flange width.

The effect of k, K_0, E_1 and E_2 on the resisting moment at 5% probability of failure is given in Tables 9, 10, 11 and 12 respectively. Three loading cases have been considered. Uniformly distributed load is chosen from these tables to summarise the results. Let the properties be as follows.

$k = 10 \qquad K_0 = 100 \qquad E_1 = E_2 = 8300\ N/mm^2$

The following table is prepared to compare the effect on the resisting moment when one of the properties is decreased or increased by 20% while others are kept constant.

Variation of the property %	Property			
	k	K_0	E_1	E_2
	Effect on the resisting moment %			
- 20	- 33.12	- 19.97	- 2.94	+ 4.52
+ 20	+ 30.22	+ 20.02	+ 3.93	-2.39

It can be seen that the resisting moment is very sensitive to k and K_0. The material property k is related to the variability in such a way that when k is larger, variability is smaller. As K_0 is the measure of the strength of the material, the increase of the resisting moment is resulted with the increase of K_0.

Table 13 shows the ultimate resisting moments and the ultimate tensile stresses of rectangular solid beams for different spans and different type of loading. Two different sets of values of k and K_0 are also considered. The span varies from 1200mm to 2400mm with an increment of 300mm. Three loading cases are considered as follows.

1. One point load at midspan.
2. Uniformly distributed load throughout the span.
3. Two equal point loads symmetrically placed at 0.333 span.

Although the cross-section is same, a reduction in the ultimate resisting moment is noticed with the increase of span. Another important observation is that for a constant span, the ultimate resisting moment is highest for case 1 and lowest for case 3. This is due to the fact that the volume which is under high tensile stress is lowest in case 1 and highest in case 3.

Tables 14 and 15 for the T beams with non-layered and layered flanges respectively, are similar to Table 13 and similar conclusions can be drawn.

Tables 16 and 16A compare the resisting moments of T beams with layered flanges and equivalent non-layered flanges. It will be of interest to note that the difference is less than 2½% for the sections considered. For practical purposes plywood can be considered as non-layered material for deriving the ultimate resisting moment of a T beam if the equivalent values of modulus of elasticity and the compressive strength are known.

Different species of plywood are considered for the flange of the T beam in Table 17. Although the modulus of elasticity of birch is 31.7% more than that of makore, the increase in the resisting moment is less than 5%. At 5% probability of failure, elastic failure (mode 1) always occurs and the compressive stress in the flange is well below the ultimate stress value. For this reason the ultimate compressive strength of the flange has very little effect on the resisting moment at 5% probability of failure and practically no advantage is gained by increasing the strength of the flange enormously. Hence it can be inferred that at 5% probability of failure, which is the basis of the assumed characteristic strength, the resisting moment of a T beam is generally governed by the tensile strength properties of the rib.

Tables 18 and 19 show how the results of the analysis of T beams can be applied to the stressed-skin panel. Normally the rib spacing is constant throughout the width of the panel and the flange width of the T beam is taken as the rib spacing. A 1200 mm wide panel with 400 mm rib spacing has been considered as three T beams with 400 mm wide flange. Table 19 shows the resisting moment contributed by the Douglas fir plywood skin for various rib spacing in a single skin panel.

TABLE 7

Bending moment and probability of failure

Bending moment (kN.m)	Prob. of failure %
1.499	0.1
2.223	5.0
2.495	15.0
2.641	25.0
2.774	37.5
2.883	50.0
2.986	62.5
3.091	75.0
3.252	90.0
3.630	99.9

E of flange = 7450 N/mm^2

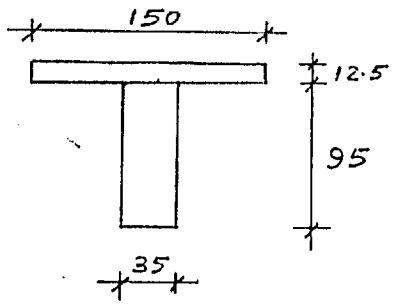
E of rib = 8300 N/mm^2

Ult.comp.stress of flange = 47 N/mm^2

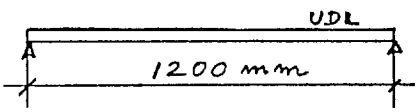
Ult.comp.stress of rib = 45 N/mm^2

k = 10

K_o = 100



Beam section



Loading arrangement

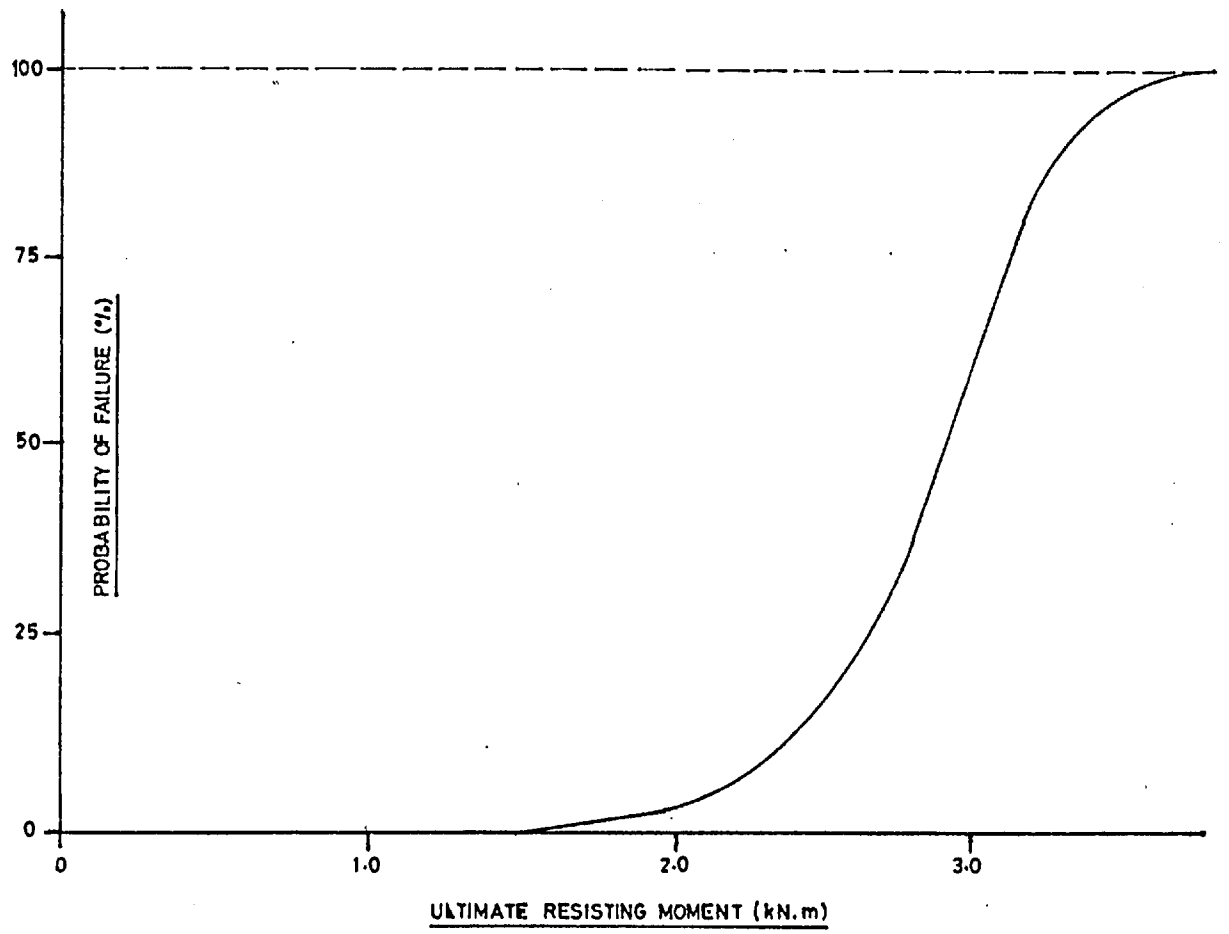
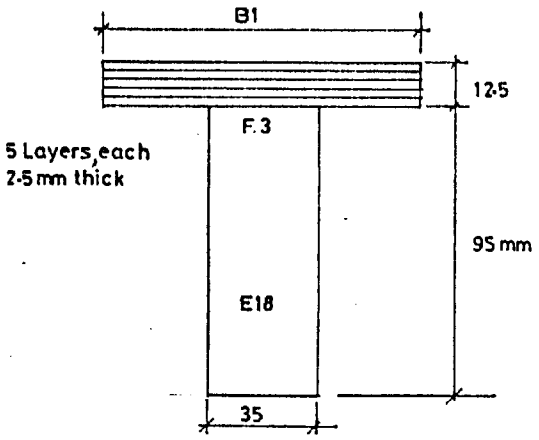


TABLE 8

Typical relationship of flange breadth with ultimate resisting moment and ultimate tensile stress.

Breadth B_1 (mm)	Ult.R.M (kN.m)	Ult.tens.stress (N/mm^2)
50	2.260	34.17
100	2.550	33.93
150	2.754	33.76
200	2.906	33.61
250	3.023	33.49
300	3.116	33.39
350	3.192	33.31
400	3.254	33.23

Mode 1 failure was predicted by the computer in all cases.



BEAM SECTION

E_1, E_3 & E_5 = 10100.00 N/mm^2

E_2 & E_4 = 400.00 N/mm^2

E_{18} = 10000.00 N/mm^2

F_1 = 53.30 N/mm^2

F_2 = 13.30 N/mm^2

F_3 = 45.00 N/mm^2

k = 16.00

K_o = 80.00

Probability of failure = 5%

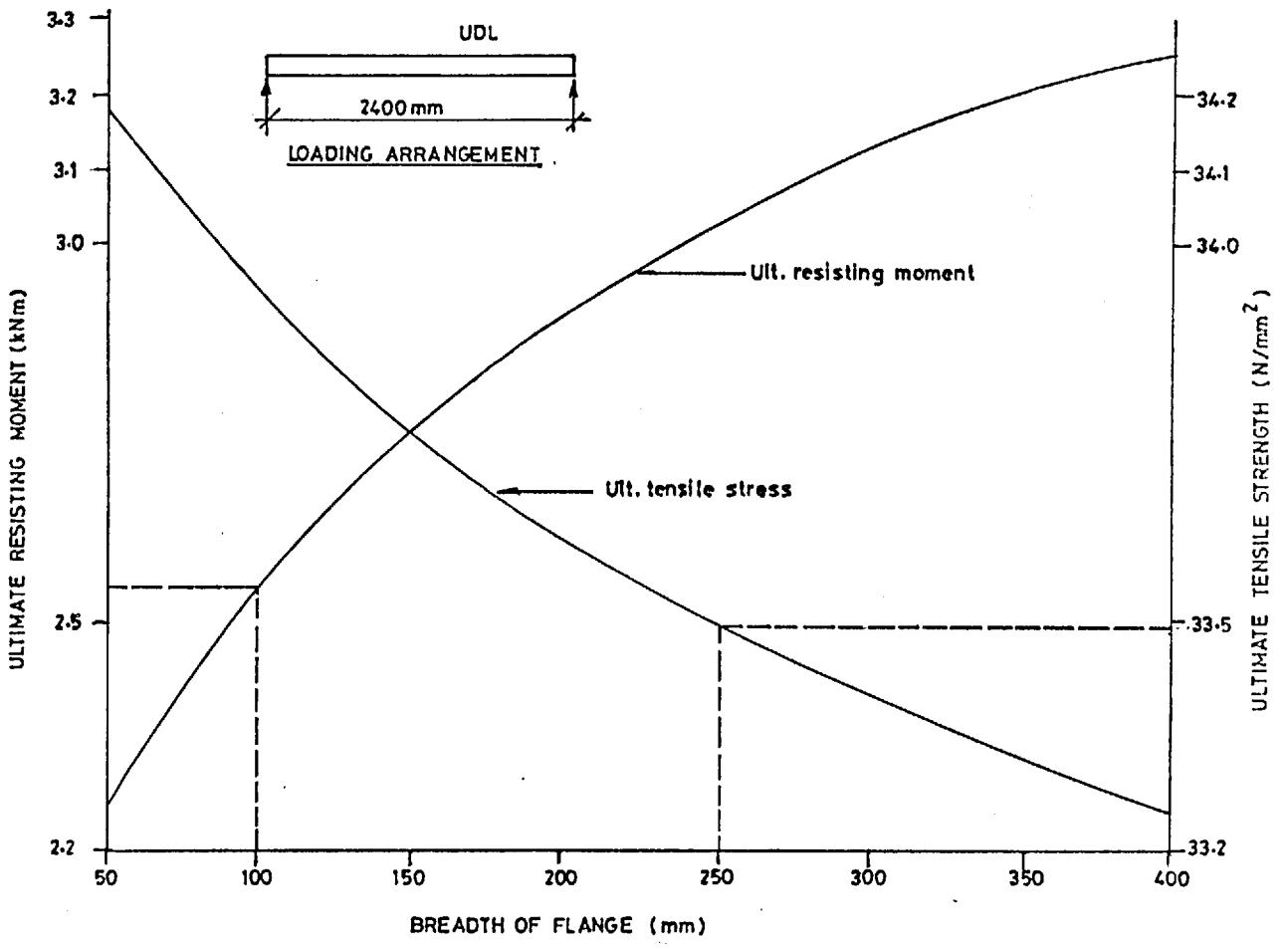


TABLE 9

Effect of k on the ultimate resisting moment

Probability of failure = 5% K_0 = 100

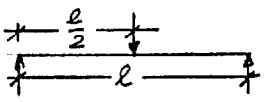
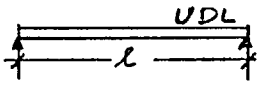
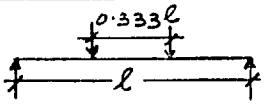
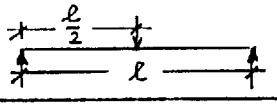
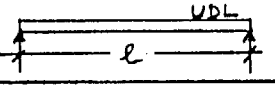
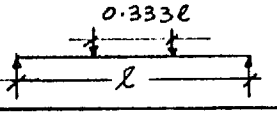
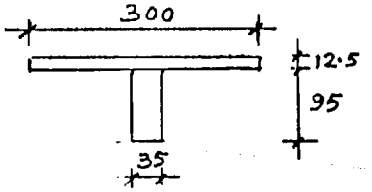
k	Type of loading and ultimate RM (kN.m)		
			
8.0	1.774	1.567	1.508
8.5	1.990	1.765	1.699
9.0	2.201	1.961	1.888
9.5	2.410	2.154	2.074
10.0	2.613	2.343	2.257
10.5	2.810	2.528	2.435
11.0	3.001	2.707	2.609
11.5	3.185	2.882	2.778
12.0	3.363	3.051	2.942

TABLE 10

Effect of K_0 on the ultimate resisting moment

Probability of failure = 5% k = 10

K_0	Type of loading and ultimate RM (kN.m)		
			
80	2.090	1.875	1.805
85	2.221	1.992	1.918
90	2.352	2.109	2.031
95	2.483	2.226	2.143
100	2.613	2.343	2.257
105	2.743	2.461	2.369
110	2.874	2.578	2.483
115	3.005	2.694	2.595
120	3.135	2.812	2.708



(Common to Tables 9, 10, 11 & 12)

E of flange = 8300 N/mm^2

E of rib = 8300 "

Ult.comp.stress of flange = 45 "

Ult.comp.stress of rib = 45 "

span = 2400 mm

TABLE 11

Effect of modulus of elasticity of flange on the ultimate resisting moment

Beam section, span and other properties of flange and rib are as per Table 9

Probability of failure = 5% k = 10 K_0 = 100

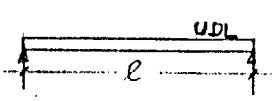
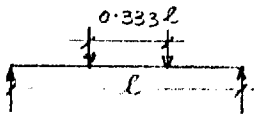
E_1 (N/mm^2)	Type of loading and ultimate RM (kN.m)		
			
6640	2.536	2.274	2.190
7055	2.557	2.294	2.209
7470	2.577	2.311	2.226
7885	2.596	2.328	2.242
8300	2.613	2.343	2.257
8715	2.629	2.380	2.271
9130	2.644	2.402	2.283
9545	2.658	2.419	2.295
9960	2.671	2.435	2.307

TABLE 12

Effect of modulus of elasticity of rib on the ultimate resisting moment

Probability of failure = 5% k = 10 K_0 = 100

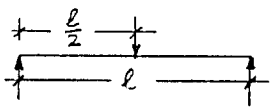
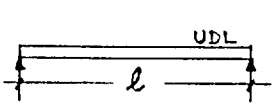
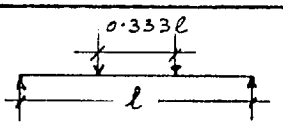
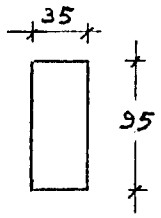
E_2 (N/mm^2)	Type of loading and ultimate RM (kN.m)		
			
6640	2.683	2.449	2.317
7055	2.665	2.428	2.301
7470	2.647	2.406	2.286
7885	2.630	2.382	2.271
8300	2.613	2.343	2.257
8715	2.596	2.329	2.243
9130	2.581	2.314	2.229
9545	2.565	2.301	2.216
9960	2.550	2.287	2.203

TABLE 13

Ultimate resisting moments and tensile stresses of rectangular solid beams for different spans and different type of loading.



Modulus of elasticity = 8300 N/mm^2

Ultimate compressive stress = 45 N/mm^2

Probability of failure = 5%

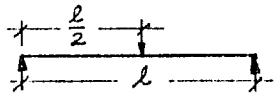
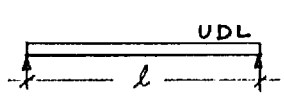
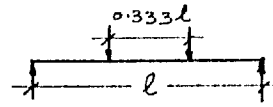
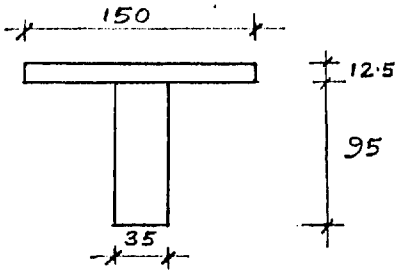
	Type of loading					
						
a) when k = 8.0 and K_0 = 120.0						
Span (mm)	Ult. R.M (kN.m)	Ultimate tens.stress (N/mm^2)	Ult. R.M (kN.m)	Ultimate tens.stress (N/mm^2)	Ult.R.M (kN.m)	Ultimate tens.stress (N/mm^2)
1200	1.289	24.49	1.139	21.62	1.096	20.82
1500	1.254	23.81	1.107	21.03	1.066	20.25
1800	1.225	23.28	1.083	20.56	1.042	19.79
2100	1.202	22.83	1.062	20.17	1.022	19.41
2400	1.182	22.45	1.045	19.84	1.005	19.09
b) when k = 10.0 and K_0 = 100.0						
1200	1.537	29.19	1.378	26.18	1.327	25.21
1500	1.503	28.54	1.348	25.60	1.298	24.65
1800	1.476	28.03	1.323	25.14	1.275	24.21
2100	1.453	27.60	1.303	24.75	1.255	23.84
2400	1.433	27.22	1.286	24.42	1.238	23.52

TABLE 14

Ultimate resisting moments and tensile stresses of a T beam with non-layered flange for different spans and different types of loading.



Modulus of elasticity of flange = 7450 N/mm^2
Modulus of elasticity of rib = 8300 N/mm^2
Ultimate comp.stress of flange = 47 N/mm^2
Ultimate comp.stress of rib = 45 N/mm^2
Probability of failure = 5%

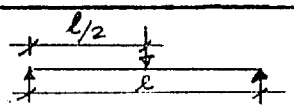
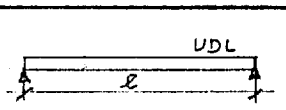
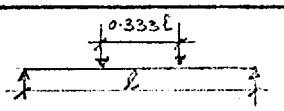
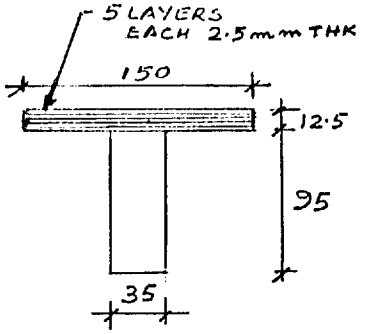
	Type of loading					
						
a) when k = 8.0 and K_o = 120.0						
Span (mm)	Ult. R.M (kN.m)	Ultimate tens.stress (N/mm^2)	Ult. R.M (kN.m)	Ultimate tens.stress (N/mm^2)	Ult. R.M (kN.m)	Ultimate tens.stress (N/mm^2)
1200	2.063	23.52	1.822	20.78	1.754	20.00
1500	2.006	22.87	1.772	20.21	1.705	19.45
1800	1.961	22.36	1.732	19.75	1.667	19.01
2100	1.922	21.92	1.699	19.37	1.635	18.65
2400	1.891	21.56	1.671	19.05	1.608	18.34
b) when k = 10.0 and K_o = 100.0						
1200	2.479	28.26	2.223	25.35	2.141	24.41
1500	2.424	27.64	2.174	24.79	2.094	23.87
1800	2.380	27.13	2.135	24.34	2.056	23.44
2100	2.343	26.72	2.102	23.97	2.024	23.08
2400	2.313	26.37	2.074	23.65	1.988	22.78

TABLE 15

Ultimate resisting moments and tensile stresses of a T beam with layered flange for different spans and different types of loading



E of first, third and fifth layer = 12016.0 N/mm^2

E of second and fourth layer = 601.0 N/mm^2

E of rib = 8300.0 N/mm^2

Ult.comp.stress of 1st,3rd & 5th layer = 67.1 N/mm^2

Ult.comp.stress of 2nd & 4th layer = 16.8 N/mm^2

Ult.comp.stress of rib = 45.0 N/mm^2

Probability of failure = 5%

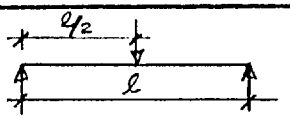
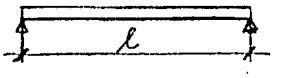
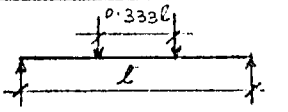
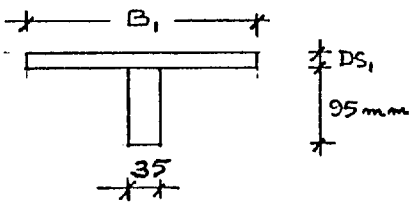
	Type of loading					
						
a) when k = 8.00 and K_o = 120.00						
Span (mm)	Ult. R.M (kN.m)	Ultimate tens.stress (N/mm^2)	Ult. R.M (kN.m)	Ultimate tens.stress (N/mm^2)	Ult. R.M (kN.m)	Ultimate tens.stress (N/mm^2)
1200	2.068	23.55	1.808	20.59	1.756	20.00
1500	2.011	22.91	1.758	20.02	1.708	19.45
1800	1.966	22.39	1.718	19.57	1.669	19.01
2100	1.927	21.95	1.686	19.20	1.637	18.65
2400	1.896	21.59	1.658	18.88	1.610	18.34
b) when k = 10.00 and K_o = 100.00						
1200	2.485	28.30	2.206	25.12	2.144	24.42
1500	2.430	26.67	2.157	24.57	2.096	23.88
1800	2.385	27.16	2.118	24.12	2.059	23.44
2100	2.349	26.75	2.086	23.76	2.027	23.09
2400	2.318	26.40	2.058	23.44	2.000	22.78

TABLE 16

Comparison of the ultimate resisting moments of the T beam with layered flange and equivalent non-layered flange.

Probability of failure = 5% Load type : Uniformly distributed load

B_1 (mm)	DS_1 (mm)	Span (mm)	Layers in layered flange	Ultimate R.M(kN.m)		% increase for non-layered flange
				Layered flange	Non-layered flange	
300	7.5	1200	3	1.722	1.726	0.23
400	7.5	1200	3	1.801	1.806	0.28
300	7.5	2400	3	1.579	1.583	0.25
400	7.5	2400	3	1.652	1.656	0.24
300	12.5	1200	5	1.904	1.921	0.89
400	12.5	1200	5	1.981	2.003	1.11
300	12.5	2400	5	1.745	1.762	0.97
400	12.5	2400	5	1.816	1.836	1.10
300	17.5	1200	7	2.057	2.100	2.09
400	17.5	1200	7	2.130	2.180	2.35
300	17.5	2400	7	1.886	1.925	2.07
400	17.5	2400	7	1.953	1.999	2.36



BEAM SECTION

Properties of the Rib

Ult.comp.stress = 45.00 N/mm^2

E = 10000.00 N/mm^2

k = 8

K_0 = 120

Properties of the layers of layered flanges

E_1 = 10100.00 N/mm^2

E_2 = 400.00 N/mm^2

F_1 = 53.30 N/mm^2

F_2 = 13.30 N/mm^2

Properties of the non-layered flanges

Modulus of elasticity (N/mm^2)	Ultimate comp.stress (N/mm^2)	No.of layers in the equivalent layered flange
6866.67	39.97	3
6220.00	37.30	5
5942.86	36.16	7

All layers are of same thickness.

Equivalent modulus of elasticity $= \frac{\Sigma(Et)}{\Sigma t}$

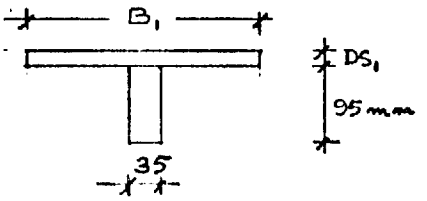
Equivalent compressive stress $= \frac{\Sigma(Ft)}{\Sigma t}$

TABLE 16A

Comparison of the ultimate resisting moments of the T beam with layered flange and equivalent non-layered flange.

Probability of failure = 5% Load type : Uniformly distributed load

B_1 (mm)	DS_1 (mm)	Span (mm)	Layers in layered flange	Ultimate R.M(kN.m)		% increase for non-layered flange
				Layered flange	Non-layered flange	
300	7.5	1200	3	2.925	2.932	0.24
400	7.5	1200	3	3.069	3.078	0.29
300	7.5	2400	3	2.801	2.807	0.21
400	7.5	2400	3	2.939	2.947	0.27
300	12.5	1200	5	3.254	3.282	0.86
400	12.5	1200	5	3.399	3.431	0.94
300	12.5	2400	5	3.116	3.142	0.83
400	12.5	2400	5	3.254	3.286	0.98
300	17.5	1200	7	3.542	3.601	1.67
400	17.5	1200	7	3.682	3.751	1.87
300	17.5	2400	7	3.390	3.447	1.68
400	17.5	2400	7	3.525	3.592	1.90



BEAM SECTION

Properties of the Rib

Ult.comp.stress = 45.00 N/mm^2

E = 10000.00 N/mm^2

k = 16

K_0 = 80

Properties of the layers of layered flanges

E_1 = 10100.00 N/mm^2

E_2 = 400.00 N/mm^2

F_1 = 53.30 N/mm^2

F_2 = 13.30 N/mm^2

All layers are of same thickness.

Properties of the non-layered flanges

Modulus of elasticity (N/mm^2)	Ultimate comp.stress (N/mm^2)	No.of layers in the equivalent layered flange
6866.67	39.97	3
6220.00	37.30	5
5942.86	36.16	7

TABLE 17

Comparison of the ultimate resisting moments for different species of Plywood flange with the same rib

Probability of failure = 5%

Flange Timber species	Properties of the veneers				Ult.RM (kN.m) when	
	Modulus of elasticity		Ult.comp.stress		k = 8	k = 10
	E_1 (N/mm^2)	E_2 (N/mm^2)	F_1 (N/mm^2)	F_2 (N/mm^2)	K_0 = 120	K_0 = 100
Birch	13300.0	532.0	59.9	15.0	1.813	2.258
Douglas Fir	12700.0	500.0	52.1	13.0	1.802	2.244
Sitka Spruce	10500.0	420.0	39.2	9.8	1.755	2.183
Makore	10100.0	400.0	53.3	13.3	1.745	2.170

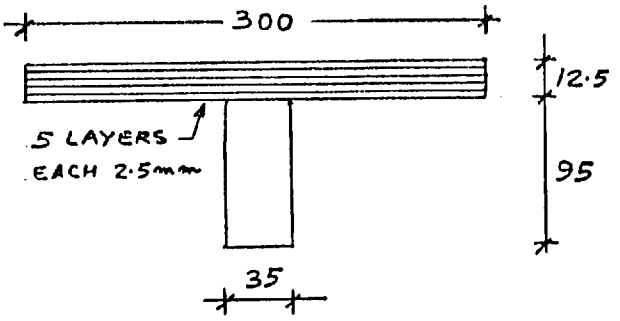
Notes: 1. Values of E_1 & F_1 are taken from PRL (1974)

2. E_2 & F_2 are assumed values.

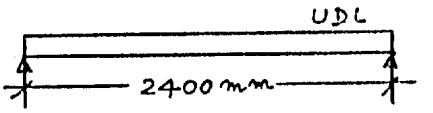
Properties of the rib

Modulus of elasticity = 10000.00 N/mm^2

Ult.compressive stress = 45.00 N/mm^2



BEAM SECTION



LOADING

TABLE 18

Ultimate resisting moments of panels with different number of ribs

Panel size = 1200 mm wide x 2400 mm long

Properties of Ribs

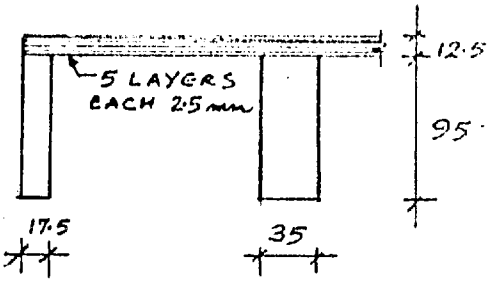
Breadth of outer ribs = 17.5 mm

Breadth of inner ribs = 35.0 mm

Depth = 95.0 mm

Modulus of elasticity = 10000.0 N/mm^2

Ultimate compressive stress = 45.0 N/mm^2



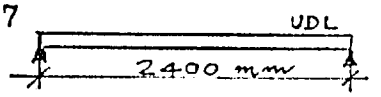
Part section

k = 8.0

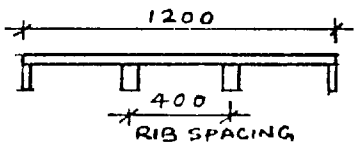
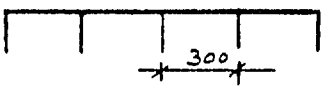
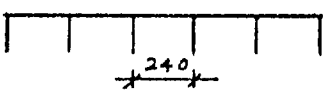
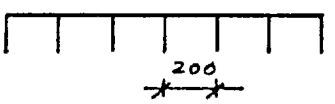
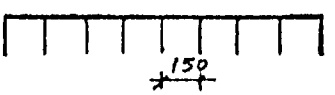
K_0 = 80.0

Properties of flanges are as given in Table 17

Probability of failure = 5%



Loading arrangement

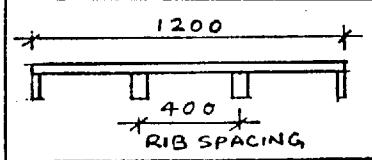
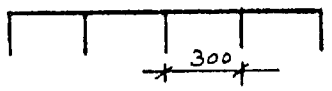
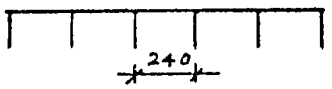
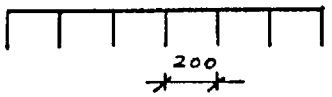
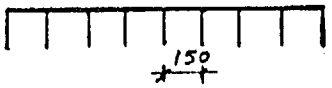
Panel Section	Ultimate resisting moment (kN.m) for different flange material			
	Birch	Douglas Fir	Sitka Spruce	Makore
	3.753	3.732	3.651	3.633
	4.836	4.808	4.680	4.656
	5.860	5.825	5.655	5.620
	6.846	6.792	6.588	6.546
	8.704	8.640	8.362	8.296

Note: Ultimate resisting moment of a 35 x 95 rib with the above properties and supporting UDL on 2400 mm span = 0.696 kN.m

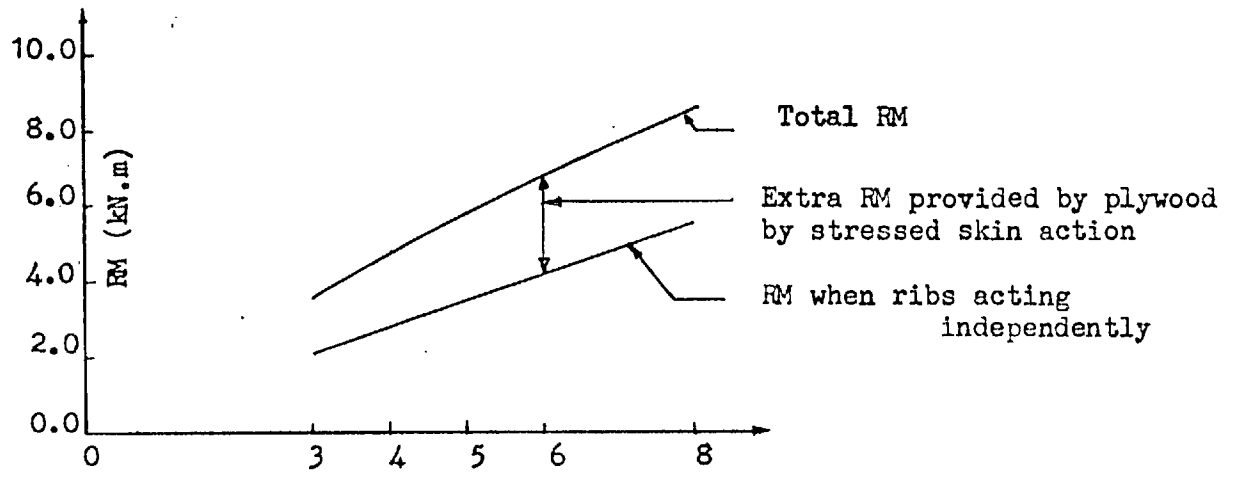
TABLE 19

Comparison of the resisting moment provided by the ribs acting independently and the resulting total resisting moment when ribs and plywood flange acting compositely as a stressed skin panel.

Reference: Panel with Douglas Fir plywood as shown in Table 18

Panel section	Total RM as stressed skin panel (kN.m)	RM of ribs if acted independently (kN.m)	% of total RM	Increase of RM due to plywood flange (kN.m)	% of total RM
	3.732	3x0.696 = 2.088	55.95	3.732-2.088= 1.644	44.05
	4.808	4x0.696 = 2.784	57.90	4.808-2.784= 2.024	42.10
	5.825	5x0.696 = 3.480	59.74	5.825-3.480= 2.345	40.26
	6.792	6x0.696 = 4.176	61.48	6.792-4.176= 2.616	38.52
	8.640	8x0.696 = 5.568	64.44	8.640-5.568= 3.072	35.56

Probability of failure = 5%

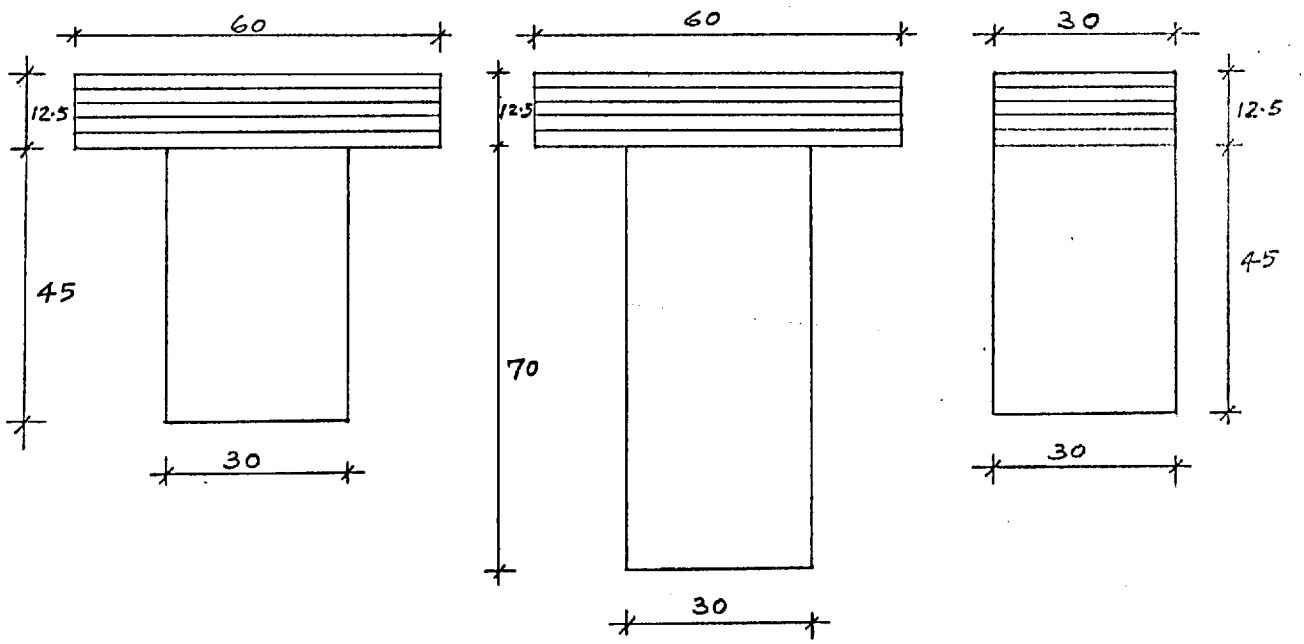


CHAPTER 6

EXPERIMENTAL INVESTIGATION

6.1 Preliminary test series

3 model beams with cross-sections as shown below were tested to ascertain the difficulties and limitations of testing the T beams with plywood flanges.



Model 1 Model 2 Model 3

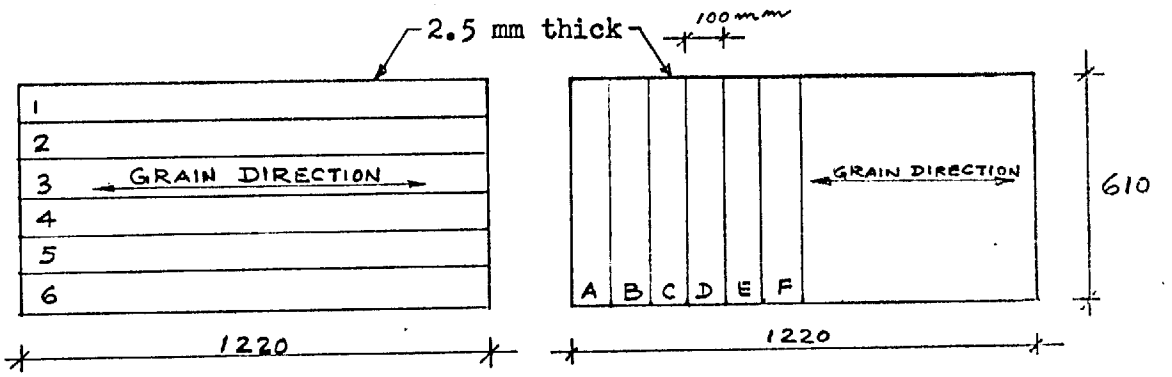
Fig. 6.1

The following details were common to all beams.

1. Flange: 5 veneers of makore with face veneers and the middle veneer parallel to the length of the beam.
2. Rib Western red cedar
3. Length 1200 mm

6.1.1. Experiments to estimate the mechanical properties of flange and rib

Flange. The plywood flange was made by gluing 5 No. 2.5 mm thick veneer strips with phenol resorcinol glue. Fig. 6.2 shows how the strips were cut from 1220 mm x 610 mm sheets.



Sheet 1 Sheet 2

Fig. 6.2

Strips 1, 2, 3 etc. have the grain parallel to the length, whereas strips A, B, C etc. have the grain perpendicular to the length.

6.1.2 Tests on the strips.

The properties to be ascertained are:

a) Ultimate compressive stress in the direction parallel to the length of the strips.

b) Modulus of elasticity in the direction parallel to the length of the strips.

a) Ultimate compressive stress

Matching pieces were cut out of the strips at the locations shown in Fig. 6.3. Two compression specimens were made from each strip by gluing the pieces. Dimensions of the test specimens and test results are given in Table 21.

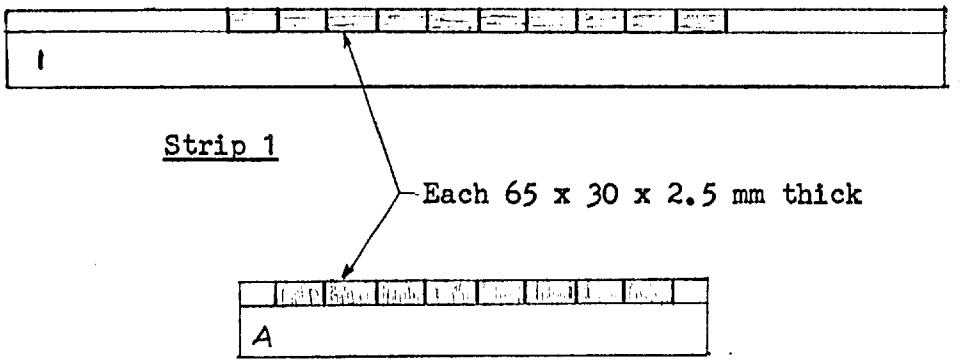


Fig. 6.3

b) Modulus of elasticity.

Modulus of elasticity parallel to the length of each strip was found by ultrasonic pulse technique, which is explained in detail later in this chapter. The test results are shown in Table 20.

6.1.3 Tests on the rib specimens.

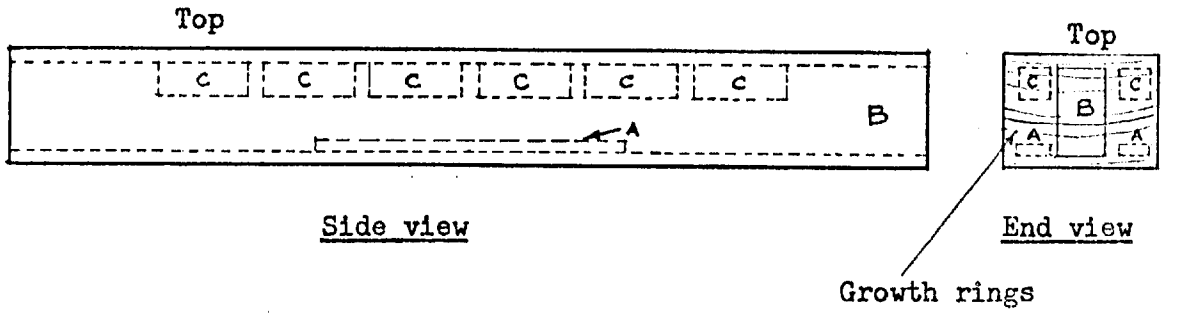
The properties to be ascertained are:

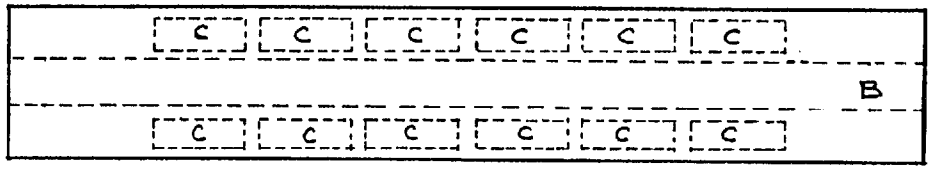
a) Ultimate compressive stress parallel to the grain.

b) Ultimate tensile stress parallel to the grain.

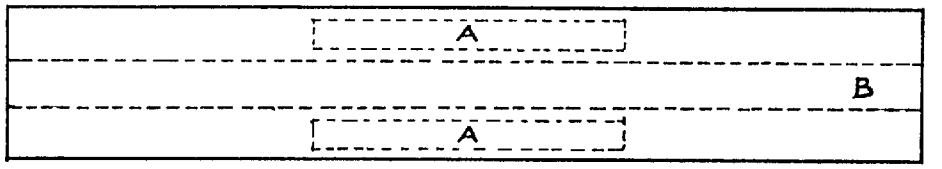
c) Modulus of elasticity parallel to the grain.

Fig. 6.4 shows the location from where the rib and the matching specimen were taken from the timber joists.





Top view



Bottom view

Fig. 6.4

A Tension specimen

B Rib

C Compression specimen

a) Ultimate compressive stress

For each rib 12 specimens 20 x 20 x 60 mm long were tested.

b) Ultimate tensile stress

For each rib 2 No. waisted test pieces as per BS 373 : 1957 were tested. As the test results were thought to be unreliable four more tension specimens were made for each rib with the waisted width as 6 mm instead of 3 mm shown in BS 373.

Both compression and tension tests were carried out on an Amsler 10 T testing machine.

c) Modulus of elasticity

Modulus of elasticity of the rib was estimated using ultrasonic pulse technique as well as static bending tests.

The results of tests a, b & c are shown in Tables 22 and 23.

Moisture content

The moisture content of the flange specimens and the rib specimens were determined by oven drying method. The results are shown in Table 24.

6.1.4 Making of the beam models

The strips were selected as shown in Fig. 6.6 and glued together to form the plywood. As the strips A, B, C etc.(with grain perpendicular to the length) were less than 1200 mm, butt jointing was resorted to make up the length. Glued plywood strips were kept in a door press overnight. Then the plywood flanges were glued to the ribs to make the beam models 1, 2 & 3 and again kept in a door press overnight. Phenol resorcinol glue was used to make plywood as well as beam models. Oversize flanges were machined to the correct width before proceeding with the tests.

"Demec" points were fixed on the models as shown in Fig. 6.5. As the thickness of the veneers was only 2.5 mm, thin strips of steel were glued on the veneers before gluing the modified Demec points. Quick setting Epoxy resin was used for fixing the Demec points.

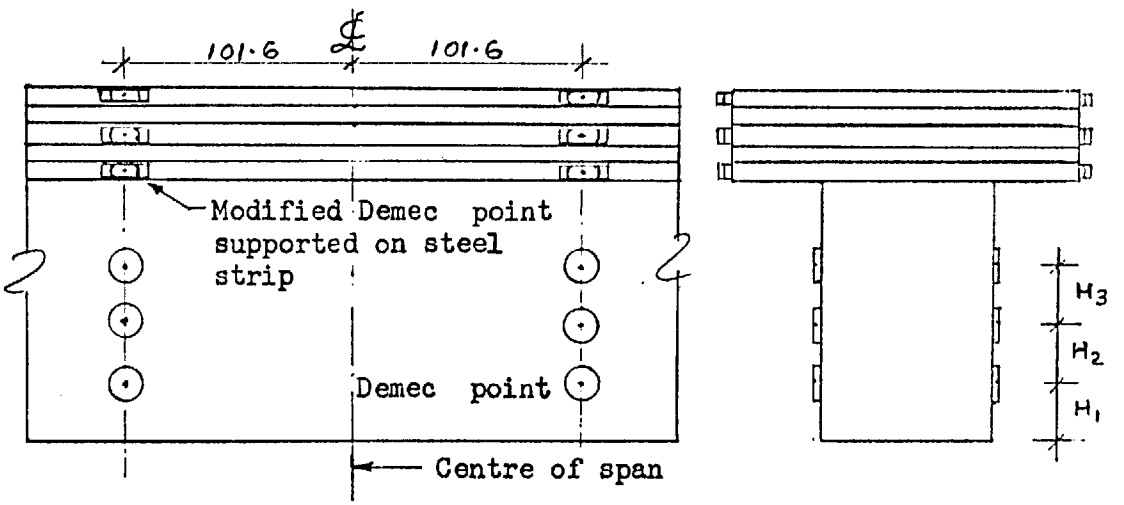


Fig. 6.5

6.1.5 Testing of model Beams.

The models were tested on a specially set up test rig. The loads were applied at $\frac{1}{3}$rd span points through a screw jack and the measure of the load was read on a proving ring. The screw jack enabled the load be kept constant for a short period at suitable intervals for strain measurements by Demec gauge. Load was increased until the model failed in bending and the ultimate load was recorded.

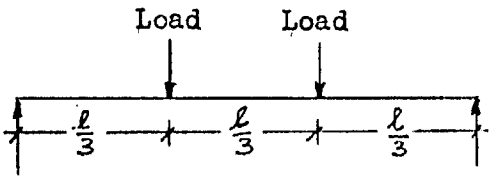


Table 25 shows the strains at different levels at different loads and the ultimate resisting moment of each model beam. The strain diagrams are also shown in Fig. 6.7. Table 26 and Fig. 6.8 show the stresses calculated from the measured strains. The stresses were derived from the formula, stress = strain x E. However, the maximum compressive stress was limited to the ultimate compressive stress obtained from the test on the component.

6.1.6 Review of Test and Test results

a) Modulus of elasticity of the veneers parallel to the grain

Ultrasonic pulse technique was found to be quick and easy. However, to estimate the value of E_{static} from $E_{Dynamic}$ (obtained by ultrasonic test), a multiplying factor must be known for each species of timber. As this factor was not known for makore, an approximate value (0.865) was adopted. This value was suggested by Nwokoye(1971) for timber, generally used for structural purposes. Alternatively, it would be advantageous to make a few rectangular beams of size 20 mm wide x 25 mm thick by gluing the veneers and subject them to static bending test and ultrasonic pulse test. The value of $\frac{E_{static}}{E_{Dynamic}}$ thus obtained will be more appropriate for

finding the value of E_{static} from the results of ultrasonic test on the veneers.

b) Modulus of elasticity of veneers perpendicular to the grain

Ultrasonic test was adopted to assess this property. It was observed that the values differ very much for different specimens. As this property has very little effect on the ultimate resisting moment of the beam, the average value is considered to be adequate.

c) Ultimate compressive stress of the veneers.

(i) Compression parallel to the grain. The height of the specimen was approximately five times its thickness. This ratio of height to thickness seems to be appropriate as the crushing failure was observed in all cases.

(ii) Compression perpendicular to the grain. Although the height to thickness ratio was reduced to four(approximate),buckling failure was observed in many cases. From this it was inferred that the height should not be more than three times its thickness to cause crushing failure of the specimen under compression test.

d) Ultimate compressive stress of the ribs

The cross-section of the specimen was 20 mm x 20 mm and the height 60 mm. This specimen was found to give reliable results.

e) Ultimate tensile stress of the ribs

From the Table 5 it will be seen that the ultimate tensile stress of the rib is the most critical property for the ultimate resisting moment of the T section. The test specimen as shown in British Standard 373 has the waisted cross section of 6 mm x 3 mm. This specimen was found to give unreliable results. When the specimens with a waisted cross section of 6 mm x 6 mm were tested it was noticed that the ultimate tensile stress was reduced by about 30 to 38% of that of the smaller cross section. This was thought to be due to the "size effect" and it

was decided to investigate this problem further as described in Chapter 5.

f) Discussion of the model test results

As timber is a very variable material, it is difficult to draw definite conclusions by testing three model beams. However, it is possible to gather many useful informations.

i) Strain across the cross-section

Fig. 6.7 shows the strain diagrams. It can be seen that the strain across the depth of the flanges of models 1 and 2 is non-linear. This may be due to the following reasons.

1. Slip at the interface of the veneers.
2. Shear lag in the protruding flanges.
3. Inaccurate readings given by the mechanical strain gauges.

Stresses were derived by using the measured values of strains and stress diagrams were drawn as shown in Fig. 6.8. It was noticed that these stress diagrams do not satisfy the equilibrium condition (compression = tension). The resisting moments calculated from the stress diagrams also were different from the actual bending moments.

Model	Internal forces	Moments
1	Compression = 1.449 x tension	Calculated RM = 0.629 x actual BM
2	Compression = 1.449 x tension	Calculated RM = 0.750 x actual BM
3	Compression = 1.003 x tension	Calculated RM = 1.151 x actual BM

Possible reasons for these discrepancies are the shear lag in the protruding flanges, the error in the assumptions of stress distribution across the cross section, and the incorrect strain measurement.

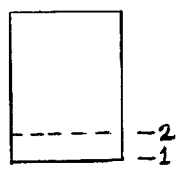
The results obtained from model 3, which has a rectangular cross section, are better than that of the other models with protruding flanges. This indicates that there is a possibility of shear lag. Shear lag produces lesser strains at the ends of the protruding flanges, and therefore the calculated total compression based on these strains should be less than actual total compression. However, even in model 1, which

shows elastic stress distribution, the total compression is much more than the total tension. Model 1 is also not affected by the assumptions of plastic stress distribution. Therefore, the shear lag and the assumptions may not have contributed much to the discrepancies.

Incorrect strain measurement may be the other reason. Using a 'Demec' strain gauge, it was difficult to measure the strain instantaneously when a particular load has been reached. In the case of the three models tested, dial gauge readings were noted when they had settled down to constant levels. Therefore, creep would have affected the strain. It is also noticed that the strain measurements are susceptible to human errors while using the mechanical strain gauges. The other alternative is the electrical strain gauge. However, more model tests are necessary to establish the reasons for the discrepancies.

(ii) Ultimate resisting moment of the model beams

The basic assumption of the theory presented in this thesis is that the beam attains its ultimate resisting moment when the stress in the extreme bottom fibre reaches the ultimate tensile stress. This assumption has an important limitation in the case of timber. Timber has different mechanical properties at different points. It is possible that the ultimate tensile strength at the level (2) may be much higher (or lower) than that at the level (1). Test on the model 1 has proved this. It was found that the ultimate collapse of the beam did not occur at the time of the failure of the extreme bottom fibre. At the ultimate collapse, the beam has sustained an additional 20% of the load at which the extreme bottom fibre first failed.



Section

The most important mechanical property required for the prediction of the ultimate resisting moment of the T section is the ultimate tensile stress of the rib. The following table compares the actual ultimate resisting moments with the calculated values using the test results of two different types of tension specimen.

Model No.	Actual ult. RM by model test (kN.m)	Using 3 mm x 3 mm Tension specimen			Using 6 mm x 3 mm Tension specimen		
		Ult.tens. stress (N/mm^2)	Calculated RM (kN.m)	Error %	Ult.tens. stress (N/mm^2)	Calculated RM (kN.m)	Error %
1	1.050	82.42	1.396	+32.95	57.83	1.080	+ 2.86
2	2.551	87.00	2.855	+11.92	53.97	2.031	-20.38
3	0.801	78.72	1.039	+29.71	54.64	0.820	+ 2.37

Two out of three test results show that the bigger the size of tension specimen, the better the estimated value of resisting moment will be.

The following table shows how the test results compare with the ultimate resisting moments estimated by using the published values for the critical mechanical properties. These values are at 12% moisture content and are as listed below.

Makore flange

E ∥ to the grain, E_1 = 10100 N/mm^2 (published value)*

E ⊥ to the grain, E_2 = 360 N/mm^2 (assumed value)

Compression ∥ to the grain, F_1 = 53.3 N/mm^2 (published value)*

Compression ⊥ to the grain, F_2 = 14.0 N/mm^2 (assumed value)

Western red cedar rib

E ∥ to the grain, E_{18} = 7000 N/mm^2 (published value)*

Compression ∥ to the grain, F_3 = 35.0 N/mm^2 (published value)*

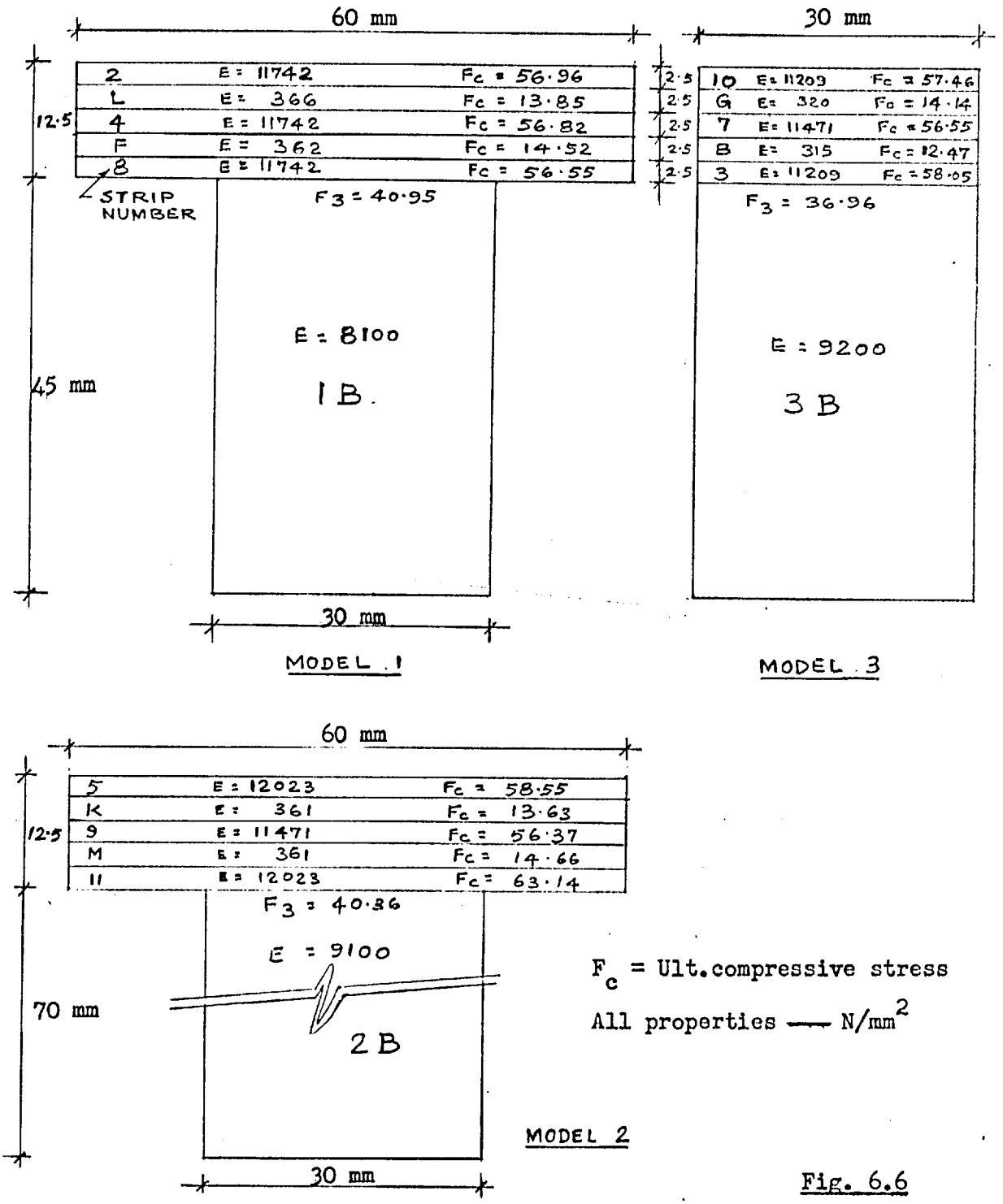
Tension ∥ to the grain, F_4 = 65.0 N/mm^2 (published value for modulus of rupture)*

* Reference:PRL(1974). Strength properties of timber.

Model No.	Actual ult.RM by model test (kN.m)	Calculated ult.RM using the properties listed above (KN.m)	Error in calculated value (%)
1	1.050	1.167	+ 11.14
2	2.551	2.316	- 9.21
3	0.801	0.912	+ 13.86

It will be noticed that the maximum error is less than 15%. This finding has an immense practical importance and has to be investigated further with more model tests. If practically acceptable results can be estimated by using the published values of the mechanical properties, difficult tests on the specimens of veneers and ribs which generally give unreliable results can be eliminated.

Properties of Flange and Rib of the model Beams



F_c = Ult. compressive stress

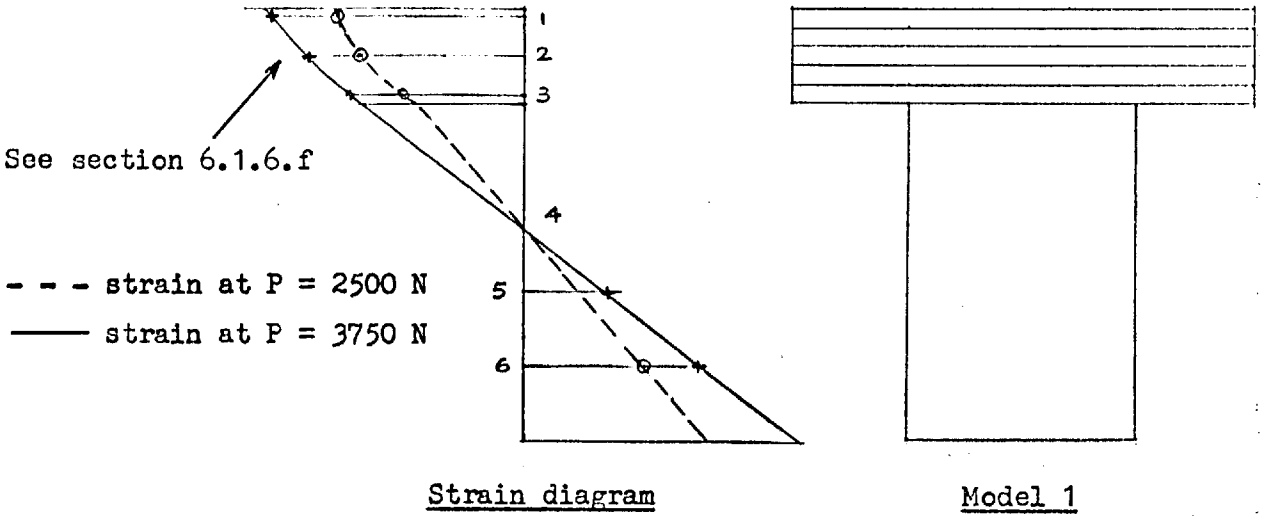
All properties —— N/mm^2

Fig. 6.6

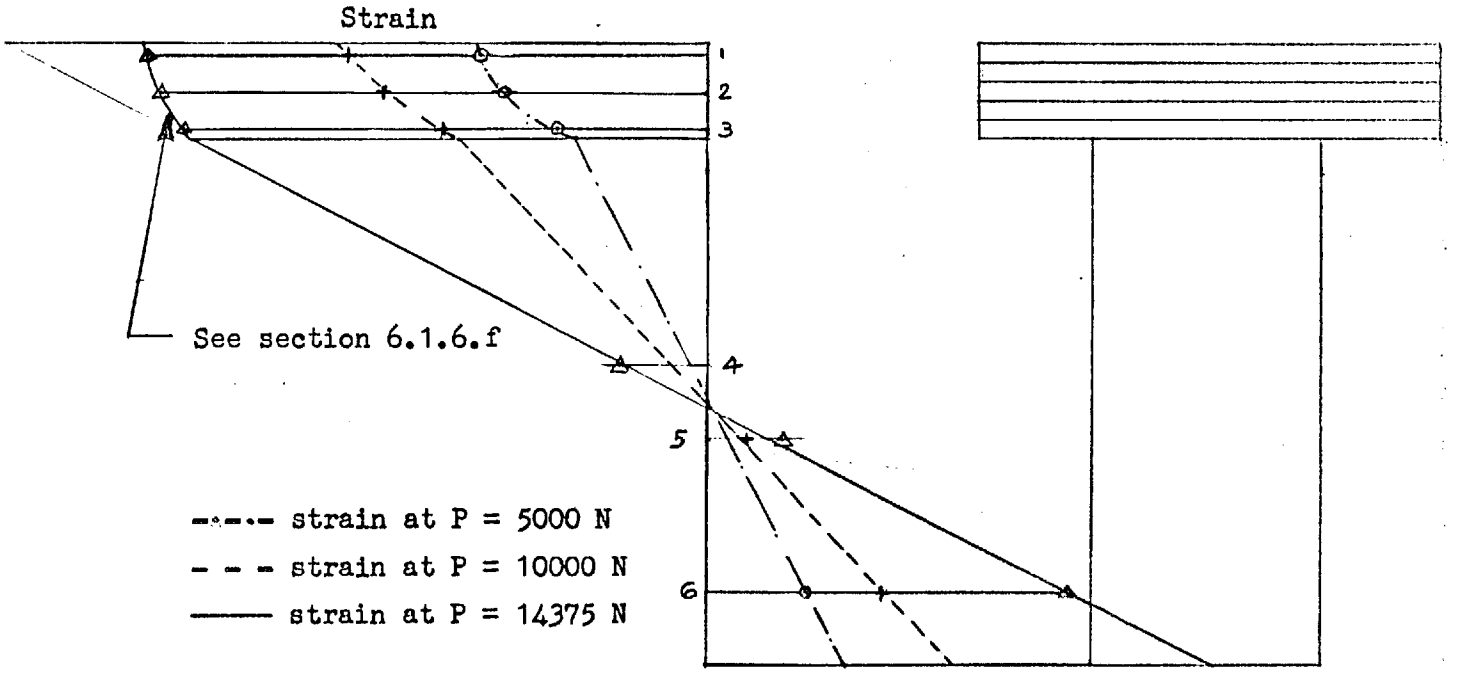
Computer input Data

Model No.	E_1	E_2	E_{18}	F_1	F_2	F_3	F_4 1st Data	F_4 2nd Data
1	11740	360	8100	56.9	13.8	40.9	82.42	57.83
2	12020	360	9100	58.5	13.6	40.3	87.00	53.97
3	11200	320	9200	57.4	14.1	36.9	78.72	54.64

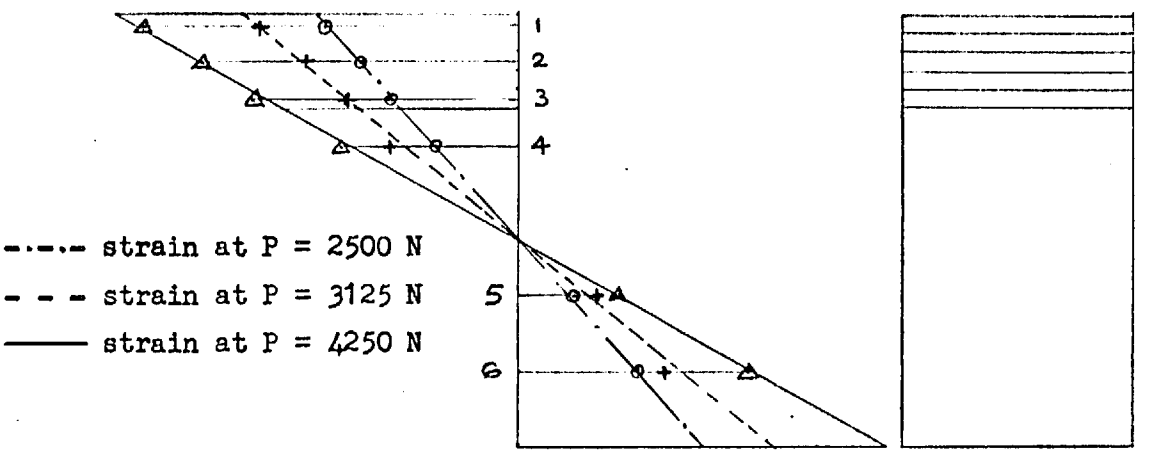
Strain diagrams of the model beams. (Reference : Table 25)



Strain diagram Model 1



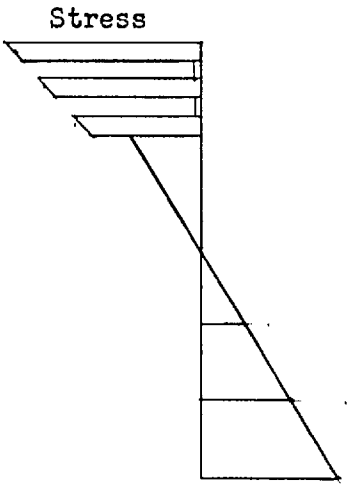
Strain diagram Model 2



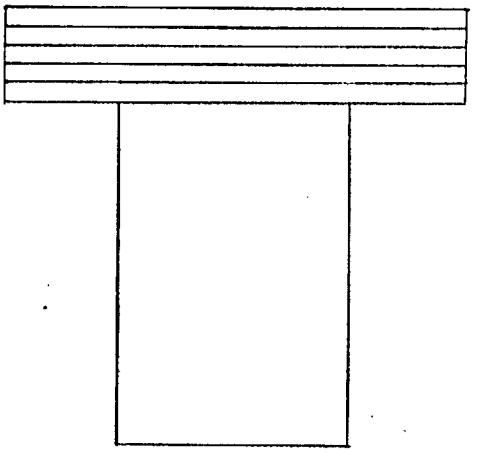
Strain diagram Model 3

Fig. 6.7

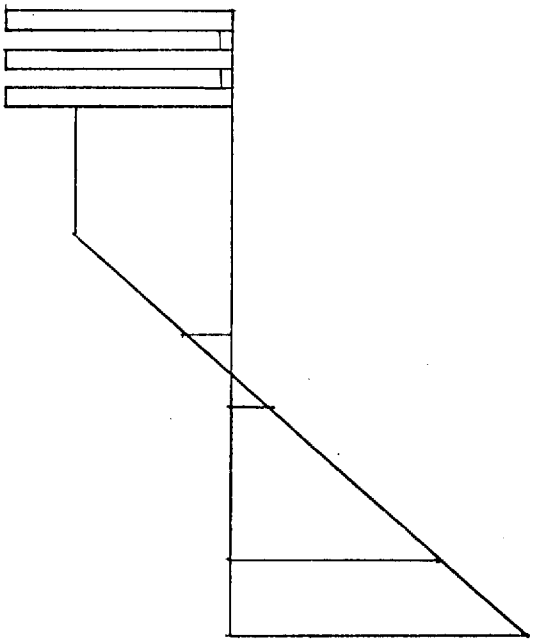
Stress diagrams of the model beams. (Reference : Table 26)



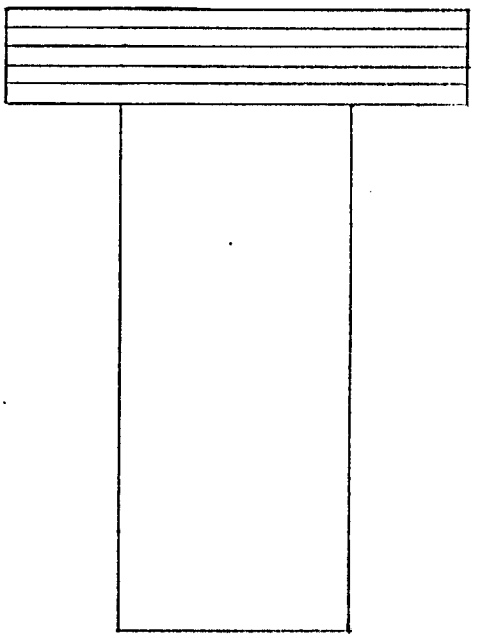
Stress diagram
(when P = 3750 N)



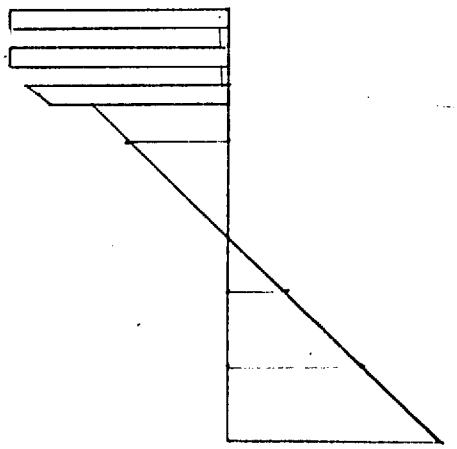
Model 1



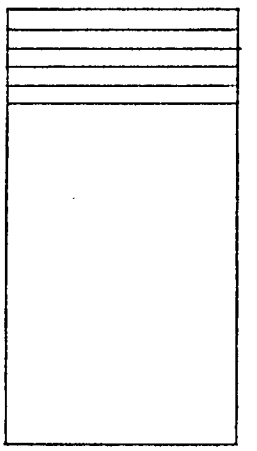
Stress diagram
(when P = 14375 N)



Model 2



Stress diagram
(when P = 4250 N)



Model 3

Fig. 6.8

TABLE 20

Results of Ultrasonic test on Veneers

Timber : Makore Thickness = 2.5 mm

$$E_{static} = 0.865\ E_{Dyn}$$

1. E Parallel to grain

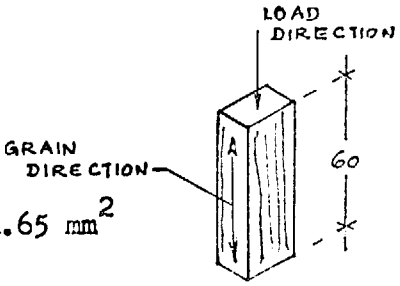
Strip No.	1	2	3	4	5	6	7	8	9	10	11
E_{Dyn} (N/mm^2)	13575	13575	12958	13575	13900	13900	13261	13575	13261	12958	13900
E_{static} (N/mm^2)	11742	11742	11209	11742	12023	12023	11471	11742	11471	11209	12023

2. E Perpendicular to grain

Strip No.	B	C	D	E	F	G	H	J	K	L	M
E_{Dyn} (N/mm^2)	364	420	308	349	419	370	254	290	417	424	417
E_{static} (N/mm^2)	315	363	266	302	362	320	220	251	361	366	361

TABLE 21

Resultsof Compression Test on Veneers



1. Compression parallel to grain

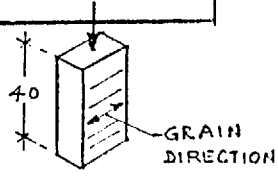
Area of cross-section = 20.07 x 12.19 = 244.65 mm^2

Stress is the average for 2 specimens

Strip No.	1	2	3	4	5	6	7	8	9	10	11
Ult.comp. stress (N/mm^2)	59.32	56.96	58.05	56.82	58.55	56.27	56.55	56.55	56.37	57.46	63.14

2. Compression perpendicular to grain

Area of cross-section = 20.07 x 10.16 = 203.91 mm^2

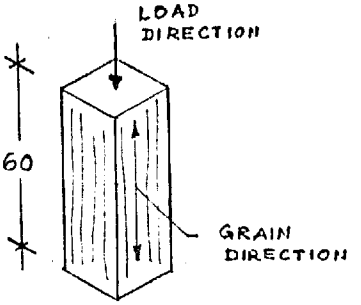


Stress is the average for 2 specimens

Strip No.	B	C	D	E	F	G	H	J	K	L	M
Ult.comp. stress (N/mm^2)	12.47	12.06	14.24	14.72	14.52	14.14	14.03	13.42	13.63	13.85	14.66

TABLE 22

Results of the Tests on the Rib specimens



1. Compression parallel to grain

Area of cross-section = 20 x 20 = 400 mm^2

Stress is the average for 10 specimens

Specimen No.	1C	2C	3C
Ult.comp.stress (N/mm^2)	40.95	40.36	36.96

2. Tension parallel to grain

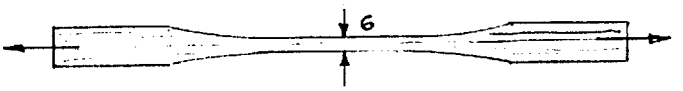
a) 

BS 373 type specimen

Minimum area of cross-section = 3 x 6 = 18 mm^2

Stress is the average for 2 specimens

Specimen No.	1A	2A	3A
Ult.tensile stress (N/mm^2)	82.42	87.00	78.72

b) 

Special specimen

Minimum area of cross-section = 6 x 6 = 36 mm^2

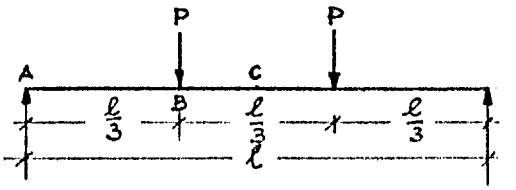
Stress is the average for 4 specimens

Specimen No.	1A	2A	3A
Ult.tensile stress (N/mm^2)	57.83	53.97	54.64

TABLE 23

3. Modulus of Elasticity of Ribs.

a) Static loading method.



$$E = \frac{Pl^3}{216\ I(\Delta_C - \Delta_B)}$$

where E = Modulus of elasticity

I = Second moment of the area

Δ_C = Deflection at C (Mid span)

Δ_B = Deflection at B

Specimen No.	1B	2B	3B
$E_{static}(N/mm^2)$	8100	9100	9200

b) Ultrasonic Pulse Technique

Specimen No.	1B	2B	3B
$E_{Dynamic}(N/mm^2)$	9820	10160	10260
$\frac{E_{static}}{E_{Dynamic}}$	0.825	0.896	0.897

TABLE 24

Moisture content of the Beam components

1. Flange specimens

Specimen No.	8	9	10
Moisture content %	9.04	9.71	10.06

2. Rib specimens

a) Tension specimens

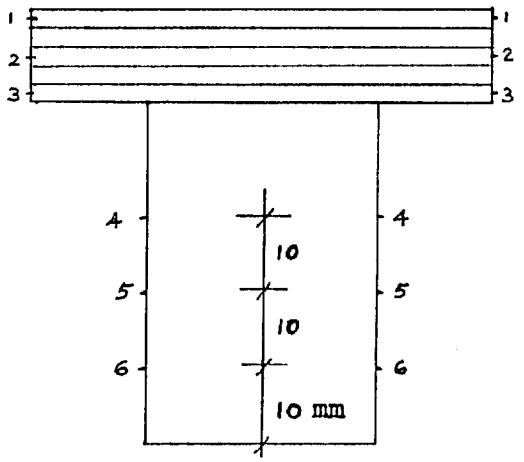
Specimen No.	1A	2A	3A
Moisture content %	10.03	9.32	9.68

b) Compression specimens

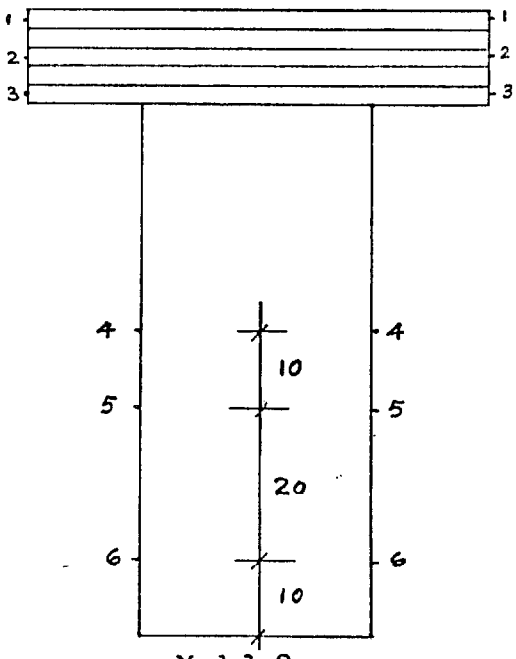
Specimen No.	1C	2C	3C
Moisture content %	10.55	9.35	9.88

TABLE 25

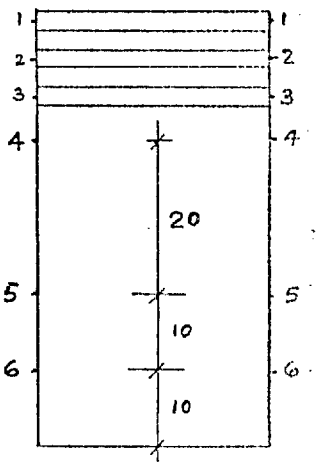
Result of the tests on the Model Beams



Model 1.

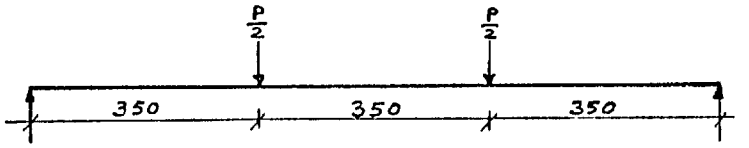


Model 2.



Model 3.

Location of the Demec points



Loading arrangement

a) Strains at various levels at different loads

- compression
+ tension

Model No.	Total load P \ level	1	2	3	4	5	6
		Average strain x 10^5					
1	2500 N	-307	-272	-195			+193
	3750 N	-415	-353	-283	- 5	+138	+289
2	5000 N	-367	-333	-246			+160
	10000 N	-591	-529	-430		+ 68	+287
	14375 N	-921	-898	-858	-140	+121	+590
3	2500 N	-317	-259	-210	-133	+ 90	+192
	3125 N	-422	-348	-284	-211	+131	+237
	4250 N	-618	-525	-440	-292	+168	+375

b) Ultimate load & ultimate resisting moment

Model No.	Ultimate load P (N)	Ult. resisting moment (kN.m)
1	6000	1.050
2	14578	2.551
3	4575	0.801

TABLE 26

Stresses at various levels calculated from strain measurements

Beam model 1. $F_1 = 56.9\ N/mm^2$ $F_2 = 13.8\ N/mm^2$ $F_3 = 40.9\ N/mm^2$

Level	Load P = 3750 N			
	Strain x 10^5	E(N/mm^2)	Strain x E (N/mm^2)	Remarks
1	415	11740	48.72	$< F_1$ ∴ Elastic
2	353	"	41.44	"
3	283	"	33.22	"
4	5	8100	0.41	$< F_3$ ∴ Elastic
5	138	"	11.18	Tension zone
6	289	"	23.41	"

Beam model 2. $F_1 = 58.5\ N/mm^2$ $F_2 = 13.6\ N/mm^2$ $F_3 = 40.3\ N/mm^2$

Level	Load P = 14375 N			
	Strain x 10^5	E (N/mm^2)	Strain x E (N/mm^2)	Remarks
1	921	12020	110.70	$> F_1$ ∴ Plastic
2	898	"	107.94	"
3	858	"	103.13	"
4	140	9100	12.74	$< F_3$ ∴ Elastic
5	121	"	11.01	Tension zone
6	590	"	53.69	"

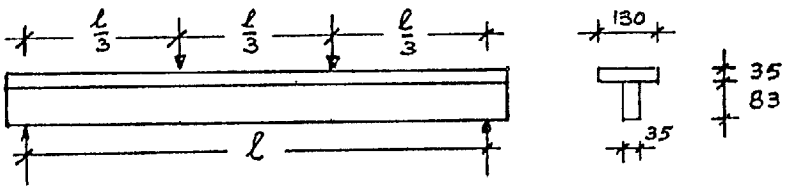
Beam model 3. $F_1 = 57.4\ N/mm^2$ $F_2 = 14.1\ N/mm^2$ $F_3 = 36.9\ N/mm^2$

Level	Load P = 4250 N			
	Strain x 10^5	E (N/mm^2)	Strain x E (N/mm^2)	Remarks
1	618	11200	69.22	$> F_1$ ∴ Plastic
2	525	"	58.80	"
3	440	"	49.28	$< F_1$ ∴ Elastic
4	292	9200	26.86	$< F_3$ ∴ Elastic
5	168	"	15.46	Tension zone
6	375	"	34.50	"

Note: Values of F_1, F_2 & F_3 are the results of the tests on the specimens.

6.2 Pilot Test series on T beams with non-layered flange to investigate the size effect problem

In order to compare the estimated and the actual ultimate resisting moments, 14 beams were tested. As the ultimate resisting moment is dependent on the volume, 3 volumes were considered. The criterion of different volume was achieved by merely changing the span and keeping the cross section as constant. The following figure shows the different beams considered.



Volume	Span l
V_1	1200 mm
V_2	1500 mm
V_3	1800 mm

To estimate the ultimate resisting moment, the following mechanical properties of the components must be known.

a) Modulus of elasticity of flange

b) Modulus of elasticity of rib

c) Ultimate compressive stress of flange

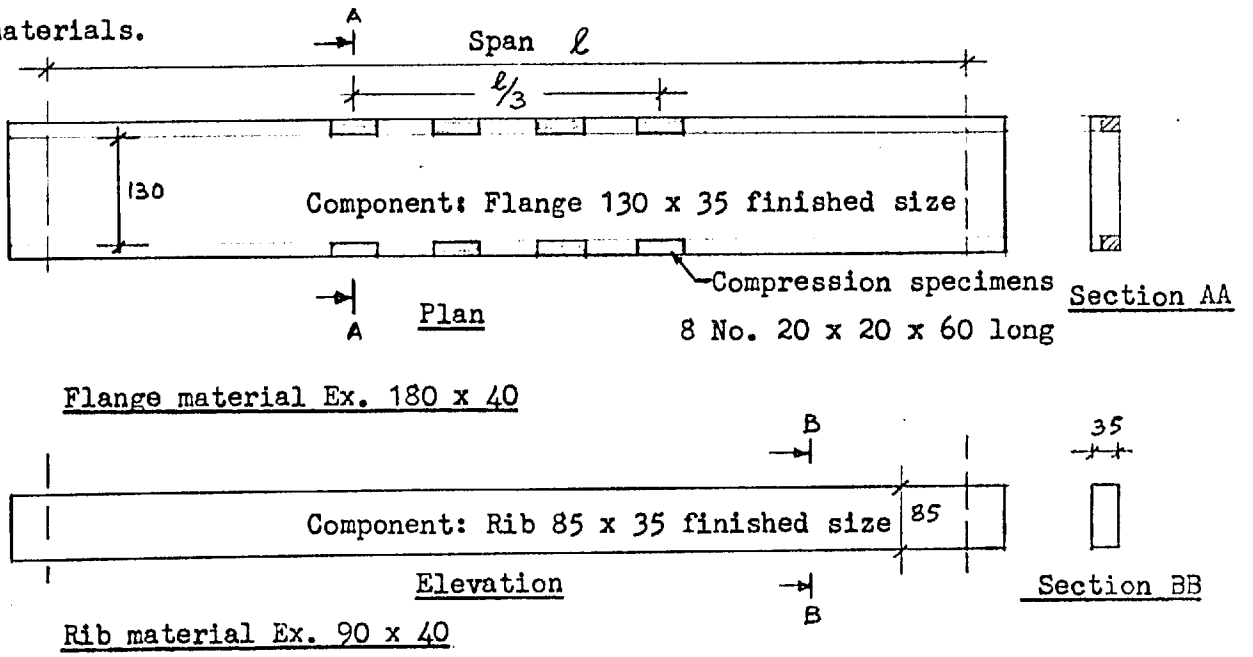
d) Ultimate compressive stress of rib

e) Ultimate tensile stress of rib

Items (a) to (d) were found by experiments. Item (e) was estimated by statistical analysis using Weibull's theory.

6.2.1 Preparation of Components and test specimens.

The timber raw materials for making the components were selected from Canadian Spruce-Pine-Fir group. When selecting the materials, care was taken to see that the defects such as knots, splits etc. were as small as possible. Nominal sizes of timber were 180x40mm and 90x40mm for flange and rib respectively. The following sketch shows the locations from where the components and the matching test specimens were taken from the raw materials.



From the geometry of the proposed T beam section and the mechanical properties of the components, it was estimated that the compressive stress level in the rib will be very low when the ultimate bending moment is reached. Therefore compression specimens were not made from the rib. As the timber raw materials were from the same group, ultimate compressive stress of the rib was assumed as the lowest value obtained when compression specimen from the flange materials were tested. This value was used as the Computer input data.

6.2.2 Experiments on Components

The following serial numbers were given to the components for the purpose of reference.

Flanges : serial numbers 1 to 14

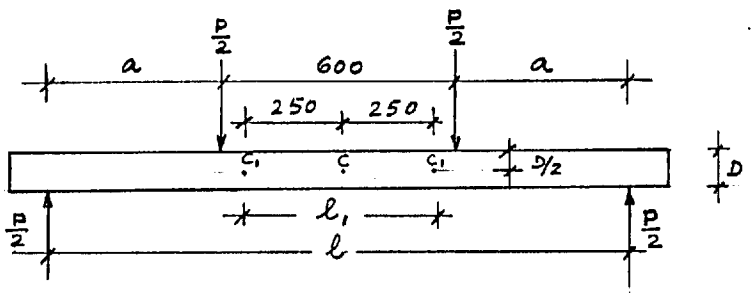
Ribs : serial numbers 15 to 28

Modulus of elasticity of flanges and ribs.

Two methods were adopted to find the modulus of elasticity.

1) Static bending test. 2) Ultrasonic pulse technique.

Static bending test. This test is broadly based upon the principle recommended by Joint Committee Rilem / CIB - 3T T-3: testing methods for timber in structural sizes. But, the dimensions are modified to suit the test specimen sizes.

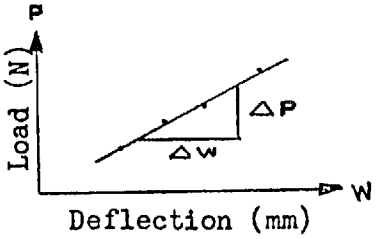


The details of the test set up are shown in Fig. 6.12

The difference between the deflections at C and C_1 is measured by the deflectometer fixed at C on a frame which is suspended from the points C_1. To achieve better accuracy two frames (one on each face) are used on the specimen and the average value of the deflection is adopted.

Deflections are measured at various loads and a load/deflection graph is drawn. The modulus of elasticity is calculated from the following formula.

$$E = \frac{\Delta P}{\Delta w} \times \frac{a l_1^2}{16\, I}$$



where E = Modulus of elasticity in bending (N/mm^2)

ΔP = An increment of load (N)

Δw = Deflection under the increment of load ΔP (mm)

a = Distance between an inner load point and the nearest support point (mm)

l_1 = Gauge length (mm)

I = Second moment of area of the section determined from its actual dimensions (mm^4)

Test results are given in Table 28

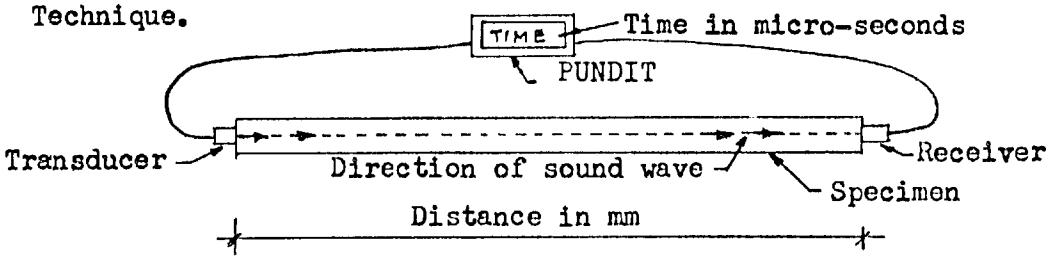
Ultrasonic pulse technique. This is a quick method of finding the modulus of elasticity. In this method the velocity of sound waves during the travel through the specimen is measured by an instrument called PUNDIT (Portable Ultrasonic Non-destructive Digital Indicating Tester). Using this information the dynamic modulus of elasticity can be calculated using the following formula.

$E_{Dyn} = mv^2$ when E_{Dyn} = Dynamic modulus of Elasticity (N/mm^2)

m = mass (Kg/m^3)

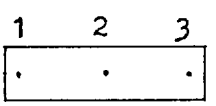
v = velocity (Km/sec)

The following sketch shows the test set up using Ultrasonic pulse Technique.

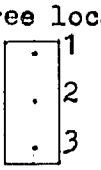


Test set up for Ultrasonic Pulse Technique

To achieve better accuracy, time is noted at three locations as shown



Components 1 to 14



Components 15 to 28

Average velocity is adopted to calculate the average E_{Dyn}. The other possible alternative is to calculate E_{Dyn} at each location and

find the average. But the differences between the latter and the former was found to be within $\pm \frac{1}{2}\%$ for the sections chosen. Calculation of E_{Dyn} using the average velocity was considered to be adequate for the specimens with small cross section.

It has been established by various researchers that E_{Dyn} is directly proportional to E_{Static}. Hence the relationship between E_{Dyn} and E_{Static} can be written as

$$E_{Static} = \eta . E_{Dynamic}$$

Nwokoye (1971) found that η is approximately equal to 0.865 for timber generally used for structural purpose. Table 29 shows the relationship between E_{Dyn} and E_{Static} for the 28 components tested for this thesis. The appropriate average value of η resulted from these limited number of tests was found to be 0.82 .

In the case of non-layered T beams, the values of E_{Static} obtained from the bending tests were adopted for computation purpose.

Ultimate compressive stress of flange.

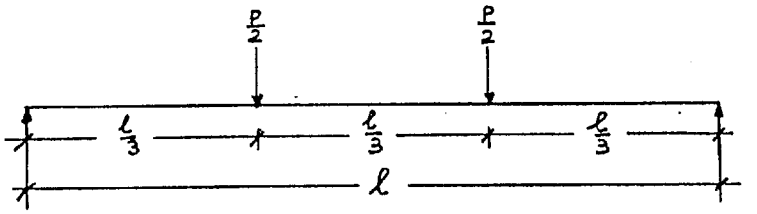
8 specimens were taken from each flange and they were tested in an Amsler 10 ton testing machine. All specimens were 20mm x 20mm in cross-section and 60mm long. These dimensions are as per the recommendations of BS 373 for small clear specimens. The average value of 8 specimens were taken as the ultimate compressive stress of the flange to which they were matched. The results are shown in Table 30.

Ultimate compressive stress of Rib.

For the T section chosen for the experiment, the ultimate compressive stress was not critical and hence no specimens were tested. As for the computer input data, the minimum value obtained from the compression tests on flange specimens which belong to the same species group of the ribs was adopted.

6.2.3 Making of the model Beams and Testing

When all the relevant mechanical properties of flanges and ribs were ascertained 14 model beams were made by gluing flanges to the webs. Phenol resorcinol glue was used. Glue pressure was provided by G clamps. In addition, 3.2mm dia x 50mm long screws were provided at 150mm centres along the glue line. The glue joint was kept under pressure over 24 hours and the tests on the beams were carried out after 48 hours. The beams were tested to destruction on a 35 ton Amsler testing machine.



Equal loads were applied at $\frac{1}{3}$rd span as shown in the sketch. Beam 1 was used for preliminary tests to find the adequacy of the test rig set up. Ultimate collapse load was noted in the case of all other beams. Beam 9 failed in longitudinal shear in the timber flange. There was a weak cleavage in the flange due to the growth ring. All other beams failed in tension in the rib. In all cases (except beam 9) the failure was sudden confirming the brittle failure of timber in tension. In few cases cracking noise was heard at about 85 to 90% of the ultimate load.

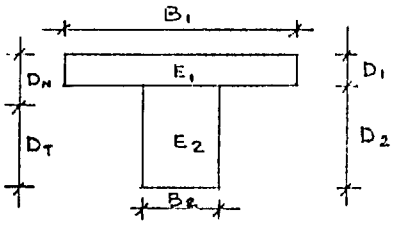
The test results are given in Table 33.

Table 34 shows the depth of neutral axis and the stress at important locations of the test beams at the ultimate load. Stresses are calculated from the ultimate bending moment. The calculations revealed that except beam 11 all other beams failed in mode 1. Failure mode of beam 11 was 2. It was not possible to identify the failure mode by visual examination. From Table 32 it will be seen that the ultimate compressive stress of the flange 11 is the least. This indicates the possibility of yield developing in the flange.

The stresses are calculated using the following procedure.

The location of elastic N.A is found by using the formula,

$$D_N = \frac{\frac{1}{2} E_1 B_1 D_1^2 + E_2 B_2 D_2 (D_1 + \frac{1}{2} D^2)}{E_1 B_1 D_1 + E_2 B_2 D_2}$$



Now flexural stiffness EI can be calculated.

$$EI = E_1 B_1 D_1 \left[\frac{D_1^2}{12} + (D_N - \tfrac{1}{2} D_1)^2\right] + E_2 B_2 D_2 \left[\frac{D_2^2}{12} + (D_T - \tfrac{1}{2} D_2)^2\right]$$

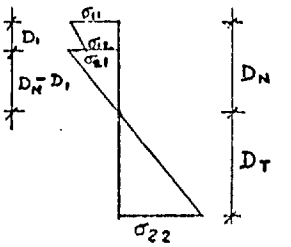
Section modulus in compression and tension are as follows.

$$Z_c = \frac{EI}{E_1 D_N} \qquad Z_t = \frac{EI}{E_2 D_T}$$

Now stresses at important points can be calculated using the ultimate bending moment.

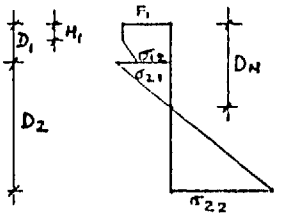
$$\sigma_{11} = \frac{BM}{Z_c} \qquad \sigma_{12} = \sigma_{11} \frac{(D_N - D_1)}{D_N}$$

$$\sigma_{22} = \frac{BM}{Z_t} \qquad \sigma_{21} = \sigma_{22} \frac{(D_N - D_1)}{D_T}$$



If the calculated values of σ_{11} and σ_{21} are less than the ultimate compressive stress of flange and rib respectively, the failure mode is 1. In the case of beam 11 it was found that σ_{11} was greater than the ultimate compressive stress of the rib. Therefore the mode of failure is 2 for beam 11. The trial and error method is adopted to find the stresses. Assume an arbitrary value for H_1.

$$D_N = \frac{D_1^2 \alpha (2 + \alpha) + \frac{\beta}{\gamma}(H_1^2 + D_1^2)}{2 D_1 (\frac{\beta}{\gamma} + \alpha)}$$



Using the known value of F_1, stresses σ_{12}, σ_{21} & σ_{22} and thereby the resisting moment of the section can be calculated. If the resisting moment is not equal to the ultimate bending moment, repeat the whole process with other values of H_1 until the error is within the acceptable limit. Stresses corresponding to the final resisting moment are given in Table 34 against beam 11.

6.2.4 Review of beam test results

Tables 35 and 36 show the comparison of the actual ultimate resisting moments from tests and the estimated resisting moments using different values of k and K_0. Table 35 is prepared by using the values of k and K_0 taken from appendix 4. The ribs of the test beams are made from the same group of timber considered in appendix 4. As explained in this appendix, the derived values of k and K_0 are unreliable. Therefore, the reliability of the estimated values of the resisting moment could be considered only as good as the reliability of the values of k and K_0. However, it will be of interest to note that the actual ultimate resisting moment is always higher than the estimated value at 99.9% probability of failure. In Table 35 estimated values of the resisting moment at 5% probability of failure also have been included.

Because of the unreliability of the values adopted in Table 35, Table 36 is prepared using different values of k and K_0 keeping one of them approximately same as that used in Table 35. The values are chosen in such a manner that the estimated resisting moment is very nearly equal to the actual ultimate resisting moment of test beam (No.4) which had the least resistance. The ratio of actual resisting moment/estimated resisting moment has been given against each beam. As the variability of the mechanical properties is very high in the case of timber, it was anticipated that the difference between the actual and estimated values will also be very high. Table 35 and 36 show that it may be possible to obtain a safe solution using Weibull's statistical strength theory. However, definite conclusions can be made only when statistically reliable values of k and K_0 are available.

TABLE 27

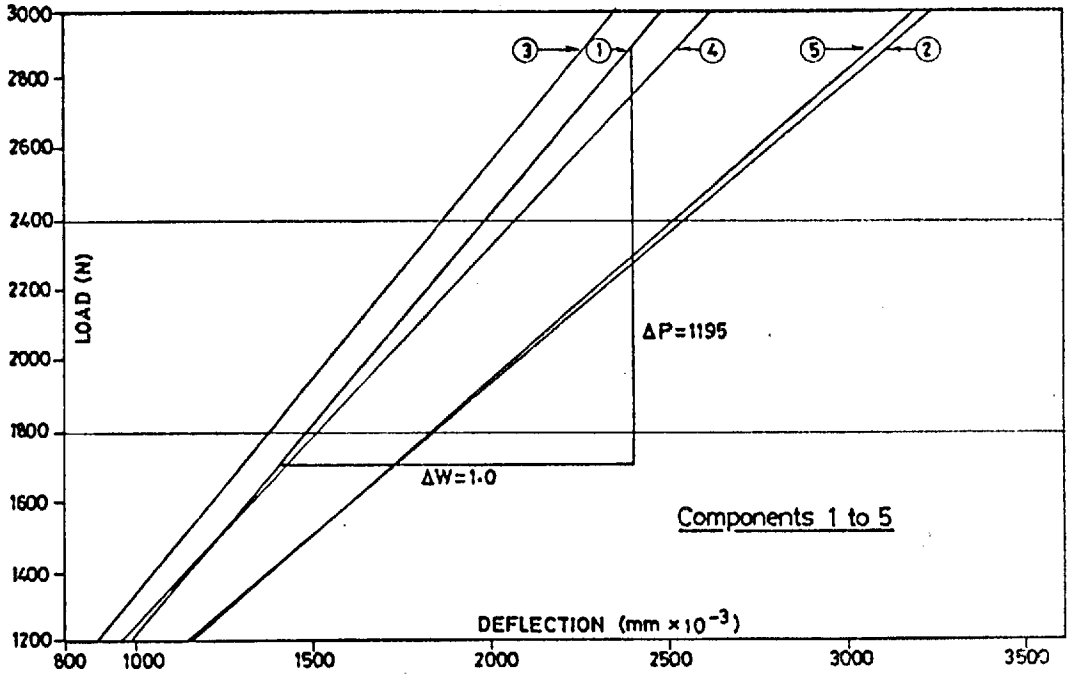
Modulus of Elasticity using Ultrasonic pulse Techinique

Component	Section	Mass m (kg/m^3)	Length (mm)	Time ($sec \times 10^{-6}$)	Velocity v (km/sec)	$E_{Dyn} = mv^2$ (N/mm^2)
1	130 × 35	400.3	1400	239	5.86	13746
2	"	471.0	1400	261	5.36	13532
3	"	546.3	1400	260	5.38	15812
4	"	447.4	1400	248	5.65	14282
5	"	384.6	1400	261	5.36	11049
6	"	387.3	1700	307	5.54	11902
7	"	407.2	1700	289	5.88	14079
8	"	418.9	1700	299	5.68	13515
9	"	396.9	1700	292	5.82	13444
10	"	452.5	1700	298	5.70	14702
11	"	412.1	2000	373	5.36	11839
12	"	470.3	2000	362	5.52	14907
13	"	413.2	2000	355	5.63	13097
14	"	456.0	2000	337	5.93	16035
15	35 × 83	452.4	1400	239	5.86	15535
16	"	393.4	1400	256	5.47	11771
17	"	486.8	1400	228	6.14	18354
18	"	489.3	1400	255	5.49	14743
19	"	491.8	1400	253	5.53	15040
20	"	526.5	1700	310	5.48	15811
21	"	500.2	1700	310	5.48	15021
22	"	319.9	1700	331	5.14	8452
23	"	546.7	1700	301	5.65	17452
24	"	506.2	1700	326	5.21	13740
25	"	559.4	2000	382	5.24	15360
26	"	425.1	2000	339	5.90	14796
27	"	547.3	2000	367	5.45	16256
28	"	438.9	2000	357	5.60	13764

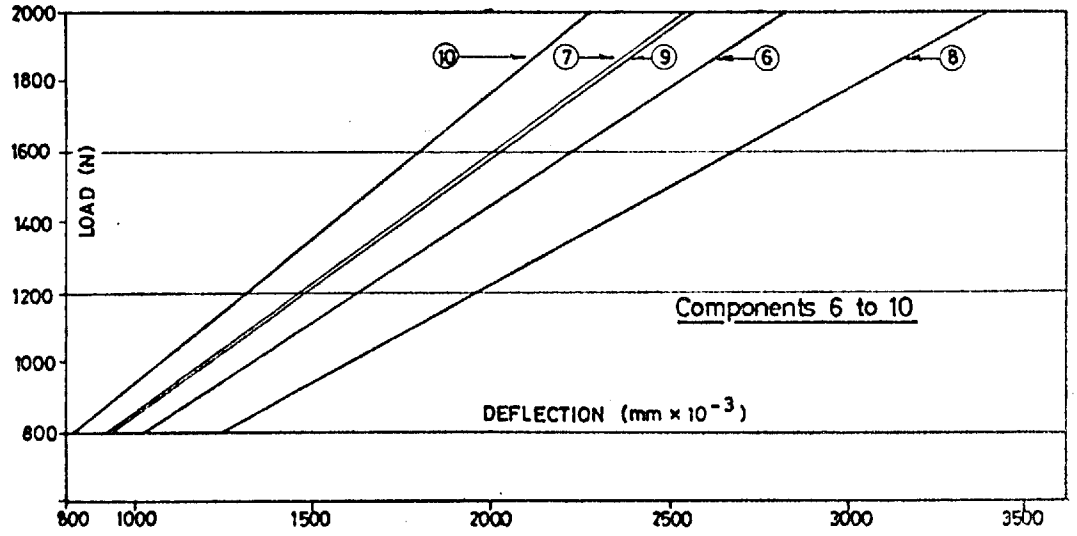
LOAD/DEFLECTION RELATIONSHIP OF THE COMPONENTS
OF THE TEST BEAMS.
STATIC BENDING TEST RESULTS.

Fig. 6.9

(a)



(b)



(c)

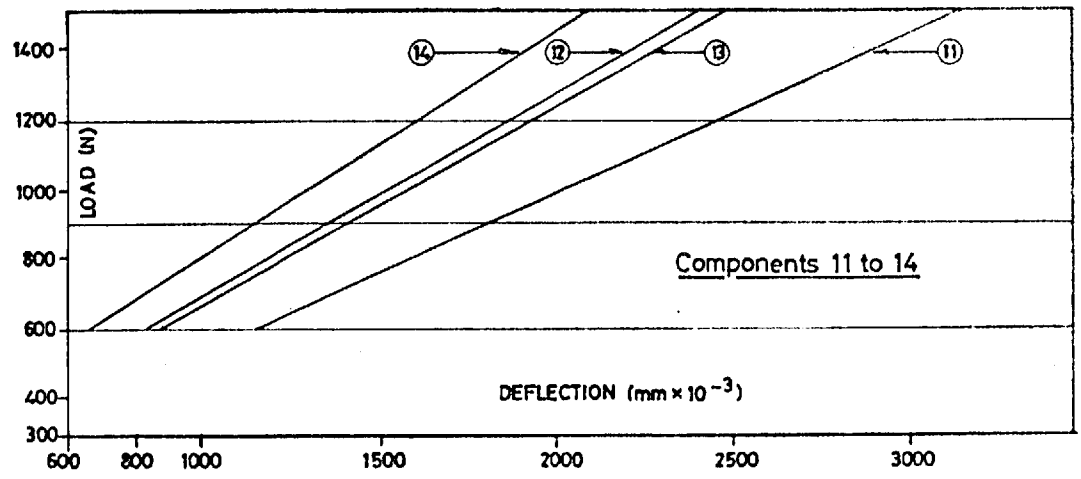
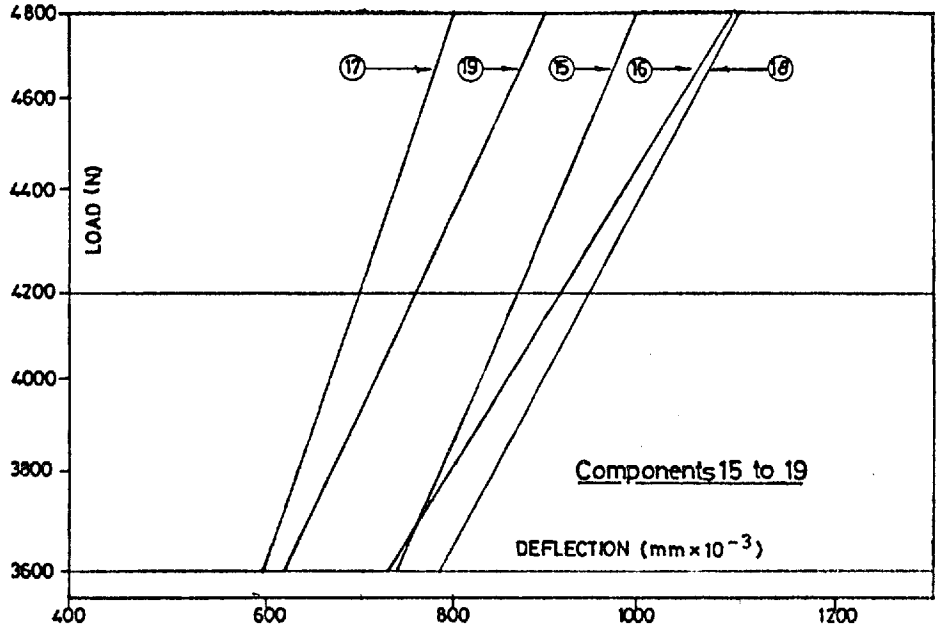
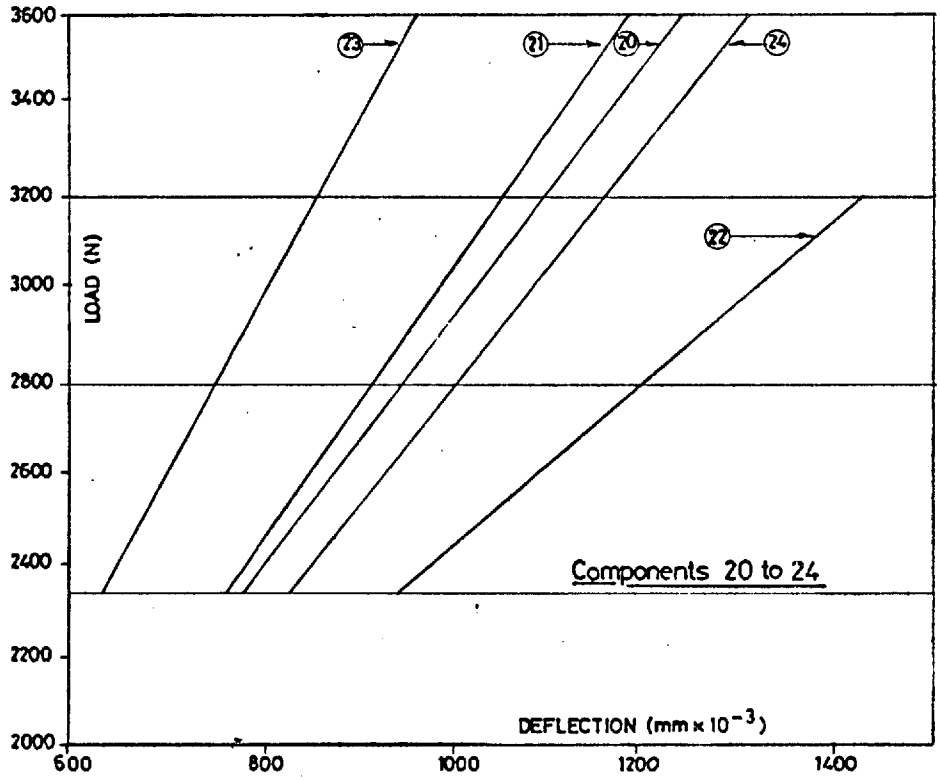


Fig 6·9 (cont.)

(d)



(e)



(f)

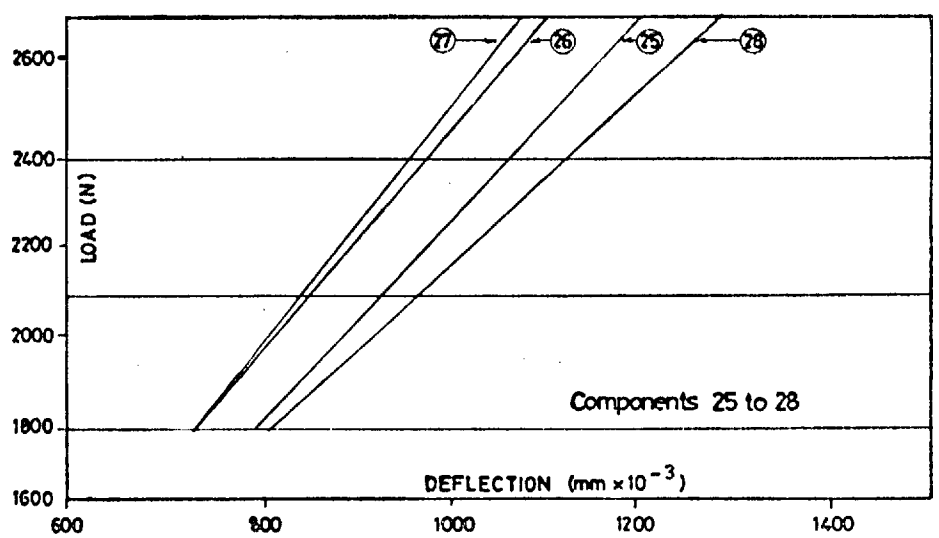


TABLE 28

Results of Static bending Test for modulus of Elasticity

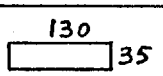
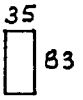
Component	Section	a (mm)	$\frac{al_1^2}{16\ I}$	$\frac{\Delta P}{\Delta w}$	l_1 = 500 mm E_{static} (N/mm^2)
1		300	10.091949	1195	12060
2	"	"	"	855	8629
3	"	"	"	1225	12363
4	"	"	"	1085	10950
5	"	"	"	890	8982
6	"	450	15.137924	660	9991
7	"	"	"	720	10899
8	"	"	"	550	8325
9	"	"	"	720	10899
10	"	"	"	810	12262
11	"	600	20.183898	445	8982
12	"	"	"	570	11504
13	"	"	"	560	11302
14	"	"	"	630	12716
15		300	2.810737	4700	13210
16	"	"	"	3300	9275
17	"	"	"	5880	16527
18	"	"	"	3790	10653
19	"	"	"	4330	12170
20	"	450	4.216105	2680	11300
21	"	"	"	2930	12353
22	"	"	"	1750	7378
23	"	"	"	3740	15768
24	"	"	"	2575	10856
25	"	600	5.621474	2160	12142
26	"	"	"	2400	13492
27	"	"	"	2550	14335
28	"	"	"	1870	10512

TABLE 29

Relationship between E_{Static} and $E_{Dynamic}$

Component	E_{Dyn}	E_{Static}	$\frac{E_{Static}}{E_{Dyn}}$
1	13746	12060	0.877
2	13532	8629	~~0.638~~
3	15812	12363	0.782
4	14282	10950	0.767
5	11049	8982	0.812
6	11902	9991	0.839
7	14079	10899	0.774
8	13515	8325	~~0.616~~
9	13444	10899	0.811
10	14702	12262	0.834
11	11839	8982	0.759
12	14907	11504	0.878
13	13097	11302	0.863
14	16035	12716	0.793
15	15535	13210	0.850
16	11771	9275	0.788
17	18354	16527	0.900
18	14748	10653	0.722
19	15040	12170	0.809
20	15811	11300	0.715
21	15021	12353	0.822
22	8542	7378	0.873
23	17452	15768	0.904
24	13740	10856	0.790
25	15360	12142	0.790
26	14796	13492	0.912
27	16256	14335	0.882
28	13764	10512	0.764

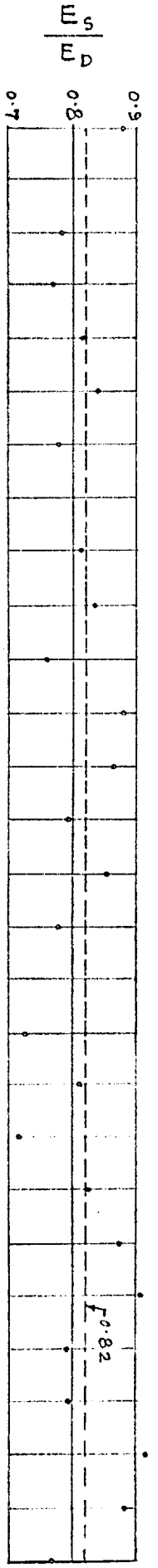


TABLE 30

Results of Compression Tests of matching specimens of Flanges

Area of cross-section = 400 mm^2

Component	Average failure Load		Ult. Comp. stress
	lb	N	N/mm^2
1	3192	14198	35.50
2	4004	17810	44.53
3	4884	21725	54.31
4	3996	17775	44.44
5	3243	14425	36.06
6	3568	15871	39.68
7	3686	16396	40.99
8	3104	13807	34.52
9	3295	14656	36.64
10	4103	18251	45.63
11	3071	13660	34.15
12	4032	17935	44.84
13	3349	14897	37.24
14	4011	17841	44.60

TABLE 31

Moisture content of the components at the time of Beam test

Component No.	Moisture content%	Component No.	Moisture content%
1	11.44	15	11.83
2	12.04	16	12.63
3	12.45	17	12.57
4	12.30	18	12.84
5	11.64	19	12.18
6	10.67	20	12.74
7	12.09	21	12.29
8	11.75	22	12.16
9	12.25	23	11.63
10	12.60	24	13.19
11	12.18	25	12.26
12	12.02	26	12.02
13	12.94	27	12.34
14	11.65	28	11.52

Average moisture content of flange material = 12.00%

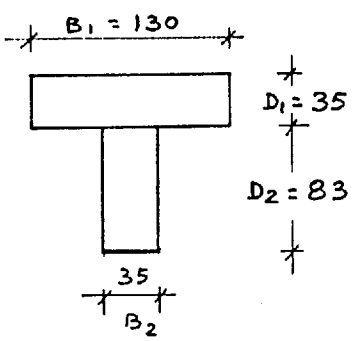
Average moisture content of rib material = 12.30%

TABLE 32

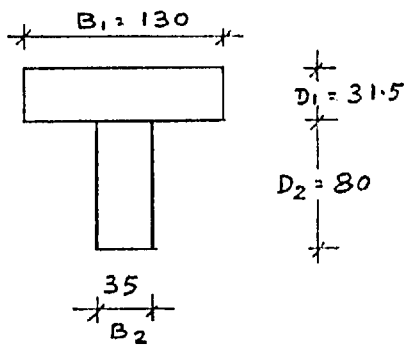
Properties of Components of Test Beams

Beam No	Span mm	Component serial number Flange	Rib	Modulus of Elasticity of Flange E_1 (N/mm^2)	Modulus of Elasticity of Rib E_2 (N/mm^2)	Ult.comp. stress of Flange F_1 (N/mm^2)
1	1200	1	15	12060	13210	35.50
2	1200	2	16	8629	9275	44.53
3	1200	3	17	12363	16527	54.31
4	1200	4	18	10950	10653	44.44
5	1200	5	19	8982	12170	36.06
6	1500	6	20	9991	11300	39.68
7	1500	7	21	10899	12353	40.99
8	1500	8	22	8325	7378	34.52
9	1500	9	23	10899	15768	36.64
10	1500	10	24	12262	10856	45.63
11	1800	11	25	8982	12142	34.15
12	1800	12	26	11504	13492	44.84
13	1800	13	27	11302	14335	37.24
14	1800	14	28	12716	10512	44.60

Ultimate compressive stress (F_3) of rib in all cases = 34.15 N/mm^2 (assumed value)



Cross-section of all Beams except Beam (5)



Cross-section of Beam (5)

TABLE 33

Results of Beam Tests

Beam	Span l m	Ultimate Load P Ton	kN	Ultimate B.M kN.m
2	1.200	3.740	37.265	7.453
3	1.200	4.455	44.390	8.878
4	1.200	2.580	25.707	5.141
5	1.200	3.160	31.486	6.297
6	1.500	2.350	23.415	5.854
7	1.500	3.170	31.586	7.896
8	1.500	2.070	20.625	5.156
9	1.500	3.325	33.130	8.283
10	1.500	2.970	29.593	7.398
11	1.800	2.870	28.597	8.579
12	1.800	1.820	18.134	5.440
13	1.800	1.975	19.679	5.904
14	1.800	2.535	25.259	7.578

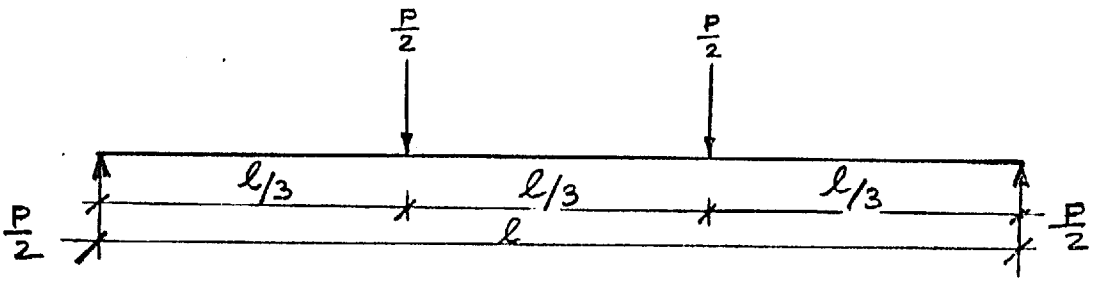
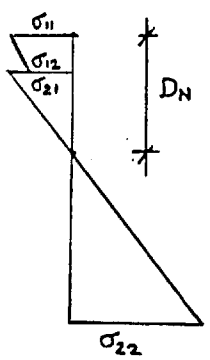


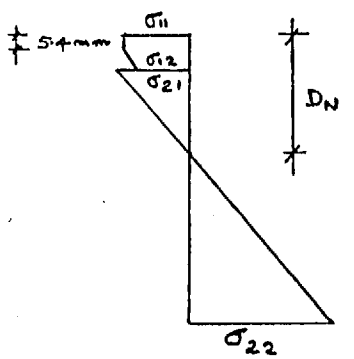
TABLE 34

Depth of N.A and stresses at important locations of the test beams at the ultimate load

Beam No.	D_N Depth of N.A (mm)	σ_{11} (N/mm^2)	σ_{12} (N/mm^2)	σ_{21} (N/mm^2)	σ_{22} (N/mm^2)	Max. Rib shear stress (N/mm^2)	Interface Rib shear stress (N/mm^2)
2	41.51	35.55	5.58	5.99	70.41	6.73	6.68
3	44.67	39.71	8.59	11.49	87.14	7.99	7.85
4	40.11	25.28	3.22	3.13	47.77	4.65	4.63
5	42.56	31.59	8.21	11.12	69.34	5.98	5.82
6	42.24	27.50	4.71	5.33	55.78	4.23	4.19
7	42.27	37.07	6.38	7.23	75.27	5.70	5.65
8	38.82	26.11	2.57	2.28	47.20	3.74	3.73
9	45.83	36.21	8.56	12.38	82.50	5.95	5.52
10	38.81	37.48	3.68	3.25	67.71	5.36	5.35
11	45.06	34.15	8.66	11.71	84.90	5.11	5.07
12	42.76	25.28	4.59	5.38	52.16	3.27	3.24
13	43.90	26.81	5.44	6.89	57.40	3.54	3.49
14	37.88	39.24	2.99	2.47	68.61	4.58	4.57



Stress diagram for all beams (except beam 11)



Stress diagram for beam 11

TABLE 35

Comparison of estimated and actual ultimate resisting moments of the Test beams.

$k = 13.14$ $K_0 = 74.95$

(values taken from appendix 4)

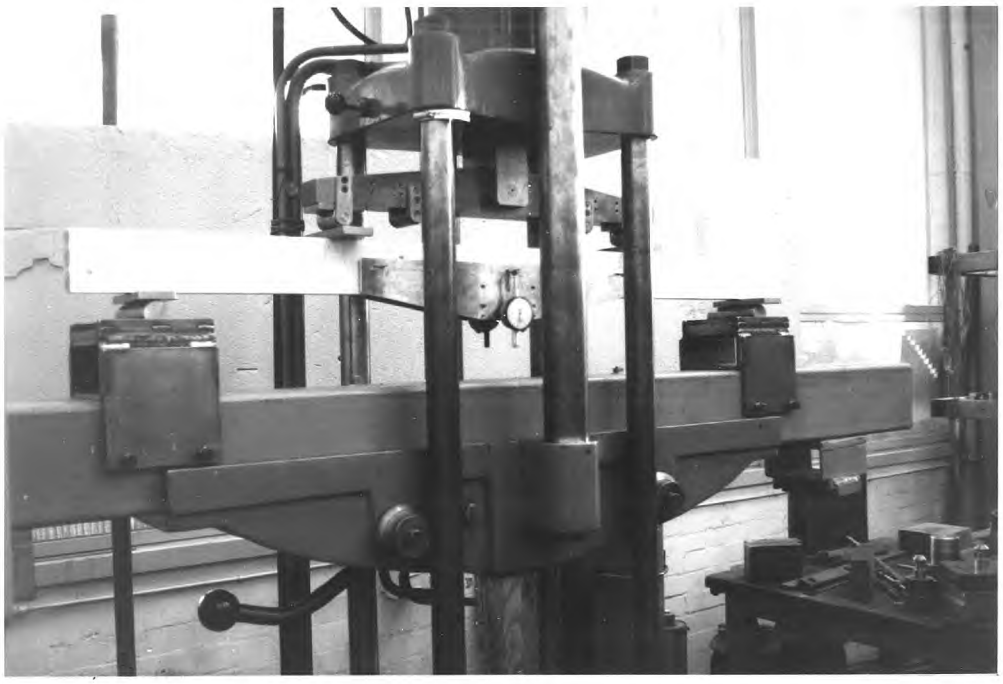
Beam No.	Span (mm)	Estimated ultimate resisting moment (kN.m)		Actual ultimate resisting moment (kN.m)
		at 5% Prob. of failure	at 99.9% prob. of failure	
2	1200	2.739	3.980	7.453
3	1200	2.645	3.842	8.878
4	1200	2.781	4.038	5.141
5	1200	2.369	3.441	6.297
6	1500	2.672	3.880	5.854
7	1500	2.671	3.879	7.896
8	1500	2.773	4.026	5.156
9	1500	2.566	3.726	8.283
10	1500	2.773	4.026	7.398
11	1800	2.560	3.717	8.579
12	1800	2.621	3.806	5.440
13	1800	2.588	3.758	5.904
14	1800	2.762	4.011	7.578

TABLE 36

Comparison of actual and estimated ultimate resisting moments using using different values of k and K_0

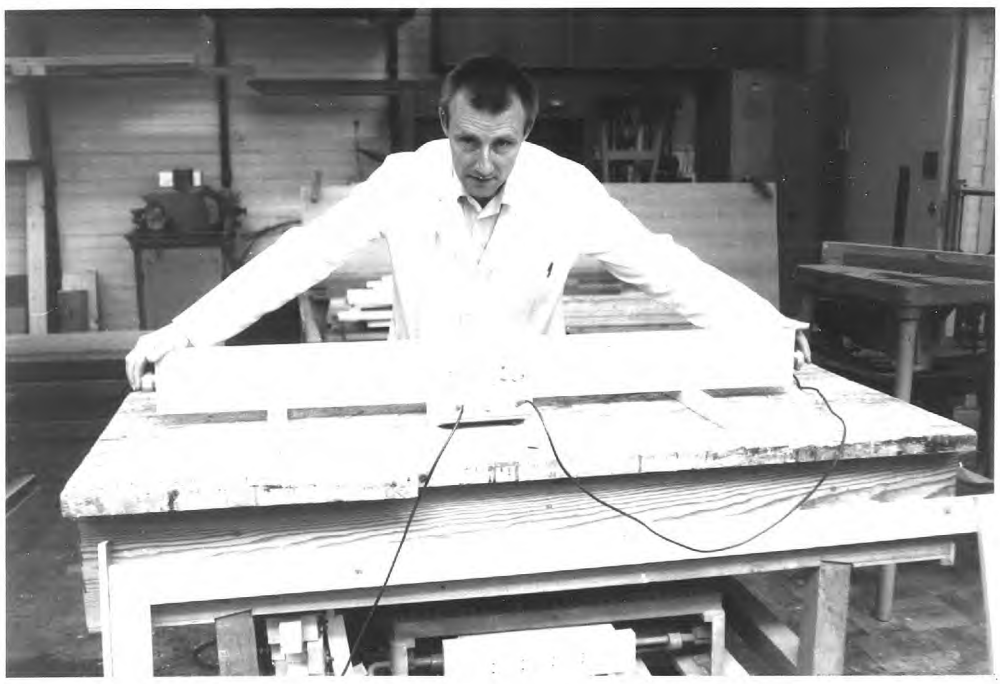
Probability of failure for estimated values = 99.9%

Beam No.	Actual ult. resisting moment from Test results (kN.m)	Estimated R.M when k = 13 K_0 = 95 (kN.m)	Actual R.M / Esti. R.M	Estimated R.M when k = 19 K_0 = 75 (kN.m)	Actual R.M / Esti. R.M
2	7.453	5.004	1.489	5.029	1.482
3	8.878	4.832	1.837	4.850	1.831
4	5.141	5.080	1.012	5.107	1.007
5	6.297	4.328	1.455	4.338	1.452
6	5.854	4.880	1.200	4.930	1.187
7	7.896	4.879	1.618	4.928	1.602
8	5.156	5.061	1.019	5.120	1.007
9	8.283	4.687	1.767	4.729	1.752
10	7.398	5.064	1.460	5.121	1.445
11	8.579	4.675	1.835	4.739	1.810
12	5.440	4.785	1.137	4.854	1.121
13	5.904	4.725	1.250	4.791	1.232
14	7.578	5.044	1.502	5.124	1.488



a) Static bending test

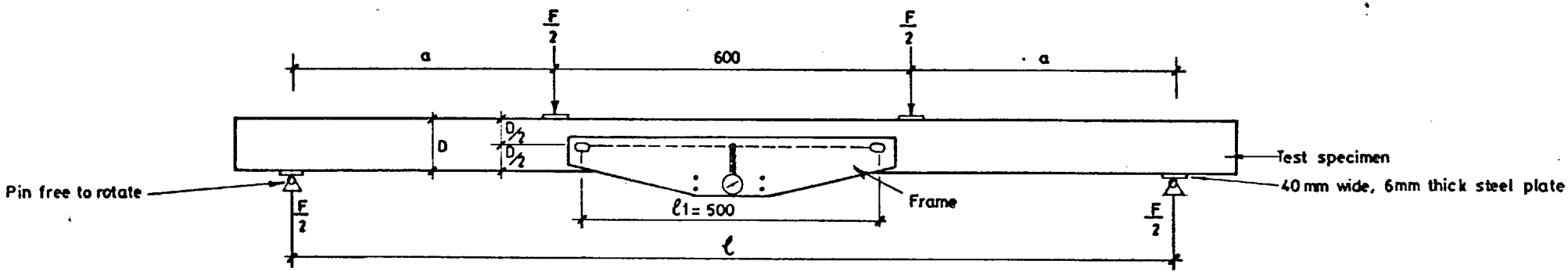
Fig. 6.10



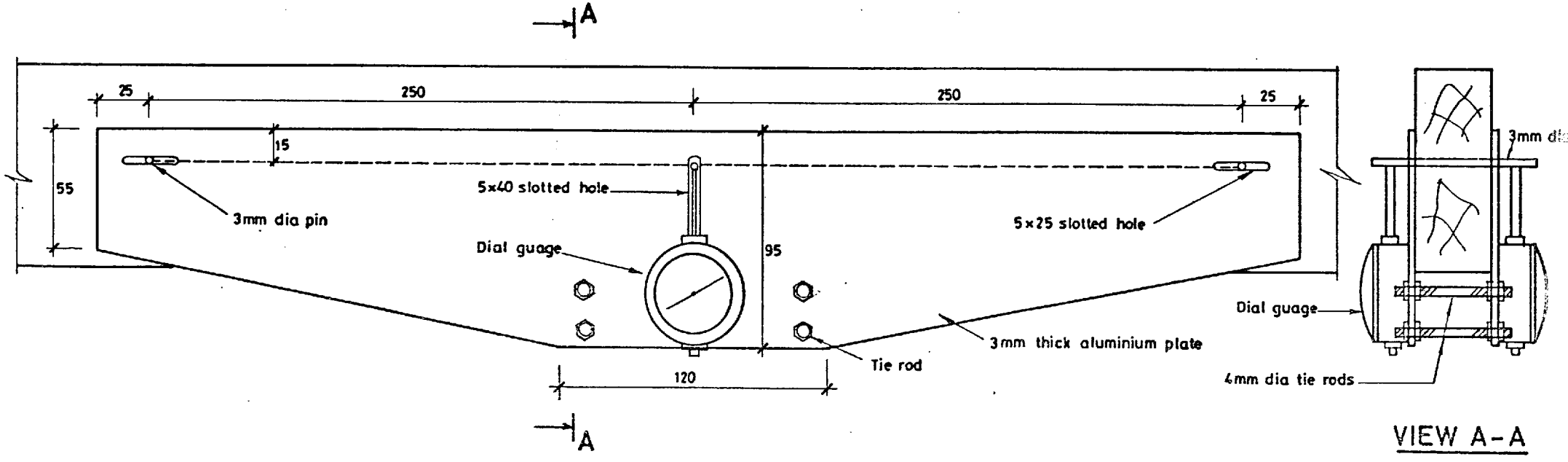
b) Ultrasonic pulse technique

Fig. 6.11

Testing arrangements for modulus of elasticity

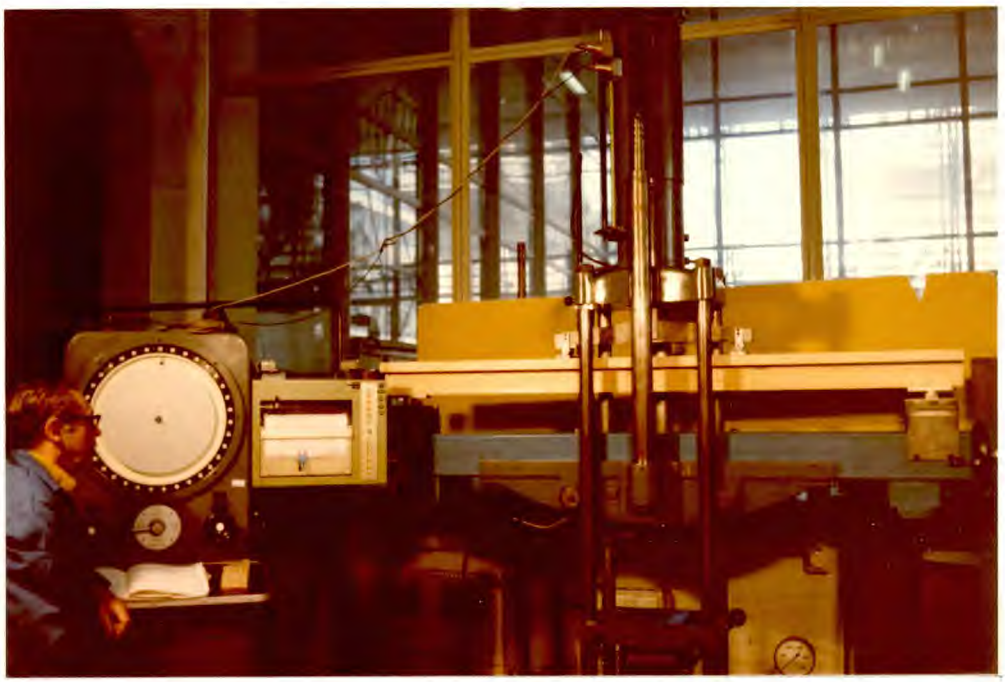


BENDING TEST TO FIND THE MODULUS OF ELASTICITY



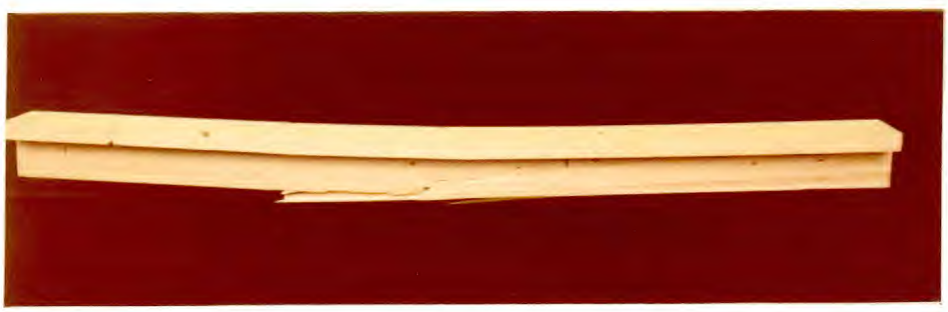
VIEW A-A

ENLARGED DETAIL OF FRAME Fig. 6·12



a) Test set up

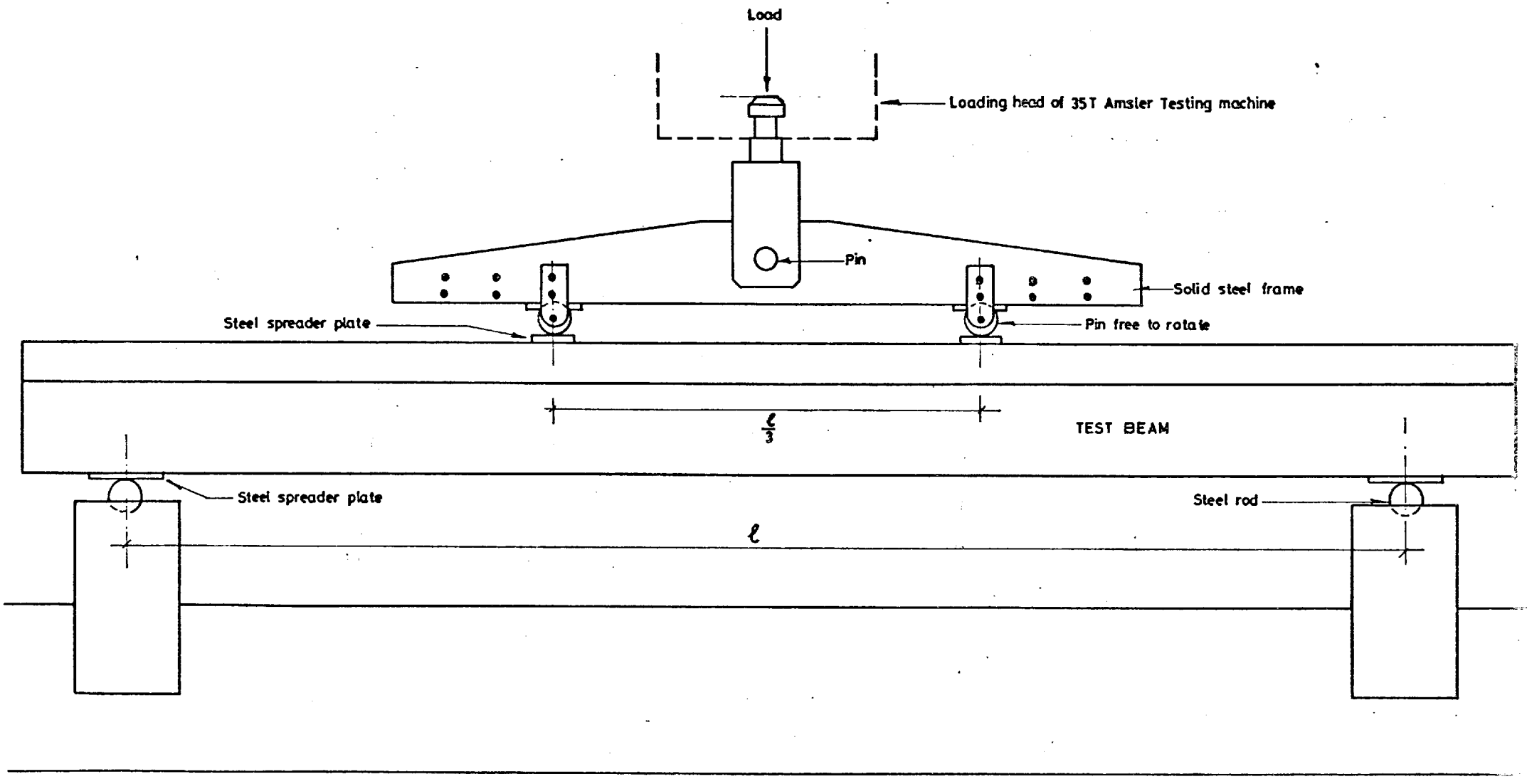
Fig. 6.13



b) Typical failed model beam

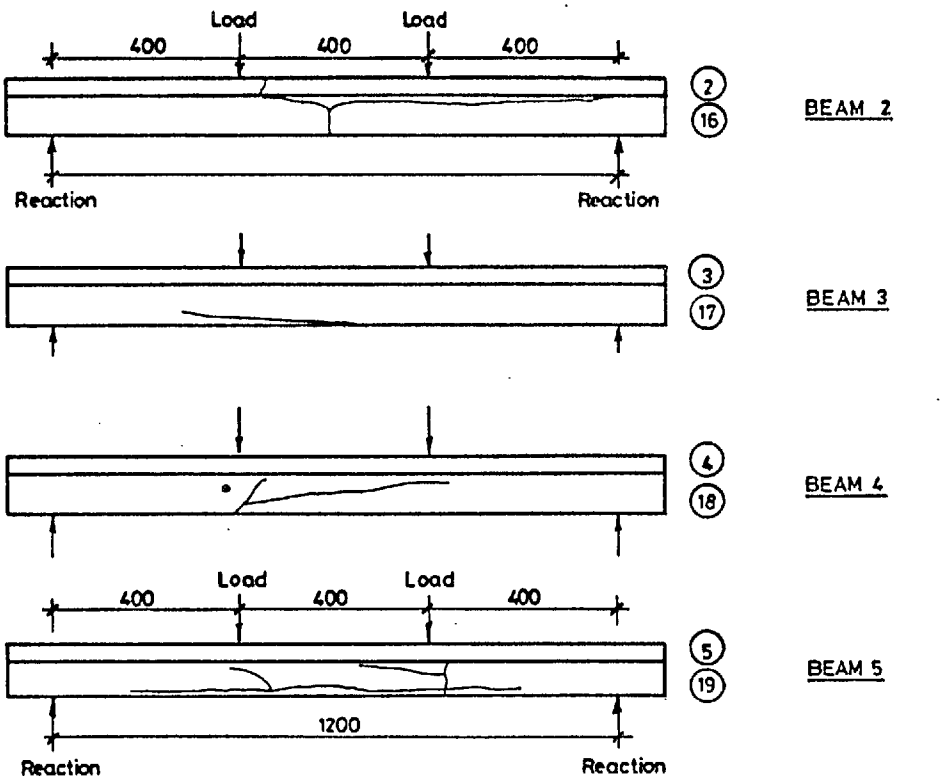
Fig. 6.14

Ultimate load test on T beam

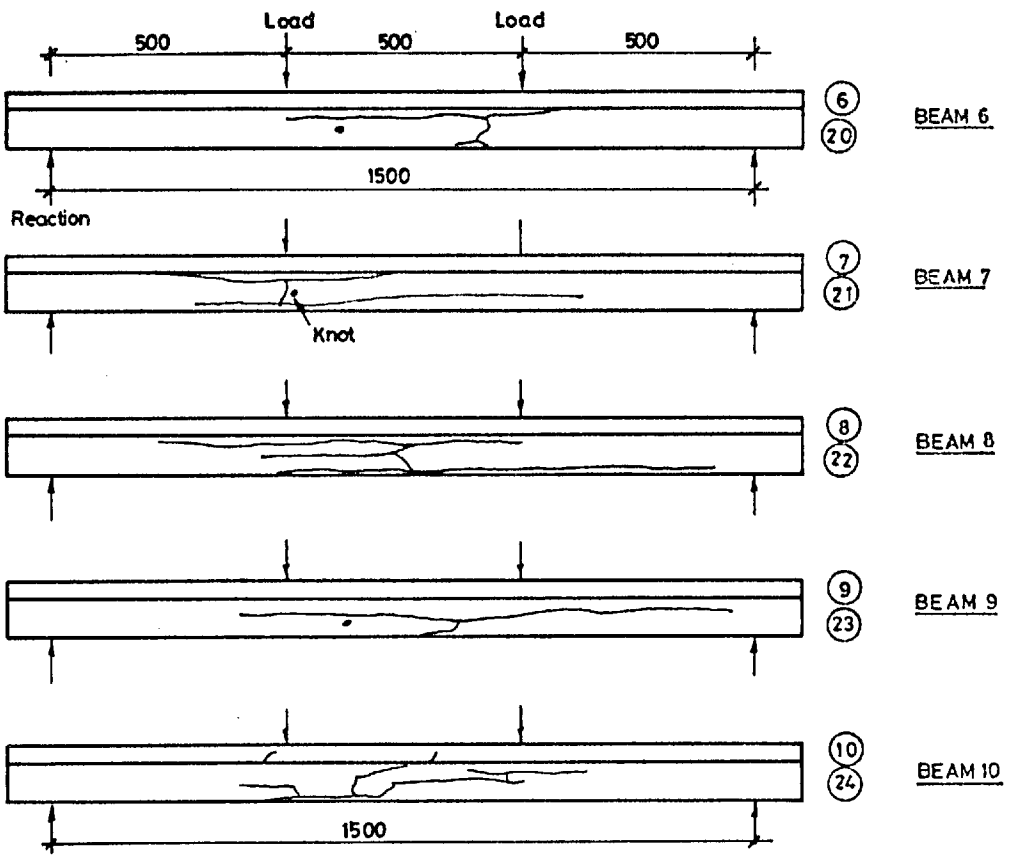


ULTIMATE LOAD TEST ARRANGEMENT Fig. 6·15

Fig. 6.16



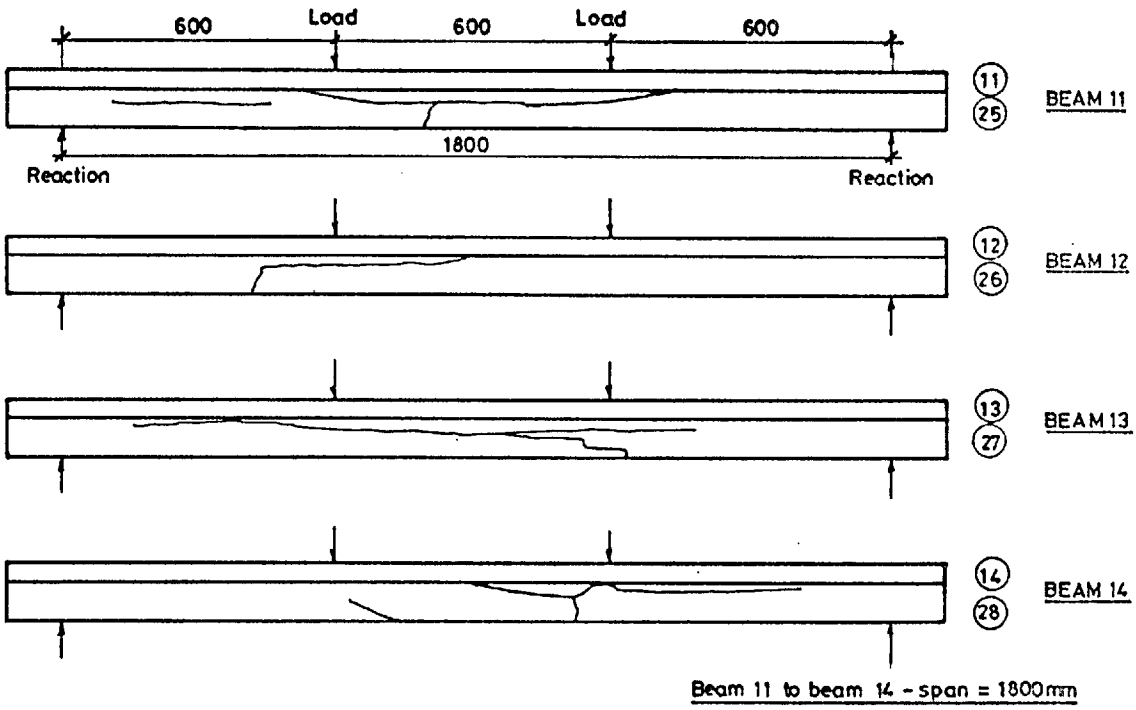
Beam 2 to beam 5 - span = 1200 mm



Beam 6 to beam 10 - span = 1500 mm

FAILURE PATTERN OF TEST BEAMS

Fig. 6.16 (cont.)


600
Load
600
Load
600
1800
Reaction
Reaction
11
25
BEAM 11
12
26
BEAM 12
13
27
BEAM 13
14
28
BEAM 14
Beam 11 to beam 14 - span = 1800mm

CHAPTER 7

Computer Programs

7.1 Introduction

Computer programs written for the analysis of T beams and I beams are described in this chapter. Beams with non-layered and layered flanges have been considered. The aim of the analysis is to find the ultimate resisting moment and the mode of failure of a particular beam. The program can be placed in two distinct categories. The programs in the first category assume that all mechanical properties of the components (including the ultimate tensile strength of the rib) are known. Volume effect on the ultimate tensile stress has not been considered here. In the second category, the probable ultimate tensile stress attained by the rib is predicted by the program from the statistical strength data. Volume effect on the ultimate tensile stress of the rib has been considered by the programs in the second category.

7.2 Computer programs

The programs are designated as follows.

First category:	a)	NOLAFT	Analysis of NON-LAYERED FLANGED T SECTION
	b)	NOLAFTI	Analysis of NON-LAYERED FLANGED T & I SECTIONS
	c)	LAYFLIT	Analysis of LAYERED FLANGED I & T SECTIONS
Second category:	a)	PNT	PROBABILISTIC ANALYSIS OF NON-LAYERED T BEAM
	b)	PLT	PROBABILISTIC ANALYSIS OF LAYERED T BEAM

7.2.1 NOLAFT This program analyses a T section with a non-layered flange, using the 'direct search method'. The essential conditions for each mode of failure are checked, starting from mode 1. When all essential conditions of a particular mode are satisfied, the detailed analysis is made to find the ultimate resisting moment of the section.

7.2.2 NOLAFTI This program is capable of analysing T section and I section with non-layered flanges, using the iteration procedure. Detailed description of the method of analysis is given in chapter 2, under the subsection 2.5.2. The iteration procedure is described in Appendix 1.

7.2.3 LAYFLIT The analysis of T section and I section with layered flanges is achieved by this program. Iteration procedure is adopted in this program also. Upto 17 layers in each flange have been considered.

7.2.4 PNT Weibull's statistical strength theory has been used in this program to predict the ultimate resisting moment of a T beam with non-layered flange at any probability of failure. The iteration procedure is the basis of the analysis.

7.2.5 PLT This program is similar to PNT. However, this program analysis T beam with layered flange.

The flow charts are given in the following pages.

FLOW CHART 1

Program NOLAFT

Flow chart for the analysis of a 'T' section with non-layered flange using 'Direct search method'.

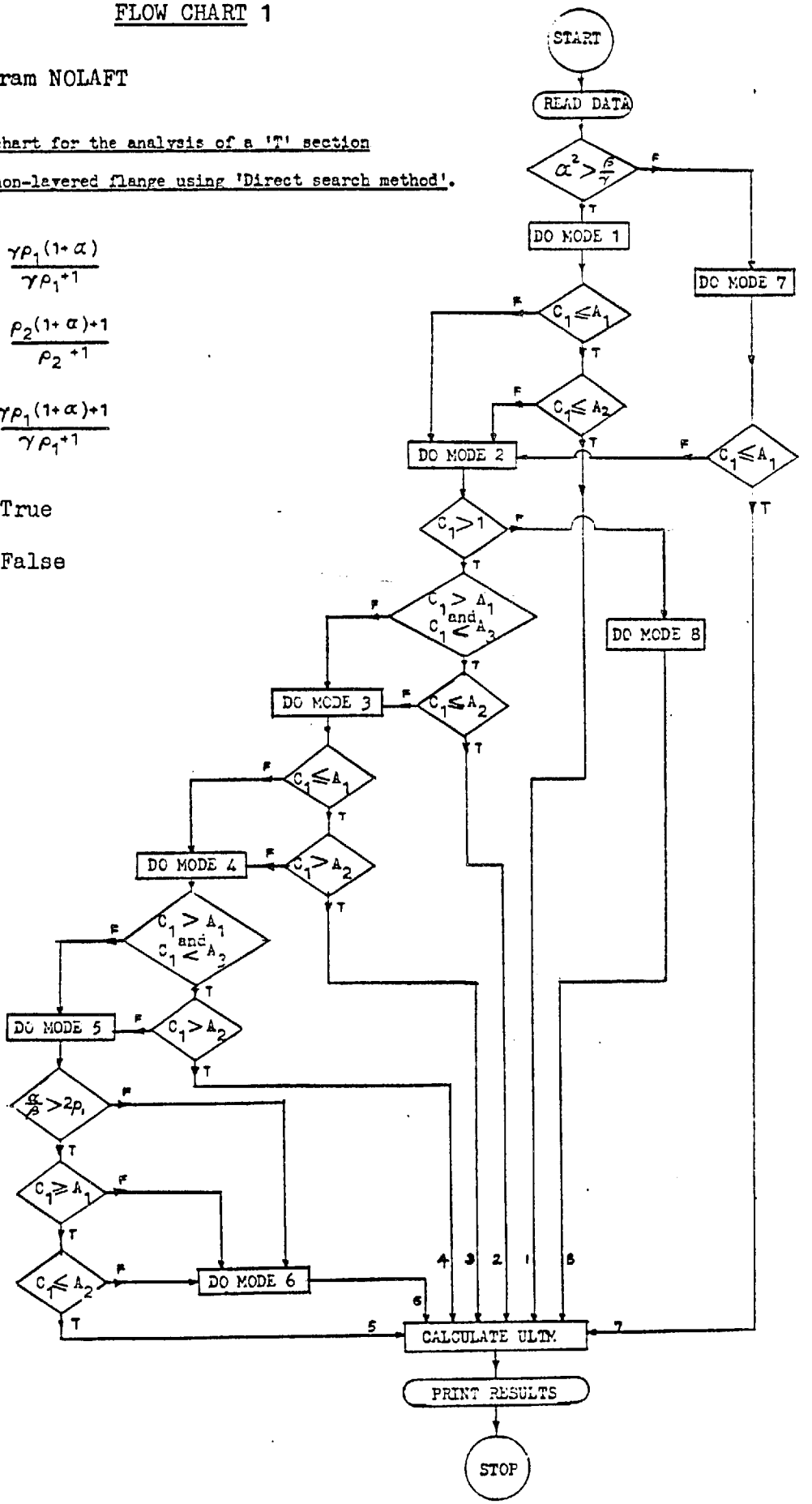
$$A_1 = \frac{\gamma\rho_1(1+\alpha)}{\gamma\rho_1+1}$$

$$A_2 = \frac{\rho_2(1+\alpha)+1}{\rho_2+1}$$

$$A_3 = \frac{\gamma\rho_1(1+\alpha)+1}{\gamma\rho_1+1}$$

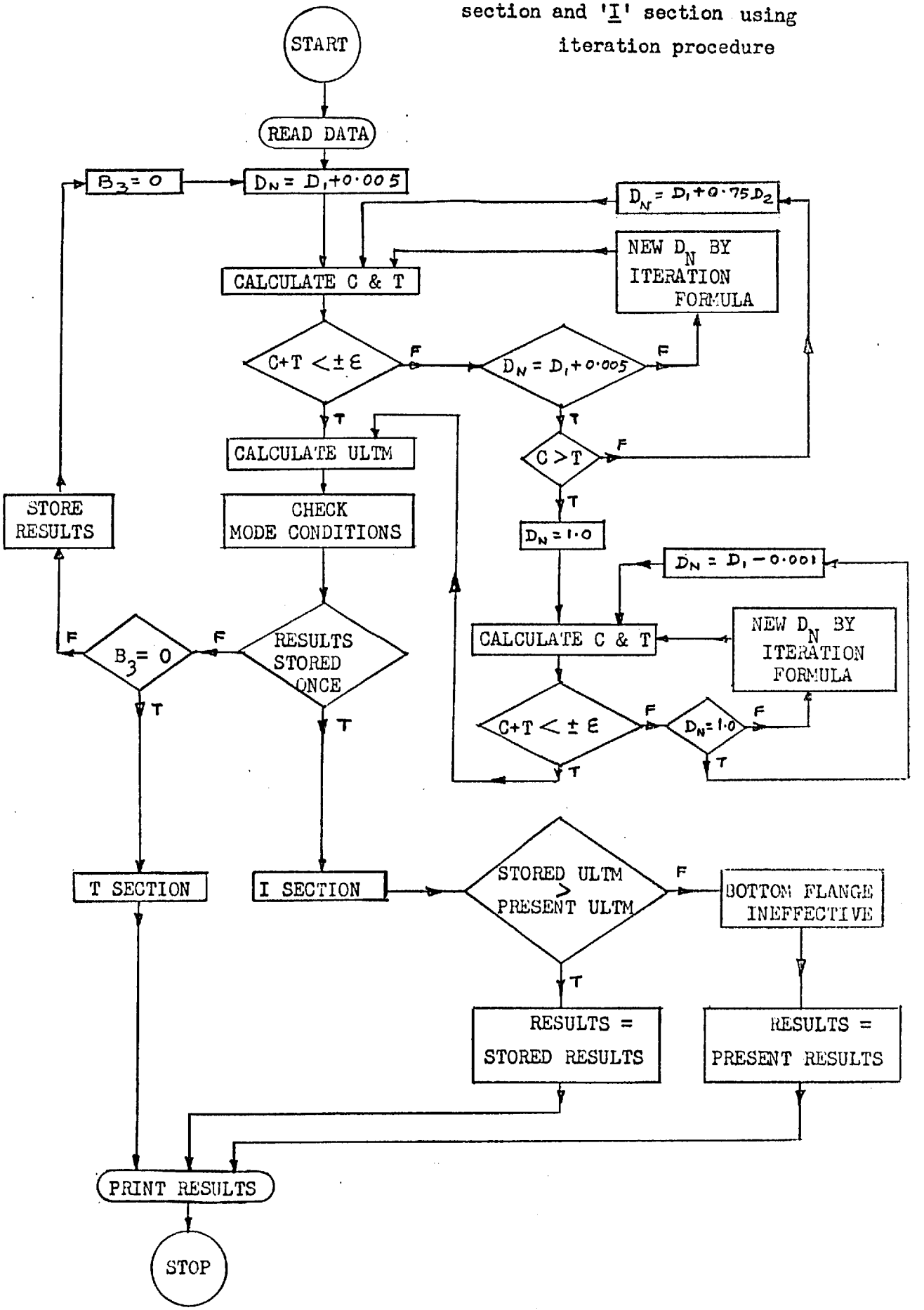
T = True

F = False



FLOW CHART 2

Flow chart for the program NOLAFTI. Analysis of NON-LAYERED FLANGED 'T' section and 'I' section using iteration procedure



Descriptions for NOLAFTI.

C = total compression

T = total tension

ε = permitted error (numerical value of F_4)

Input data: B_1, B_2, B_3, D_1, D_2, D_3, E_1, E_2, E_3, F_1, F_3, F_4 & F_5

Output : D_N, H_1, H_2, H_3, ULTM & Failure mode

Optional output: σ_{11}, σ_{12}, σ_{21}, σ_{22}, σ_{31} & σ_{32}

Program LAYFLIT.

Analysis of LAYERED FLANGED 'I' section and 'T' section.

Flow chart for the program LAYFLIT is same as that of NOLAFTI with minor modifications to allow for the layers in the flanges.

The following list shows the comparision of statements in NOLAFTI and the equivalent statements in LAYFLIT

NOLAFTI	LAYFLIT
$D_N = D_1 + 0.005$	$D_N = D_{S1} + 0.005$
$D_N = D_1 + 0.75D_2$	$D_N = D_{S1} + 0.75D_{18}$
$D_N = 1.0$	$D_N = D_1$

Input data: B_1, B_{18}, B_{19}, N_1, N_2, D_1, D_2, D_3, D_4, ... D_{N_1}, D_{18}, D_{19}, D_{20}, D_{21}, ... $D_{(18+N_2)}$, E_1, E_2, E_{18}, E_{19}, E_{20}, F_1, F_2, F_3, F_4, F_5 & F_6

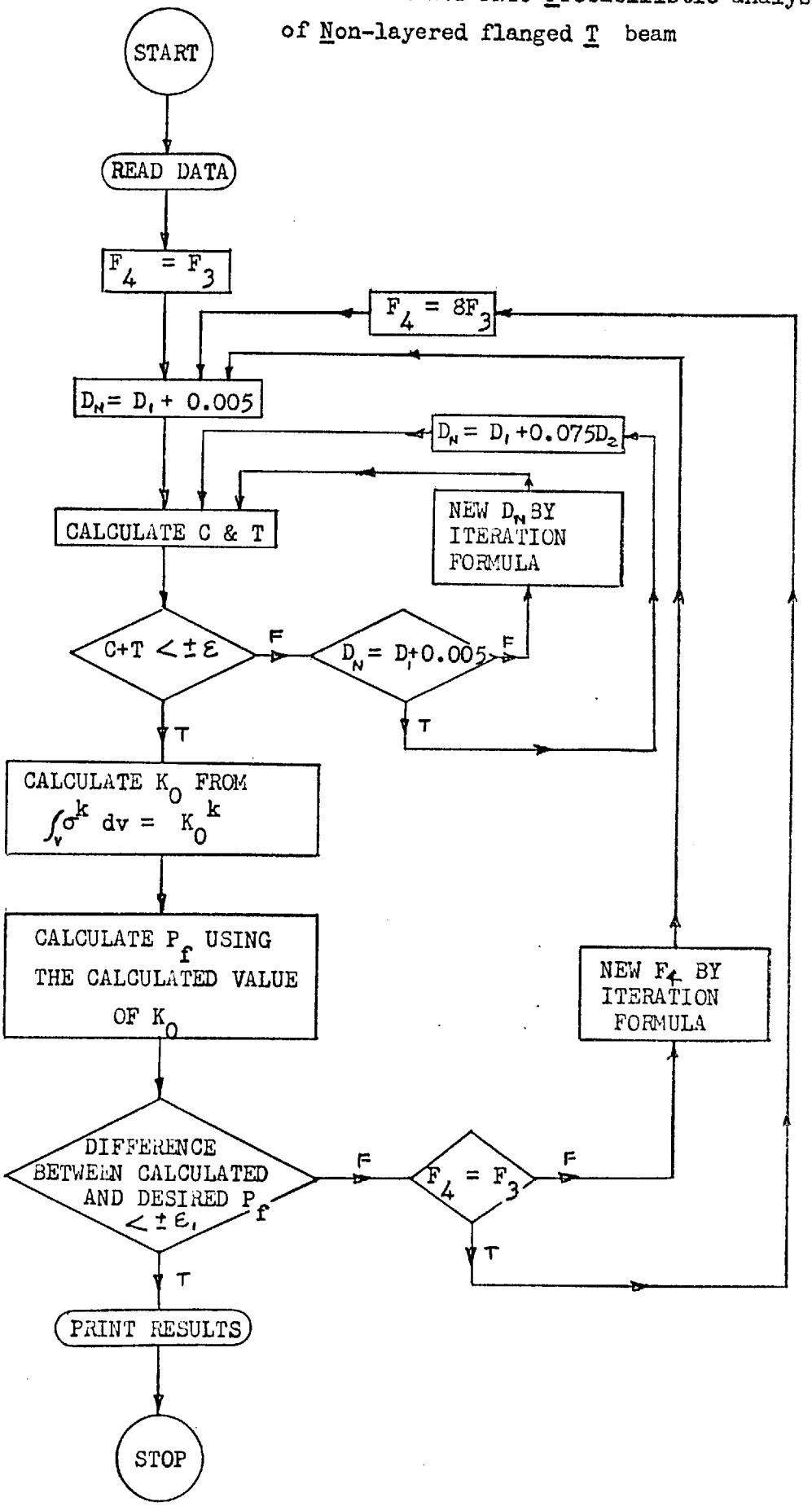
Output : D_N, H_1, H_2, H_3, ULTM & Failure mode.

Optional output: σ_{i1}, σ_{i2} where i = 1 to N_1 σ_{181} & σ_{182}

σ_{j1}, σ_{j2} where j = 19 to $(18 + N_2)$

FLOW CHART 3

Flow chart for PNT. Probabilistic analysis of Non-layered flanged T beam



Program PNT

Input data : B_1, B_2, D_1, D_2, S, G, E_1, E_2, F_1, F_3, SK, BK_{01} & PF_1

where,

S = span

G = The ratio of the distance between the two point loads and the span. For UDL put G = 1.0

SK = k

BK_{01} = K_0 at 50% probability of failure. These values of k and K_0 are obtained from the test results as described in section 5.12

PF_1 = Desired probability of failure.

Output : D_N, H_1, H_2, ULTM & failure mode

Ultimate tensile stress in rib (σ_{22}) at the given probability of failure.

Optional output : σ_{11}, σ_{12}, σ_{21} & σ_{22}

Maximum interface shear stress and rib shear stress.

Program PLT

Probabilistic analysis of Layered flanged T section.

Flow chart for the program PLT is same as PNT with minor modifications to allow for the layers in the flange.

Input data : B_1, B_{18}, N_1, D_1, D_2, D_3, ... D_{N_1}, D_{18}, S, E_1, E_2, E_{18}, F_1, F_2, F_3, SK, BK_{01}, PF_1 & G

Output : D_N, H_1, H_2, ULTM & Failure mode.

Ultimate tensile stress in rib (σ_{182}) at the given probability of failure.

Optional output : σ_{i1}, σ_{i2} where i = 1 to N_1 σ_{181} & σ_{182}

Maximum interface shear stress and rib shear stress.

CHAPTER 8

Summary, conclusions & future work

8.1 Summary

The ultimate load behaviour of single skin and double skin panels with rigid connection between flanges and ribs has been investigated theoretically, treating them as a series of T beams and I beams respectively.

A brief survey of the previous work connected with the elastic behaviour of the stressed-skin panels and the ultimate load behaviour of the timber beams has been given in chapter 1.

The next three chapters are devoted to the analysis of T sections and I sections with non-layered and layered flanges. Engineer's bending theory, modified with an assumption of trapezoid-like stress distribution in the compression zone, is the basis of the analysis. Chapter 2 describes the derivation of the governing equations for the failure modes of a T section with a non-layered flange. At the end of this chapter, two procedures of analysing T sections with the aid of the computer are given. The first procedure is based upon the 'direct search method', whereas the second is an iteration procedure.

Chapter 3 deals with the analysis of I sections with non-layered flanges by using iteration procedure.

In chapter 4, T sections and I sections with layered flanges are analysed. Initially, governing equations for each mode of failure of the T section are derived. When plasticity occurs in the flange, an incremental analysis has been adopted to obtain the final solution. In this analysis the depth of yield penetration is increased layer by layer and the equilibrium condition is checked at each time. An alternative iteration procedure, which automatically considers all possible types of

stress distribution also has been described. At the end of chapter 4, the description of the analysis of I sections with layered flange is given. The routine is the same as that of the analysis of a T section using the iteration procedure. However, the bottom flange also is considered in the case of I section.

Weibull's statistical strength theory has been used in chapter 5 to tackle the size effect problem. T beams with non-layered and layered flanges have been considered in the analysis. The application of Weibull's theory to predict the ultimate tensile stress attained by the rib of a T beam at any probability of failure has been shown. The loading cases considered are as follows.

a) Uniformly distributed load throughout the span.

b) Two point loads symmetrically placed about the centre of the span.

The derivation of the statistical tensile strength parameters of the timber beams from bending test results also has been described in this chapter.

Experimental investigation on layered and non-layered T beams are described in chapter 6. Three beams, each with a layered flange, have been used in the preliminary tests. Strength properties, including the ultimate tensile stress of the rib, are found by testing small matching specimens. The ultrasonic pulse technique was used to find the modulus of elasticity of the veneers. However, in the case of the rib, both ultrasonic and static loading methods have been used and the results compared. Description of the pilot test series on T beams with non-layered flanges to investigate the size effect problem is also given in chapter 6. The ultimate tensile stress attained by the rib of each beam is estimated from a statistical analysis of strength data obtained from tests conducted at Princes Risborough Laboratory.

In chapter 7, descriptions of the computer programs for the analysis of T beams and I beams are given. Seperate programs have been written in Fortran language for the analysis of beams with non-layered and layered flanges. In the case of layered flanges, upto 17 layers in each flange have been considered. Weibull's statistical strength theory has been used in two programs to predict the ultimate tensile stress attained by the rib of a T beam which has a non-layered or layered flange.

8.2 Conclusions

At the end of chapter 2, two procedures of analysing T sections with the aid of the computer are given. Although the first procedure, which uses a 'direct search method', can be used for a T section with non-layered flange, it is not recommended for T sections with layered flanges and I sections. It is a tedious procedure which checks almost every mode of failure to obtain the correct solution. This procedure becomes very inefficient in the case of sections with layered flanges which have to be subjected to incremental analysis when plasticity occurs in the top flange. The alternative routine using the iteration procedure, which automatically considers all possible types of stress distribution, is found to be most appropriate for I sections and T sections with layered flanges.

It has been found that the ultimate resisting moment of the T section is very sensitive to ultimate tensile stress of the rib (Table 5).

In the preliminary tests on three models, two results show close agreement with the estimated ultimate resisting moment using the modified engineer's bending theory. The accuracy of the estimated value depends upon the knowledge of the tensile strength of the rib at the most vulnerable location. These limited number of tests also show that bigger the size of the matching tension specimens, the better the chance of getting a more realistic value of the tensile strength. However, more model tests are needed to draw definite conclusions.

Tests on more models are also necessary to establish the suitability of mechanical gauges for measuring the strain of the timber T beams with layered flanges. If electrical strain gauges are used in conjunction with the mechanical gauges a fair comparison can be made.

Sufficient statistical strength data was not available to test the method of predicting the ultimate resisting moments of T beams using Weibull's statistical strength theory and to reach definite conclusions. However, the results of the pilot test series and the ultimate resisting moments estimated by using the few available statistical data (although inadequate) appears to show that the ultimate load analysis with the aid of statistical strength theory might provide a safe solution.

8.3 Future work

The research work presented in this thesis can be considered as a basic step for the ultimate load analysis of stressed skin panels. To understand the behaviour of the panels completely, more work has to be done by way of research and model testing. The future work falls into two types.

(1) Theoretical work in the following areas.

   (a) Application of size effect analysis to the bottom flange which resists tensile stresses.

   (b) Effect of large deflections and shear lag on the ultimate resisting moment.

   (c) Ultimate load analysis of the panel as a whole, without splitting into T beams or I beams.

(2) Experimental work to find the following:

   (a) Statistical tensile strength properties (k and K_0) of the materials.

   (b) The ultimate load behaviour of the stressed-skin panel models.

BIBLIOGRAPHY

Amana, E. J. (1967). Applications of orthotropic plate theory to stiffened plywood plates. Ph.D. thesis. London.

Barrett, J. D. (1974). Effect of size on tension perpendicular-to-grain strength of Douglas-Fir. Wood and Fiber. Vol.6(2). pp. 126-143.

Barrett, J. D., Foschi, R. O. and Fox, S. P. (1975). Perpendicular-to-grain strength of Douglas-Fir. Can. J. Civ. Eng. Vol. 2. pp. 50-57.

Beghtel, S. C. and Norris, C. B. (1959). Strength of wood beams of rectangular cross section as effected by span-depth ratio. U.S. Forest Serv., FPL Report 1910. Madison.

Bohannan, B. (1966). Effect of size on bending strength of wood members. USDA Forest Service. Research paper FPL 56. Madison.

Booth, L. G. and Pierce, C. B. (1971). The theoretical behaviour of plywood panel stiffened with timber beams. IUFRO. Section 41. Madison.

B.S.I. (1957) BS373. Methods of testing small clear specimens of timber. London.

Comben, A. J. (1957). The effect of depth on the strength properties of timber beams. FPR Spe. Report No. 12. HMSO. London.

Curry, W. T. (1954). The strength properties of plywood. Part 2. Effect of the geometry of construction. FPR Bulletin No. 33 HMSO. London.

Dietz, A. G. H. (1942). Stress-Strain Relations in Timber Beams (Douglas-Fir). A.S.T.M Bulletin No. 118, October 1942. pp. 19-27.

Foschi, R. O. (1969). Stress distribution in plywood stressed-skin panels with longitudinal stiffeners. Dept. of Fisheries and Forestry. Canadian Forestry Service. Publication No. 1261.

Foschi, R. O. and Barrett, J. D. (1976). Longitudinal shear strength of Douglas Fir. Can. J. Civ. Eng. Vol. 3. pp. 198-208.

Foschi, R. O. (1979). Lectures on brittle fracture. Mechanical Engineering Department, Imperial College, London.

Freas, A. D. and Selbo, M. L. (1954). Fabrication and design of glued laminated wood structural members. U.S. Dept. Agr. Tech. Bulletin 1069.

Kollmann,F. F. P. and Cote, W. A. (1968). Principles of wood science and technology. Vol.1. Springer-Verlag, Berlin.

Liska, J. A. (1942). Tentative method of calculating strength and modulus of elasticity of plywood in compression. Revised in 1950. Again revised in 1955 (No. 1315). FPL. Madison.

Markwardt, L. J. and Freas, A. D. (1946). Approximate methods of calculating the strength of plywood. FPL. Madison.

Newlin, J. A. and Trayer, G. W. (1924). Form factors of beams subjected to transverse loading only. Nat. Advisory Comm. Aeron. Rep. 181. (see US. Forest Prod. Lab. Report 1310 - (1941)

Nwokoye, D. N. (1971). A method of estimating safe stresses for structural timber from non-destructive tests. Report to CIRIA, London.

Princes Risborough Laboratory (1974). Strength properties of timber. MTP Construction, Lancaster, England.

Ramos, A. N. (1961). Stress-strain distribution in Douglas-Fir beams within plastic range. USDA Forest Service. Forest Products Laboratory, Madison.

RILEM/CIB-3TT-3 (1978). Testing methods for timber in structural sizes. Materiaux et Constructions. Vol.11. No.66. Nov-Dec. pp. 445-452

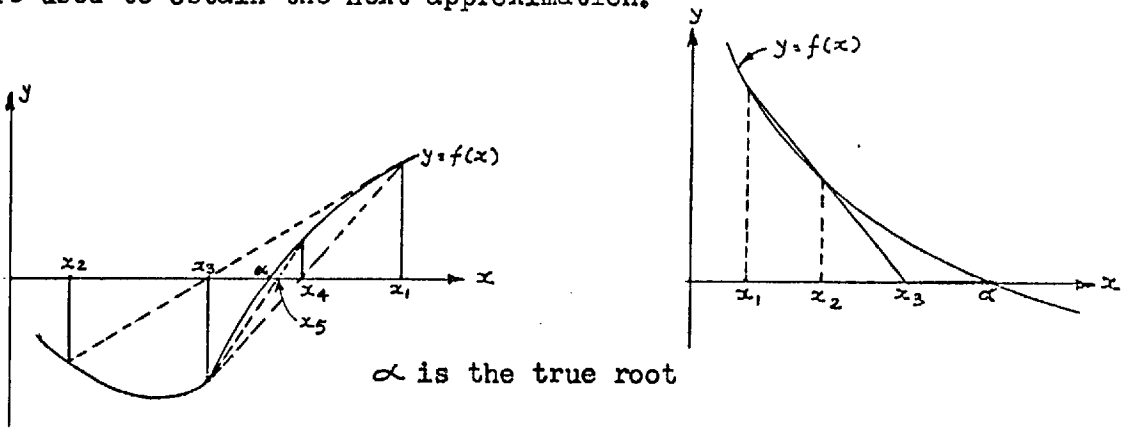
Tottenham, H. (1958). The effective width of plywood flanges in stressed skin construction. TDA research report E/RR/3. London.

Weibull, W. (1939). A statistical theory of the strength of materials. Proc. Roy. Swed. Inst. Eng. Res. No. 151, Stockholm.

APPENDIX 1

Iteration Procedure.

The iteration procedure adopted in this thesis is a combination of the method of False Position and the modified version of the Secant method. In both methods two initial approximation must be available to derive the next approximate value. In the former, the true root always lies in between the two approximate values when the next value is derived. That is, the value of the function is negative in one location and positive in the other. In the latter method the function need not have opposite signs at two locations but the last two approximations are used to obtain the next approximation.



The method of false position — The Secant method

Fig. A

Refer to Fig. B

In the method adopted for this thesis two initial values x_1 and x_2 are chosen to satisfy the requirements of the method of false position. Let $f(x_1)<0$ and $f(x_2)>0$. The third approximate value x_3 is derived using the iteration formula,

$$x_3 = x_1 + \frac{(x_2-x_1)\ f(x_1)}{f(x_1)-\ f(x_2)}$$

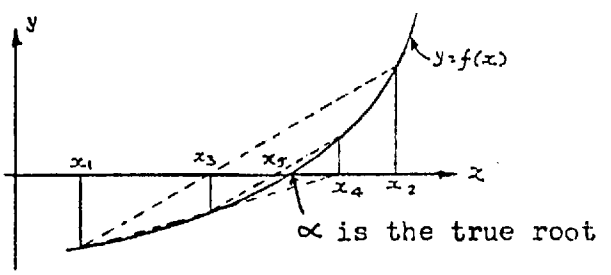


Fig.B

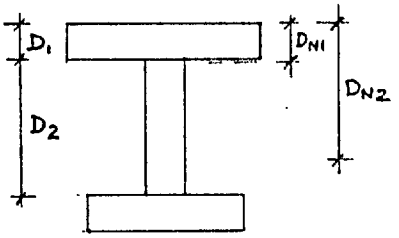
Let $f(x_3)<0$. If the method of false position was adopted x_2 and x_3 would have been automatically chosen to derive x_4. But the magnitude of $f(x_1)$ and $f(x_2)$ are compared and whichever value of x gives the smaller error is chosen along with x_3 to derive x_4. In this particular case x_1 and x_3 are used to derive x_4. This is a deviation from the secant method where the second and third values of x should have been used to obtain x_4.

It is found that this iteration procedure is appropriate for the analysis of T and I sections. Depth of neutral axis D_N is calculated by checking equilibrium equation. $C+T \not> \epsilon$ where ϵ is an acceptable small error.

Let the first and second approximation of D_N be D_{N1} and D_{N2} respectively, where

$D_{N1} = D_1 + 0.005$ mm

$D_{N2} = D_1 + 0.75\, D_2$



We know the correct value of D_N lies between D_{N1} and D_{N2}.

$(C+T)_{D_{N1}} = F_1$(Negative)

$(C+T)_{D_{N2}} = F_2$(Positive)

D_{N3} is calculated from the iteration formula $D_{N3} = D_{N1} + (D_{N2}-D_{N1})\frac{F_1}{(F_1-F_2)}$

The magnitude of F_1 and F_2 are compared and if $F_1 < F_2$, D_{N1} and D_{N3} are adopted to find the next approximate value of D_N; otherwise D_{N2} and D_{N3} are adopted. This process is repeated until a value of D_N is obtained such that $(C+T)_{D_N} \not> \epsilon$.

By working out many examples it is found that seven or less iterations are sufficient to obtain an acceptable value of D_N. As a further precaution there is a provision in the computer program to stop the iterations after 10 routines and to print out a message to that respect.

APPENDIX 2

FORTRAN PROGRAM FOR ITERATION ALGORITHM

```
      SUBROUTINE  ITER(D1, D2, ER, DN)
C     ALGORITHM:  ITERATION TO FIND DN
      DN1  =  D1 + 0.005
      DN2  =  DN1
      CALL SUB 1 (DN1, F1)
      IF (ABS(F1).LT.ER) GO TO 103
C     ER IS THE MAXIMUM PERMITTED ERROR
      DN2  = D1 + 0.75 * D2
      CALL SUB 1 (DN2, F2)
      I = 1
      IF (ABS(F2).LT.ER) GO TO 103
100   DN3 = DN1 + (DN2 - DN1)*F1/(F1 - F2)
      IF (ABS(F1).LT.ABS(F2) ) GO TO 101
      DN1 = DN2
      F1  = F2
101   DN2 = DN3
      CALL SUB 1 (DN2, F2)
      IF (ABS(F2).LT.ER) GO TO 103
      I  = I + 1
      IF (I.EQ.11) GO TO 102
      GO TO 100
102   PRINT, "CONVERGENCE PROBLEM. ERROR =", F2
103   PRINT, "DN = ", DN2
      RETURN
      END
```

APPENDIX 3

Application of Gauss Quadrature

The integral $\int_V \sigma^k dv$ can be written in the following form.

$$\int_V \sigma^k dv = Z \int_A^B \int_c^D f_1(x)\ f_2(y)dx\ dy = Z\ I \qquad \text{where Z is a constant.}$$

The evaluation of integral I using Gauss quadrature technique is shown in the following steps.

$$I = \int_A^B \int_c^D f_1(x)\ f_2(y)dx\ dy \qquad 1.$$

By transformation of co-ordinates of integration

$$I = \frac{(B-A)}{2}\ \frac{(D-C)}{2} \int_{-1}^{+1} \Psi_1(u)du \int_{-1}^{+1} \Psi_2(v)dv \qquad 2.$$

where,

$$x = (1-u)\frac{C}{2} + (1+u)\frac{D}{2} \quad \text{i.e} \quad x = \phi_1(u) \text{ and } \Psi_1(u) = f_1(\phi_1(u))$$

$$y = (1-v)\frac{A}{2} + (1+v)\frac{B}{2} \quad \text{i.e} \quad y = \phi_2(v) \text{ and } \Psi_2(v) = f_2(\phi_2(v))$$

Adopting n number of points for integration along x and y axis for convenience,

$$\int_{-1}^{+1} \Psi_1(u)du = \sum_{i=1}^{n} H_i\ \Psi_1(u_i)$$

where u_i = position of the point

H_i = weight coefficient for the position u_i

Similarly,

$$\int_{-1}^{+1} \Psi_2(v) = \sum_{i=1}^{n} H_i\ \Psi_2(v_i)$$

when n is the same for both integrals, $u_i = v_i$

Reference: Zienkiewicz, O. C. (1971). Finite element method in Engineering science. 2nd Ed. McGraw-Hill, London.

The following example illustrates the application of Gauss quadrature technique.

$$\text{Evaluate } I = \int_2^5 \int_3^6 x^2 y^3 \, dx \, dy$$

To choose the number of points, the following formula is adopted.

$$2n - 1 = \text{order of equation} = 5$$

$$\therefore \quad n = 3$$

From Tables, when n = 3

(Approximate values rounded off to 4 significant figures)

u (or v)	H
$u_1 = -0.7746$	0.5556
$u_2 = +0.7746$	0.5556
$u_3 = 0.0000$	0.8889

$$\phi_1(u_1) = (1 - 0.7746)\frac{3}{2} + (1 + 0.7746)\frac{6}{2} = 5.6619,$$

$$\psi_1(u_1) = f_1(\phi_1(u_1)) = 5.6619^2 = 32.057$$

$$\phi_1(u_2) = (1 + 0.7746)\frac{3}{2} + (1 - 0.7746)\frac{6}{2} = 3.3381,$$

$$\psi_1(u_2) = f_1(\phi_1(u_2)) = 3.3381^2 = 11.143$$

$$\phi_1(u_3) = (1 - 0.0)\frac{3}{2} + (1 + 0.0)\frac{6}{2} = 4.5000$$

$$\psi_1(u_3) = f_1(\phi_1(u_3)) = 4.5^2 = 20.250$$

$$\sum_{i=1}^{3} H_i \, \psi_1(u_i) = 0.5556 \times 32.057 + 0.5556 \times 11.143 + 0.8889 \times 20.25$$

$$= \underline{42.002}$$

Similarly,

$$\phi_2(v_1) = (1 - 0.7746)\frac{2}{2} + (1 + 0.7746)\frac{5}{2} = 4.6619,$$

$$\psi_2(v_1) = f_2(\phi_2(v_1)) = 4.6619^3 = 101.318$$

$$\phi_2(v_2) = (1 + 0.7746)\,\frac{2}{2} + (1 - 0.7746)\,\frac{5}{2} = 2.3381,$$

$$\psi_2(v_2) = f_2(\phi_2(v_2)) = 2.3381^3 = 12.782$$

$$\phi_2(v_3) = (1 - 0.0)\,\frac{2}{2} + (1 + 0.0)\,\frac{5}{2} = 3.5000,$$

$$\psi_2(v_3) = f_2(\phi_2(v_3)) = 3.5^3 = 42.875$$

$$\sum_{i=1}^{3} H_i\,\psi_2(v_i) = 0.5556 \times 101.318 + 0.5556 \times 12.782 + 0.8889 \times 42.875$$

$$= \underline{101.506}$$

Using equation 2,

$$I = \frac{(5-2)}{2} \times \frac{(6-3)}{2} \times 42.002 \times 101.506 = \underline{9592.77}$$

Check

$$\int_2^5 \int_3^6 x^2 y^3\,dx\,dy = \left[\frac{x^3}{3}\right]_3^6 \cdot \left[\frac{y^4}{4}\right]_2^5 = \left[\frac{216}{3} - \frac{27}{3}\right] \cdot \left[\frac{625}{4} - \frac{16}{4}\right]$$

$$= 63 \times \frac{609}{4} = \underline{9591.75}$$

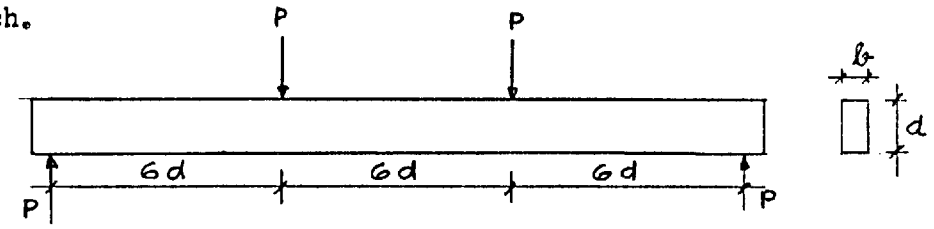
$$\text{Error} = \frac{(9592.77 - 9591.75)}{9591.75}\,100 = +\,0.0106\%\ \text{very small}$$

Note: If exact values of the Gauss points u_i and weight coefficients H_i were used, the above example would give the exact result.

APPENDIX 4

Bending test results obtained from the Princes Risborough Laboratory (PRL)

It was possible to obtain some test data from the PRL for the timber belonging to the "Spruce-Pine-Fir" group. The materials for the model beams were selected from the same batch of timber joists that were used in the PRL bending tests. The PRL test set up was as shown in the sketch.



From the available test data, the beams which failed before the extreme top fibre attained the ultimate compressive stress, were only chosen to derive the value of k and K_0. The failure mode was confirmed by testing two specimens (20 x 20 x 60mm long) taken from the compressive zone outside the middle third span of the tested beams. Ultimate tensile stress at the extreme bottom fibre was calculated using the simple bending formula.

$$\text{Ultimate tensile stress} = \text{Ultimate bending moment} \times \frac{6}{bd^2}$$

The ultimate tensile stress at the extreme bottom fibre is given below in the ascending order.

1) Cross-section b x d = 37.8 x 87.5mm Number of beams = 30

Ultimate tensile stress (N/mm^2)

17.60	17.70	19.90	22.30	23.50	24.60	25.50	26.70	26.80
30.00	30.10	30.40	30.80	31.70	34.40	34.70	35.10	35.40
35.60	36.70	37.60	37.90	38.10	39.20	39.30	40.00	40.70
42.90	42.90	46.50						

average stress = 32.49 N/mm^2

2) Cross section b x d = 37.8 x 181.3mm Number of beams = 27

Ultimate tensile stress (N/mm^2)

14.50	16.10	19.50	19.80	21.20	21.60	21.80	23.70	24.20
24.70	25.10	26.80	27.30	29.50	29.60	30.30	31.30	32.00
33.33	33.80	36.10	37.60	39.50	40.30	41.50	41.70	42.40

average stress = 29.08 N/mm^2

Derivation of k and K_0 from the test results.

$\sigma_1 = 32.49\ N/mm^2$ $V_1 = 37.8 \times 87.5 \times 6 \times 87.5 = 1736437.5mm^3$

$\sigma_2 = 29.08\ N/mm^2$ $V_2 = 37.8 \times 181.3 \times 6 \times 181.3 = 7454845.7mm^3$

From equation (5.58)

$$k = \frac{\ln V_2 - \ln V_1}{\ln \sigma_1 - \ln \sigma_2} = \frac{15.824375 - 14.367346}{3.4809324 - 3.3700507} = \frac{1.4570288}{0.1108817} = 13.14$$

From equation (5.59)

$$K_0 = \sigma_2 \left[\frac{V_2(k+3)}{2\,(k+1)^2} \right]^{\frac{1}{k}} = 29.08 \left[\frac{7454845.7 \times 16.14}{2 \times 14.14^2} \right]^{\frac{1}{13.14}} = 75.95$$

Note: It should be noted that the above value of k and K_0 are derived only for illustrative purpose and are not reliable due to the following reasons.

1. Test results were available for only two volumes. If the graph had been drawn using three or more volumes, better results would have been obtained.

2. Number of specimens considered in each volume was too small to give statistically reliable average stress.